Al-Quds University

Deanship of Graduate Studies

Faculty of Health Profession

Medical Imaging Technology

Deep Clustering Approaches for Carotid Artery Calcification Detection in Panoramic Radiographs for Enhancing Cardiovascular Risk Prediction

Nadeen Khaled Ibrahim Erekat

M.Sc. Thesis

Jerusalem - Palestine

1447/ 2026

Deep Clustering Approaches for Carotid Artery Calcification Detection in Panoramic Radiographs for Enhancing Cardiovascular Risk Prediction

Prepared By:

Nadeen Khaled Ibrahim Erekat

Supervisor: **Prof. Radwan Qasrawi**

Co-Supervisor: **Dr. Hussien ALMasri**

This Thesis submitted in partial fulfillment of requirements for the degree of Master of Medical Imaging Technology Faculty of Graduate studies - Al-Quds University

1447/2026

Al-Quds University

Deanship of Graduate Studies

Faculty of Health Profession

Medical Imaging Technology

Thesis Approval

Deep Clustering Approaches for Carotid Artery Calcification Detection in Panoramic Radiographs for Enhancing Cardiovascular Risk Prediction

Prepared by: **Nadeen Khaled Ibrahim Erekat**

Registration No: **22312348**

Supervisor: **Prof. Radwan Qasrawi**

Co-Supervisor: **Dr. Hussien ALMasri**

The master's thesis was submitted and accepted on: 8/1/2026

The names and signatures of the examining committee members are as follows:

1- Head of Committee: Prof. Radwan Qasrawi Signature:

2- Co-Supervisor: Dr. Hussein ALMasri Signature:

3- Internal Examiner: Dr. Mohammad Hjouj Signature:

4- External Examiner: Prof. Derar Eleyan Signature:

Jerusalem - Palestine

1447 / 2026

Dedication

I dedicate this work first and foremost to my mother and father, whose unwavering love, sacrifices, and constant encouragement carried me through every step of this journey. Your belief in me gave me strength when mine wavered, and your support remains the foundation of everything I have achieved.

To my husband, my partner and steady support, thank you for your patience, understanding, and for standing beside me through the long days and longer nights. Your presence made this path lighter and my determination stronger.

To my beloved child, still young yet already my greatest motivation, I dedicate this achievement as a promise to keep learning, to keep striving, and to hope for a future where I will see you grow into the successful and kind person, I know you can become.

To my professors and mentors, thank you for opening the first doors on this path, for sharing your knowledge generously, and for guiding me with care and integrity. Your support shaped not only this research, but also the researcher I am becoming.

This work was not built by effort alone; it is the result of many hands and many hearts. It was carried by the quiet strength of those who stood behind it, by the love that lifted me when I was tired, the guidance that steadied my steps, and the patience that made every difficult season bearable. I carry your presence in these pages, and I offer this milestone as a shared triumph, with sincere gratitude and lasting pride.

Nadeen Khaled Ibrahim Erekat

Declaration

I certify that this thesis submitted for the degree of Master is the result of my own research, except where otherwise acknowledged, and that this study (or any part of the same) has not been submitted for a higher degree to any other university or Institution.

Signed:

Nadeen Khaled Ibrahim Erekat

Date: 8/1/2026

Acknowledgements

In the name of Allah, the Most Gracious, the Most Merciful. Peace and blessings be upon our Prophet Muhammad. All praise is due to Allah for granting me strength, patience, and guidance throughout this journey. Without His support, this work would not have been possible. I am deeply grateful to my mother and father for their endless love, prayers, sacrifices, and unwavering belief in me. Your encouragement carried me through the most demanding moments and remains the foundation of everything I have achieved. I also extend my sincere appreciation to my family for their constant support and understanding.

I acknowledge the academic and institutional support that made this thesis possible. I would like to express my heartfelt gratitude to my supervisor, Dr. Radwan Al-Qasrawi, for his exceptional guidance, mentorship, and continuous support. His insightful feedback, scientific rigor, and encouragement were instrumental in shaping this thesis and pushing me to strive for excellence. I also acknowledge Dr. Hussein Al-Masri, co-supervisor of this thesis, for serving on the supervisory team and for his formal academic oversight throughout the study. I also extend my appreciation to the academic staff involved in the supervision and administrative process of this thesis for their time and support. Furthermore, I would like to thank the Dental Clinics affiliated with Al-Quds University for granting access to patient data and radiographs, which were critical to the study. Their cooperation and the support from the College of Dentistry made this work possible.

Finally, I would like to acknowledge the support I received at home throughout the completion of this thesis, particularly the patience and understanding shown during long working hours and periods of limited availability. I extend my appreciation to my husband, my family, and my child for their continued support throughout the research and writing process. This steady support, in both time and spirit, made it possible to maintain focus and momentum until the final stage and helped me meet the demands of this project with consistency and perseverance. I am also thankful to all those who contributed, directly or indirectly, to bringing this work to completion, and I deeply value the assistance I received.

Nadeen Khaled Ibrahim Erekat

Abstract

Cardiovascular disease remains a leading cause of death worldwide, making early identification of vascular risk markers essential for prevention. Carotid artery calcifications can occasionally be visualized on panoramic dental radiographs, offering an opportunistic indicator of atherosclerotic burden during routine dental care. Yet, manual identification is challenged by inter-reader variability and the presence of anatomical mimics, and many published AI solutions rely on supervised learning that requires large, densely labeled datasets. This thesis investigates an alternative pathway by developing an unsupervised deep clustering framework for carotid region analysis on panoramic radiographs, and by integrating questionnaire-based risk factor modeling to support broader cardiovascular risk stratification.

This single-center retrospective cross-sectional observational study included 1,107 panoramic radiographs acquired between February 2025 and August 2025 during routine dental examinations at Abraj Dental Clinics affiliated with Al-Quds University, in collaboration with the Faculty of Dentistry. In addition, a cross-sectional questionnaire sub-study was prospectively administered to a subset of participants (n = 438) to capture cardiovascular risk profiles and support complementary non-imaging analyses. The imaging cohort comprised 48% males and 52% females, with an age range of 18–85 years and a mean age of approximately 40 years. Preprocessing consisted of contrast enhancement using Contrast Limited Adaptive Histogram Equalization (CLAHE) followed by extraction of bilateral carotid regions of interest (ROIs), resized to 128×128 pixels. To represent each ROI, a dual feature strategy was adopted. Interpretable handcrafted radiographic features were computed to quantify intensity distributions, texture patterns, and edge- and morphology-related cues potentially associated with calcification. In parallel, deep representations were learned using a convolutional autoencoder pretrained for 300 epochs with mean squared error loss and a low-dimensional latent space, producing compact feature vectors suitable for downstream clustering.

Four clustering methods were evaluated: K-Means, hierarchical clustering, Gaussian Mixture Models, and Deep Embedded Clustering (DEC). Clustering quality was assessed using internal validation metrics that do not require ground truth labels, including the Silhouette score, Davies–Bouldin index, and Calinski–Harabasz index. To connect unsupervised clustering outcomes to clinical relevance, the thesis adopted a patient-level validation strategy, where each patient contributed left and right ROI assignments. A high-risk validation subset of 21 patients was defined using confirmed cardiovascular disease history or documented carotid calcifications in clinical records. Patient-level accuracy was calculated based on the proportion of high-risk patients grouped into the dominant high-risk

cluster. Model interpretability was further supported using GradCAM++ visualization to highlight salient ROI regions consistent with expected calcification-related patterns.

DEC achieved the strongest clustering performance across the internal metrics, with a Silhouette score of 0.214, a Davies–Bouldin index of 1.752, and a Calinski–Harabasz index of 524, indicating improved within-cluster cohesion and between-cluster separation relative to baseline methods. Patient-level validation also favored DEC, which achieved 95.2% accuracy in aggregating high-risk patients into a dominant cluster with fewer anomalous cases compared with K-Means, hierarchical clustering, and GMM.

To incorporate non-imaging determinants of cardiovascular risk, prospectively administered questionnaire data were analyzed for 438 participants (220 high risk, 218 low risk). Univariate association testing using chi-square statistics with Cramér's V suggested notable associations with age, physical activity, sleep duration, sedentary time, dietary behaviors, selected health awareness indicators, and mental health measures such as relaxation difficulty and feelings of worthlessness. A Random Forest classifier trained on questionnaire features achieved high predictive performance (accuracy = 0.9318, ROC AUC = 0.9821, F1 = 0.9291), and feature importance analysis highlighted socioeconomic factors and psychological distress-related variables among influential predictors alongside age and lifestyle behaviors.

In conclusion, this thesis demonstrates that unsupervised deep clustering of anatomically defined carotid ROIs on panoramic radiographs can yield coherent groupings aligned with clinically defined high-risk status, while offering an interpretable and label-efficient screening support pathway. Combining imaging-based signals with questionnaire-derived risk factors may further strengthen cardiovascular risk stratification and support targeted referral for confirmatory vascular assessment. Future work should incorporate gold-standard vascular confirmation, multi-site external validation, and longitudinal outcome linkage to establish clinical reliability and generalizability.

Keywords: panoramic radiographs, carotid arteries calcifications, Deep Embedded Clustering, convolutional autoencoder, CLAHE, cardiovascular risk factors, Random Forest, GradCAM++.

Table of Contents

Declaration I

Acknowledgements II

Abstract III

List of Tables VIII

List of Figures IX

Abbreviations X

Chapter One 1

1.1. Introduction 1

1.2. Background 1

1.3. Problem Statement 3

1.4. Research Significance 4

1.5. Research Aim and Objectives 5

1.6. Research Questions 5

1.7. Thesis contributions 6

Chapter Two 8

2.1. Literature Review 8

2.2. Background 9

2.2.1. Epidemiology and pathophysiology of CVD: burden (global and Palestine) and why CACs matter: 9

2.2.2. Imaging approaches for carotid disease, with panoramic radiography (PR) as an opportunistic tool: 11

2.2.3. Evidence linking PR-detected CACs to future stroke and ischemic heart disease: prognostic signal and limitations: 12

2.2.4. Artificial intelligence in panoramic imaging: methods, performance, and clinical integration: 13

2.2.5. Modifiable risk factors that may influence carotid artery calcifications (CACs): 14

2.3. Artificial Intelligence in Panoramic Dental Radiography 22

2.4. Panoramic Dental Radiographs and Cardiovascular Disease: Revealing the Link 25

2.4.1. Early signals and conceptual groundwork: 25

2.4.2. Prevalence and risk-factor correlates (who has PR-visible CAC, and what does it track with?): 27
2.4.3. Concordance with vascular imaging (do PR findings align with ultrasound/CT?): 31
2.4.4. Clinical outcomes (does a PR finding predict events and established disease?): 33
2.4.5. Diagnostic utility, reliability, and practice pathways (can clinicians use PR signals consistently and safely?): 36
2.5. Utilizing Artificial Intelligence to Detect Carotid Artery Calcifications from Panoramic Dental Radiographs 39
2.6. Unsupervised Representation Learning and Deep Clustering for CAC Risk Stratification 46
2.7. Research Gap and Rationale 47

Chapter Three 50
3.1. Methodology 50
3.2. Dataset and Study Population 50
3.3. Image Preprocessing and ROI Extraction 51
Stage 1: DICOM Loading and Normalization 51
Stage 2: Region of Interest (ROI) Extraction 51
Stage 3: Contrast Enhancement 52
Stage 4: Noise Reduction 52
3.4. Feature Extraction 52
3.4.1. Hand-Crafted Radiographic Features: 53
3.4.2. Deep Learned Features via CNN Autoencoder: 54
3.5. Clustering Methods 54
3.6. Patient-Level Validation Methodology 56
3.6.1. Patient-Level Cluster Assignment 56
3.6.2. Accuracy Calculation: 57
3.6.3. Visualization Strategy 57
3.7. Clustering Quality Metrics 57
3.8. Explainability via GradCAM++ 58
3.9. Implementation Details 60
3.10. Validation 60

3.10.1. Imaging-based validation strategy: 60
3.10.2. Questionnaire sub-study and analysis plan: 61

Chapter Four 62
4.1. Results 62
4.2. Image Preprocessing 62
4.3. Clustering Quality Evaluation 63
4.4. Patient-Level Validation Results 65
4.4.1. High-Risk Patient Accuracy: 65
4.4.2. Cluster Distribution Analysis: 66
4.5. Visual Analysis of Clustering Results 66
4.6. GradCAM++ Interpretability Analysis 68
4.8. Cardiovascular Risk Factors Univariate Analysis 69

Chapter Five 76
5.1. Discussion 76
5.2. Finding Discussion 76
5.3. Strengths of the Study 79
5.4. Practical and Operational Challenges 79
5.5. Limitations and Potential Sources of Bias 80
5.6. Implications for Clinical Practice and Public Health 80
5.7. Future Directions and Outlook 81

Chapter Six 82
6.1. Conclusion 82
6.2. Summary of the Study 82
6.3. Main Conclusions 83
6.4. Implications and Outlook 83
6.5. Final Remarks 84
References 85
Appendix A: Letter of Research Ethical Committee (REC) approval 106
Appendix B: Consent form and questionnaire 107
الملخص: 113

List of Tables

Table 2.1: Key studies linking CACs on panoramic radiographs to cardiovascular outcomes 22
Table 2.2: Comparison of methodologies and performance metrics across reviewed studies 44
Table 4.1: Clustering Quality Metrics Comparison 62
Table 4.2: High-Risk Patient Distribution Across Clusters 65
Table 4.3: Patients risk assessment descriptive analysis 69
Table 4.4: Patients risk assessment univariate analysis 70
Table 4.5: Random Forest prediction performance 71

List of Figures

Figure 2.1: Stages in atherosclerosis progression 9
Figure 2.2: Panoramic dental radiograph with carotid artery calcification 10
Figure 4.1: The Complete Preprocessing Pipeline for the Proposed Model 62
Figure 4.2: Clustering Quality Metrics Comparison 63
Figure 4.3: Patient-Level Clustering Performance Across Methods 64
Figure 4.4: PCA Projections of the Feature Spaces for All Clustering Methods 67
Figure 4.5: GradCAM++ Visualization of Saliency Maps 68
Figure 4.6: Top 15 Most Important Questionnaire-Based Predictors of Cardiovascular Risk 73

Abbreviations

AHA:	American Heart Association	**MESA:**	Multi-Ethnic Study of Atherosclerosis
AI:	Artificial Intelligence	**MI:**	Myocardial Infarction
AUC:	Area Under the Curve	**MRA:**	Magnetic Resonance Angiography
BMP-2:	Bone Morphogenetic Protein-2	**MRI/MR:**	Magnetic Resonance Imaging
BVO:	Bilateral Vessel-Outlining	**MSE:**	Mean Squared Error
CAC:	Carotid Artery Calcification	**NOX2:**	NADPH Oxidase 2
CAD:	Coronary Artery Disease	**oPt:**	Occupied Palestinian Territory
CBCT:	Cone Beam Computed Tomography	**PCA:**	Principal Component Analysis
CH:	Calinski–Harabasz Index	**PM2.5:**	Particulate Matter ≤ 2.5 μm
cIMT:	Carotid Intima–Media Thickness	**PR:**	Panoramic Radiograph
CNN:	Convolutional Neural Network	**PREDIMED:**	Prevención con Dieta Mediterránea (Spanish Trial)
CTA:	Computed Tomography Angiography	**R-CNN:**	Region-Based Convolutional Neural Network
CT:	Computed Tomography	**RCT:**	Randomized Controlled Trial
CVA:	Cerebrovascular Accident	**ROC:**	Receiver Operating Characteristic
CVD:	Cardiovascular Disease	**ROI:**	Region of Interest
DB:	Davies–Bouldin Index	**RQ:**	Research Question
DEC:	Deep Embedded Clustering	**RUNX2:**	Runt-Related Transcription Factor 2
DSA:	Digital Subtraction Angiography	**SCORE:**	Systematic Coronary Risk Evaluation
DUS:	Duplex Ultrasound	**SHS:**	Second-Hand Smoke

eNOS:	Endothelial Nitric Oxide Synthase	**TIA:**	Transient Ischemic Attack
F1:	F1-Score (Harmonic Mean of Precision and Recall)	**TMJ:**	Temporomandibular Joint
GMM:	Gaussian Mixture Model	**UPF:**	Ultra-Processed Food
HPA:	Hypothalamic–Pituitary–Adrenal Axis	**VGG16:**	Visual Geometry Group 16-Layer Network
hs-CRP:	High-Sensitivity C-Reactive Protein	**WHO:**	World Health Organization
KL:	Kullback–Leibler (Divergence)	**YOLO:**	You Only Look Once
MACEs:	Major Adverse Cardiovascular Events		

Chapter One

1.1. Introduction

This chapter sets the scene for the thesis by framing cardiovascular disease as a leading yet largely preventable cause of death and disability, with particular attention to stroke and ischemic heart disease. It then introduces panoramic radiography and carotid artery calcifications as an unexpected but promising window into subclinical vascular disease, especially in contexts where access to formal vascular imaging is limited. Against this background, the chapter articulates the core problem that motivates the study, explains why it matters clinically and for public health in settings such as Palestine, and develops the overall aim together with specific research objectives and questions. It concludes by outlining the main contributions the thesis seeks to make in advancing the opportunistic use of panoramic radiographs, and in linking imaging-visible calcifications to broader behavioral and cardiometabolic risk profiles.

1.2. Background

Cardiovascular disease (CVD) remains the foremost contributor to global morbidity and mortality, with ischemic heart disease and stroke accounting for a substantial proportion of preventable loss of life (Roth et al., 2020; World Health Organization, 2025). A persistent challenge across many health systems, particularly in low-resource environments, is that risk often becomes clinically apparent only after irreversible vascular injury has occurred. Early identification of individuals at elevated risk is therefore central to effective prevention. Conventional vascular imaging modalities, such as Doppler ultrasound or CT angiography,

provide reliable assessment but are not routinely accessible in settings with limited infrastructure, high service demand, and fragmented referral pathways.

Panoramic radiography (PR), in contrast, is widely available, routinely performed, and comparatively inexpensive. In many populations, including Palestine, PR is often one of the most common imaging examinations obtained during adulthood. Importantly, carotid artery calcifications (CACs) may be incidentally visualized within the carotid window on PRs, and evidence from multiple cohorts suggests that these calcifications carry prognostic value for future cerebrovascular and coronary events (Bengtsson et al., 2019; Garoff et al., 2019, 2025; Gustafsson et al., 2018; Lim et al., 2021). This positions PR as a potentially valuable, opportunistic screening tool, one that could enable earlier vascular risk flagging without introducing new costs, appointments, or workflow disruptions to dental practice.

Despite this potential, adoption of PR-based CAC assessment remains limited. Human interpretation is difficult because of anatomical variability, overlapping structures, and the presence of numerous mimics such as triticeous cartilage and stylohyoid ligament ossifications (Aoun & Nasseh, 2018; Wadia, 2021). Inter-reader consistency is variable and can be limited, criteria for defining CAC morphology remain heterogeneous, and few dental clinics have structured pathways for communicating incidental findings to primary-care or cardiology services (Janiszewska-Olszowska et al., 2022; Prados-Privado et al., 2022; Yoon et al., 2014). Artificial intelligence (AI) methods have begun to address some of these issues by automating detection and reducing subjectivity (Litjens et al., 2017; Schwendicke et al., 2020); however, most existing work is limited by small, single-centre datasets, narrow binary classification tasks, and insufficient consideration of CAC morphology, laterality, and clinical workflow integration (Arzani et al., 2025; Ding et al., 2023; Turosz et al., 2023). Moreover, current AI studies rarely integrate imaging findings with behavioral and cardiometabolic risk domains, even though CVD risk is fundamentally multifactorial (Havranek et al., 2015; Levine et al., 2021).

Deep clustering methods offer an emerging alternative to conventional supervised models. These approaches can exploit the essential structure of image data to group patterns associated with distinct morphological or risk-related phenotypes, even when labelled data are scarce (Caron et al., 2018; Xie et al., 2016). When applied to panoramic radiographs, deep clustering may help differentiate clinically meaningful CAC subtypes, capture subtle variations that avoid binary classifiers, and support more significant risk stratification. Integrating such approaches with simple patient-level risk factors may create a scalable mechanism for transforming incidental dental imaging into an actionable early-warning signal for vascular disease. This thesis explores how deep clustering can be leveraged to detect, characterize, and contextualize carotid artery calcifications on panoramic radiographs, with the goal of advancing opportunistic CVD risk prediction, particularly in resource-limited environments such as Palestine.

1.3. Problem Statement

Cardiovascular disease often presents only after substantial vascular injury, and in resource-constrained settings this challenge is increased by delayed diagnosis, fragmented care pathways, and limited access to advanced imaging. Although panoramic radiographs are ubiquitous and low-cost, and CACs detected on these images have been associated with elevated risk of stroke and coronary events, the current diagnostic landscape does not provide a consistent, validated, or workflow-ready method for extracting cardiovascular risk information from these routinely acquired images (Arzani et al., 2025; Schwendicke et al., 2020).

Three interconnected gaps shape the core problem. First, identifying CACs on panoramic radiographs is still challenging in everyday practice. Dentists and radiologists often have to navigate anatomical variations and several structures that can mimic true calcifications, which leads to inconsistent readings. Existing AI models do not fully solve this issue; many are built on small, single-centre datasets, lack solid external validation, and treat CACs as simple yes/no findings, without capturing morphology or laterality, features that appear relevant for estimating cardiovascular risk. Second, when CACs are detected on PRs, they are rarely interpreted alongside behavioral or cardiometabolic factors, even though these factors are central to determining a person's overall cardiovascular risk. As a result, PR-based CAC findings often remain isolated imaging observations rather than meaningful components of a broader risk assessment. Third, there is no standardized pathway for what should happen when a dentist encounters a possible CAC on a panoramic radiograph. Without clear guidance on documentation, communication with patients, or when referrals should be made, the outcome is often inconsistent: some patients may be falsely reassured, while others may be referred unnecessarily. Both situations reduce the preventive value that early detection could offer.

Deep clustering approaches offer a promising way forward. These methods can identify underlying patterns in PR images, support more detailed, morphology/appearance-aware clustering of CAC-related patterns (beyond a simple present/absent output), and reduce reliance on large labelled datasets, an important advantage in contexts such as Palestine, where annotated medical images are scarce. However, the potential of deep clustering for CAC detection has not been systematically examined, nor has it been linked to patient-level risk factors or embedded into a workflow that dentists can realistically adopt.

For these reasons, the central problem addressed in this study is the lack of a reliable, interpretable, and deployable framework that can convert an already-acquired panoramic radiograph into a meaningful early indicator of cardiovascular risk. This gap spans technical needs (accurate, morphology-aware clustering and stratification of CAC-related patterns), clinical needs (risk interpretation informed by both imaging and patient characteristics), and organizational needs (a simple, actionable referral pathway suited to low-resource dental environments). Closing these gaps is essential to determine whether opportunistic CAC

screening using PRs can move from theoretical potential to practical impact as an early-warning tool for vascular disease.

1.4. Research Significance

Cardiovascular disease places a heavy burden on communities that have limited access to preventive screening and timely diagnostic services. This challenge is particularly evident in settings such as Palestine, where financial constraints, shortages in specialized healthcare personnel, and fragmented referral systems make early detection of vascular risk difficult. In this context, it becomes essential to explore practical, affordable approaches that can identify risk earlier and more efficiently. Panoramic radiographs offer a compelling opportunity: they are widely available in dental clinics, routinely taken for oral health needs, and require no additional appointments or cost. If carotid artery calcifications visible on these images can be detected reliably and interpreted within the broader context of an individual's health risks, they could serve as a valuable early-warning tool for cardiovascular disease.

The importance of this thesis stems from addressing the technical and operational barriers that currently prevent PR-based CAC detection from becoming clinically useful. Although previous studies have shown that CACs can predict adverse cardiovascular events, their detection on PRs remains inconsistent. Variability in human interpretation, differences in calcification morphology, and the presence of structures that mimic CACs often lead to uncertainty. Meanwhile, many AI models developed so far rely on small datasets and simplified binary labels that fail to capture the more detailed morphological patterns that may hold clinical relevance. Deep clustering introduces a promising direction by learning more important, morphology-aware features directly from the images, reducing the need for large labelled datasets, an advantage that is particularly meaningful in Palestine, where access to annotated medical imaging is limited and scalable AI solutions must be lightweight and practical.

The study also holds significance because it positions CAC detection within a broader view of cardiovascular risk. Radiographic findings alone offer only part of the picture; behavioral and cardiometabolic factors play an equally crucial role in determining overall risk. By integrating morphology-aware CAC findings with simple and low-cost risk indicators, this research examines whether panoramic radiographs can meaningfully complement existing early-detection strategies. This approach aligns with global trends promoting prevention, early identification, and the use of accessible data sources to reach individuals before symptoms appear.

Our research contributes to an area that has received little attention: the practical integration of CAC detection into routine dental workflows. Without clear guidance on interpretation, documentation, and follow-up, even highly accurate AI models are unlikely to be adopted. By incorporating interpretability, structured reporting, and workflow design from the outset, this thesis advances the discussion from theoretical modelling toward real-world implementation in low-resource settings.

1.5. Research Aim and Objectives

The aim of this thesis is to develop, evaluate, and contextualize an unsupervised deep clustering framework for organizing carotid artery regions on panoramic radiographs into risk-related imaging phenotypes, and to explore how these imaging-derived groupings relate to simple behavioral and cardiometabolic risk profiles in a resource-limited setting.

Objective 1: To design and implement a deep clustering framework capable of identifying, grouping, and characterizing calcification-related CAC patterns in panoramic radiographs, with an emphasis on morphology-aware feature learning.

Objective 2: To compare the performance of deep embedded clustering (DEC) with classical unsupervised clustering methods (K-means, hierarchical clustering, and Gaussian mixture models) using combined hand-crafted and deep features derived from carotid-region panoramic radiograph ROIs.

Objective 3: To examine how image-derived carotid clustering patterns relate to questionnaire-based cardiovascular risk profiles, and to evaluate whether questionnaire-based machine-learning models provide a complementary view of cardiovascular risk that is consistent with the unsupervised image-derived groupings.

1.6. Research Questions

RQ1: How effectively do deep clustering methods detect and differentiate carotid artery calcification (CAC) patterns on panoramic radiographs, including separation from frequent anatomical mimics?

RQ2: To what extent do morphology-aware clustering features, such as density, shape, laterality, and spatial extent, improve the characterization of CAC-related patterns beyond the binary present/absent framing commonly used in prior work?

RQ3: How does the performance of deep clustering-based CAC models compare with traditional unsupervised clustering methods (K-Means, hierarchical, GMM) in terms of detection accuracy, robustness within the study cohort, and what are the implications for future external validation and generalizability?

1.7. Thesis contributions

This thesis offers several key contributions to advancing the use of panoramic radiographs as an opportunistic tool for cardiovascular risk detection. First, it curates a structured carotid-ROI dataset derived from panoramic radiographs and a morphology-aware feature set (density/shape/spatial-extent cues). The dataset is supported by available clinical documentation and study-defined reference criteria, and explicitly acknowledges and documents common anatomical mimics, providing a dependable foundation for reproducible model development and evaluation.

Second, the thesis introduces a deep clustering framework specifically designed for the carotid region on panoramic radiographs. This approach moves beyond the binary present/absent framing commonly used in prior work by capturing latent morphological patterns and enabling a more detailed and clinically relevant characterization of CACs.

The third contribution is a comparative evaluation that positions deep clustering alongside conventional clustering baselines. This analysis examines performance**,** within-cohort robustness, and interpretability, and discusses implications for future external validation and generalizability. These factors are essential when considering deployment in low-resource clinical environments. By highlighting where deep clustering excels and where it may need support from complementary methods, the study offers practical insights into real-world applicability.

The thesis proposes a multi-modal risk integration interpretation model that combines imaging-derived CAC cluster groupings with simple behavioral and cardiometabolic indicators. This integrated approach explores whether panoramic radiographs can realistically function as early-warning signals for cardiovascular risk. The study also

discusses referral and reporting considerations that are aligned with dental workflows, making the proposed system more feasible for implementation in everyday practice.

Chapter Two

2.1. Literature Review

This chapter situates the thesis within the intersecting clinical and methodological literature on cardiovascular disease, panoramic dental imaging, and artificial intelligence. It begins by grounding the work in the epidemiology and biology of atherosclerosis and stroke and ischemic heart disease, clarifying why carotid artery calcifications are meaningful vascular markers and why routine panoramic radiographs can serve as an opportunistic window for risk flagging in dental care. It then broadens to the rapidly expanding landscape of AI in panoramic radiography, showing how modern computer vision systems can standardize detection, localization, segmentation, and quality control on images already acquired in everyday practice.

Building on this technical foundation, the chapter synthesizes the clinical evidence linking calcifications visible on panoramic radiographs to carotid ultrasound indicators and to future cardiovascular and cerebrovascular events, while emphasizing interpretive challenges such as mimics, variable cervical coverage, and the need for confirmatory vascular imaging and clear referral communication. The focus then narrows to AI systems developed specifically for automated carotid calcification detection on dental radiographs, summarizing representative model designs, ROI guided pipelines, evaluation strategies, and recurring limitations in external validation and reporting of morphology.

In parallel with supervised CAC detectors, the chapter also introduces ROI-guided unsupervised representation learning and deep clustering as a complementary strategy for patient-level pattern discovery and risk stratification when reliable lesion annotations are limited. Finally, the chapter consolidates these threads to define the research gap that motivates this thesis, namely the need for a practical, interpretable, and workflow ready pathway that can stratify carotid region patterns from panoramic images and contextualize imaging derived risk groups using the questionnaire domains captured in this study.

2.2. Background

To frame the aims of this study and the pathway to our goals, this section reviews a connected set of themes. First, it outlines the epidemiology and pathophysiology of cardiovascular disease (CVD) and atherosclerosis, emphasizing the clinical significance of carotid artery calcifications (CACs) and the regional burden of CVD. Second, it surveys imaging approaches for carotid disease with a focus on panoramic dental radiography (PR) as an opportunistic tool, covering CAC appearance, common radiographic mimics, and interpretive challenges. Third, it synthesizes evidence linking PR-detected CACs to adverse cardiovascular outcomes, highlighting prognostic implications and current limitations. Fourth, it introduces the role of artificial intelligence (AI) in panoramic imaging, summarizing approaches spanning detection/segmentation pipelines and data-driven representation learning, and highlighting how AI may support more consistent risk flagging and referral-oriented decision support from routine dental images. Finally, this section maps modifiable and contextual risk factors that may shape CAC prevalence, severity, or early appearance (e.g., chronic stress, diet quality, sleep continuity and duration, environmental noise, air pollution, tobacco use, drinking-water source/quality, relevant medications, sedentary behavior, and physical activity), together with health-system context (awareness, preventive attitudes, and access to care). Collectively, this synthesis clarifies why opportunistic CAC findings on panoramic radiographs, interpreted alongside risk profiles, warrant systematic attention and underpin the thesis's subsequent questions and aims.

2.2.1. Epidemiology and pathophysiology of CVD: burden (global and Palestine) and why CACs matter:

Cardiovascular diseases (CVDs) remain the leading global cause of death, with an estimated 19.8 million CVD deaths in 2022, ~85% attributable to heart attack and stroke (World Health Organization, 2025). Consistent with this, Global Burden of Disease analyses rank ischemic heart disease and stroke as the top drivers of mortality and disability, showing the scale of preventable vascular risk and the need for earlier, scalable risk identification beyond specialty cardiology services (Roth et al., 2020). In the occupied Palestinian territory (oPt), official yearbooks and health information reports similarly place CVD at or near the top of

mortality among noncommunicable diseases, showing a substantial regional burden and the value of opportunistic screening pathways (Massad Marwa Qadadha Mervett Isbeih Khalid Abu Saman et al., 2022; *The Palestinian Ministry of Health*, 2022; World Health Organization, 2023).

Pathobiologically, these events arise from atherosclerosis, a chronic inflammatory disease of large and medium arteries that evolves from endothelial dysfunction and lipid retention to fibroatheroma and ultimately arterial calcification (Figure 2.1), with biomechanical consequences relevant to plaque stability and thrombosis (Libby et al., 2019). Calcification spans a spectrum from micro- to macro-deposits within the plaque and is a recognized hallmark of advanced lesion biology on histopathology and imaging (Jebari-Benslaiman et al., 2022).

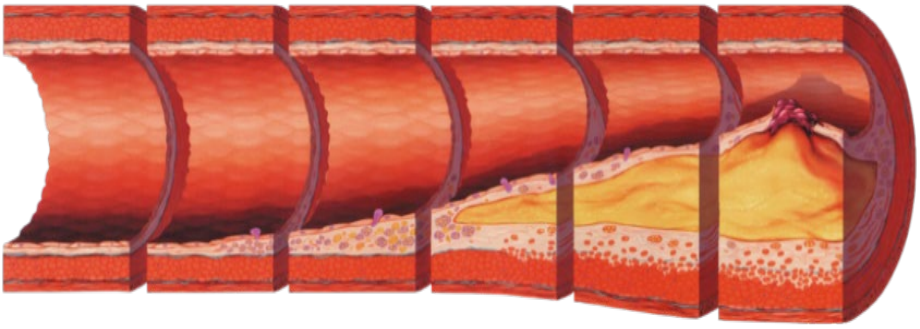

Figure 2.1: Stages in atherosclerosis progression (McGill et al., 2008).

From left to right, the panels illustrate a normal arterial wall, early lipid deposition ("fatty streak"), development of a lipid-rich atherosclerotic plaque, formation of a fibroatheroma with a necrotic core, and an advanced, calcified, rupture-prone plaque with overlying thrombus

Within this trajectory, carotid artery calcifications (CACs) occasionally visible on panoramic dental radiographs (PRs) (figure 2.2) are clinically meaningful markers: seminal dental literature first documented their recognition on PRs, and modern cohort studies show that PR-detected CACs are associated with future stroke and ischemic heart disease (Bengtsson et al., 2019; Friedlander & Lande, 1981). Moreover, morphology matters, bilateral vessel-outlining calcifications carry particularly strong prognostic signals, and recent work links defined CAC shapes on PRs with adverse cardiovascular signs on ultrasound (Bladh et al., 2024; Garoff et al., 2019).

The public-health implication follows: while ultrasound or CT/MR angiography remain excellent diagnostic tools, they are rarely used for asymptomatic populations and can be resource-intensive; by contrast, opportunistic case-finding from routine PRs, images already captured in dental care, can surface high-risk candidates at minimal marginal cost, provided detection is reliable, standardized, and tied to clear referral pathways (Friedlander & Lande, 1981; World Health Organization, 2025).

Figure 2.2: Panoramic dental radiograph with carotid artery calcification (Alsweed et al., 2019)

2.2.2. Imaging approaches for carotid disease, with panoramic radiography (PR) as an opportunistic tool:

Standard vascular imaging for carotid disease includes duplex ultrasound (DUS) for first-line stenosis assessment, and CT angiography (CTA) or MR angiography (MRA) when cross-sectional or pre-operative detail is needed; digital subtraction angiography (DSA) remains the invasive reference but is reserved for select indications (Adla & Adlova, 2015; Anderson et al., 2000; National Imaging Associates, 2025). In contrast, panoramic dental radiographs, acquired routinely for oral care, incidentally image the C3–C4 region near the carotid bifurcation, allowing opportunistic detection of carotid artery calcifications (CACs) at essentially zero marginal cost (Bengtsson et al., 2019). Classical and contemporary dental studies describe CACs on PRs as radiopaque nodules, vertical linear streaks, or vessel-outlining silhouettes inferior-posterior to the mandibular angle (Friedlander & Lande, 1981).

Interpretation on PRs is nontrivial because several soft-tissue calcifications can mimic CAC, notably calcified triticeous cartilage and stylohyoid/thyroid cartilage ossifications, as well as calcified lymph nodes, tonsilloliths, sialoliths, and phleboliths. Careful attention to location and shape helps: triticeous cartilage is typically small, ovoid, and more medial than atheroma; lymph-node calcifications are irregular/lobulated; tonsilloliths cluster superior and medial to the ramus (Aoun & Nasseh, 2018; CEE Noffke et al., 2015). Inter-observer variability further complicates screening on PRs, reinforcing the need for standardized descriptors and, where feasible, confirmatory vascular imaging for positive cases (Yoon et al., 2014).

Head-to-head dental imaging comparisons suggest PRs are high-specificity, lower-sensitivity for CAC relative to CBCT, fitting a triage role rather than a definitive vascular study; nonetheless, multiple clinical series and reviews report that CACs detected on PRs frequently correspond to atherosclerotic disease on ultrasound and are associated with cardiovascular risk (Alves et al., 2014; Möst et al., 2023). Recent morphology-aware work adds that vessel-outlining, particularly bilateral patterns, on PRs align with more severe ultrasound findings of cardiovascular disease, supporting the development of reporting templates that capture both presence and shape of CAC (Bladh et al., 2024; Karlsson et al., 2025).

2.2.3. Evidence linking PR-detected CACs to future stroke and ischemic heart disease: prognostic signal and limitations:

A growing body of evidence, spanning cross-sectional, cohort, and systematic reviews, supports the association between carotid artery calcifications (CACs) visible on panoramic radiographs (PRs) and cardiovascular disease. Cross-sectional analyses show clinically meaningful correlations: in women over 50, PR-detected CACs were significantly associated with hypertension and prior myocardial infarction (MI) (Moshfeghi et al., 2014). More recently, in a large retrospective study, Brar et al. found that CAC-positive patients had substantially higher adjusted odds of both cerebrovascular accident (CVA) and coronary artery disease (CAD) compared with age- and sex-matched controls (cases = 314; controls = 276) (Brar et al., 2024). Earlier, Almog et al. synthesized practice-based evidence and argued that CACs seen near the carotid bifurcation on PRs can flag patients at increased stroke risk and warrant medical referral, helping convert an incidental dental finding into preventive cardiovascular action (Almog et al., 2004). Longitudinal studies strengthen the prognostic signal. In the Malmö Diet and Cancer cohort, baseline CACs on PRs predicted incident stroke and ischemic heart disease over roughly a decade of follow-up (~10–13 years), even after adjustment for conventional risk factors (Bengtsson et al., 2019). Garoff et al. 2019 showed that bilateral vessel-outlining (BVO) calcifications, described as plaque-tracing opacities, identify individuals at particularly high risk of major vascular events, with higher annual event rates than other CAC patterns or controls (Garoff et al., 2019). More

recent replication in an independent sample (n = 212) found that BVO morphology on PR remained an independent predictor of major adverse cardiovascular events (MACEs), with multivariable hazard ratios ≈2.4, and that this radiographic phenotype outperformed carotid ultrasound plaque area as a risk marker over ~7 years of follow-up (Garoff et al., 2025). Morphologic refinement also improves risk discrimination: in a population sample (n = 414), defined CAC shapes on PRs correlated with carotid ultrasound markers of disease severity, with vessel-outlining patterns showing the strongest associations, refining how PR features map to pathophysiology (Bladh et al., 2024). Systematic reviews converge on the same conclusion while noting heterogeneity and a need for standardized criteria and prospective designs: a 2021 review concluded that patients with CACs on PRs are more likely to experience stroke/TIA/MI and revascularization (with bilateral vessel-outlining highlighted as an independent marker), though effect sizes vary across studies and designs (Lim et al., 2021); a 2022 review agreed PR can detect calcified carotid atheroma but emphasized the need for standardized diagnostic criteria and prospective multicenter trials before routine risk-stratification is adopted (Prados-Privado et al., 2022). Together, these data support PR-detected CACs, especially specific morphologies, as a pragmatic, opportunistic signal of systemic atherosclerotic risk, while also clarifying present limitations in standardization, referral pathways, and external validation. Table 2.1 shows some key studies that linking CACs on panoramic radiographs to cardiovascular outcomes.

2.2.4. Artificial intelligence in panoramic imaging: methods, performance, and clinical integration:

Artificial intelligence (AI) has rapidly become a mainstay of medical image analysis, with convolutional neural networks (CNNs) and related architectures delivering robust performance in classification, detection, and segmentation tasks and offering a path to more standardized, objective reporting (Chan et al., 2020; Litjens et al., 2017; Schwendicke et al., 2020). In panoramic radiography (PR), early proof-of-concept work showed that deep detectors can localize atherosclerotic carotid plaques even from small datasets, for example, a Faster R-CNN model trained on 65 PRs achieved sensitivity ~75% and specificity ~80%, demonstrating feasibility despite limited data (Kats et al., 2019). Subsequent CNN studies trained on larger cohorts reported clinically meaningful accuracy for carotid artery calcification (CAC) screening: a transfer-learning pipeline evaluated on 500 patients reached recall 0.87 and specificity 0.97 at the patient level, directly supporting referral workflows (Amitay et al., 2023). Reader-study designs also suggest AI can lift general dentists' diagnostic accuracy for soft-tissue calcifications on PRs, including CAC, narrowing expertise gaps in routine care (Song et al., 2022). Model classes have diversified beyond CNNs. Vision transformer hybrids (e.g., Faster R-CNN + Swin Transformer) trained on curated PR sets reported strong detection performance for CAC (AUC ≈ 0.95; F1 ≈ 0.89), and outperformed purely convolutional baselines (Vinayahalingam et al., 2024). Cascaded networks now integrate image-level triage with lesion-level segmentation: CACSNet

couples a classifier and a segmenter to handle morphologic variability and anatomic overlap, achieving AUC 0.996, accuracy 0.985, sensitivity 0.980, and

specificity 0.988 for image-level classification, while producing lesion masks (Dice ≈ 0.72) that can anchor standardized reports and morphology-aware flags (S. W. Yoo et al., 2024). At the evidence-synthesis level, a 2025 systematic review and meta-analysis pooling PR/CBCT AI studies estimated pooled sensitivity 0.92 and specificity 0.96 for CAC detection, indicating that AI systems can function as effective screening/risk-flagging tools when embedded in dental imaging pipelines (Arzani et al., 2025).

Clinically, these systems can do more than classify: they standardize nomenclature and measurements, reduce inter-observer variability, and surface explainable cues (e.g., heatmaps, lesion contours) that dovetail with morphology-linked risk, thereby supporting structured PR reports (presence, laterality, shape), automatic referral prompts to vascular imaging, and scalable opportunistic risk stratification from images already acquired in routine dental care (Schwendicke et al., 2020). When paired with established prognostic evidence for PR-detected CACs, especially high-risk morphologies, AI becomes a practical bridge between dentistry and preventive cardiology, turning incidental findings into timely, standardized cardiovascular follow-up (Vinayahalingam et al., 2024; S. W. Yoo et al., 2024).

2.2.5. Modifiable risk factors that may influence carotid artery calcifications (CACs):

CACs on panoramic radiographs are a radiographic expression of atherosclerosis, that is, calcified atherosclerotic plaque within the carotid wall, and thus reflect the same inflammatory and mineralization biology that hardens arteries (Borba et al., 2016; Brar et al., 2024; Friedlander & Lande, 1981). Factors that accelerate atherogenesis (e.g., chronic vascular inflammation), disturb calcium-phosphate balance, or impair vascular repair can plausibly increase the prevalence, severity, or earlier appearance of CACs via mechanisms such as vascular smooth-muscle osteogenic transformation and microcalcification within plaques (Demer & Tintut, 2014; S. J. Lee et al., 2020; Libby et al., 2019). This section briefly maps the key modifiable domains measured in the questionnaire, so the imaging-derived clustering risk groups can be interpreted in a risk-aware, patient-centered manner.

2.2.5.1. Psychosocial stress (and depressive symptoms):

Chronic psychosocial stress and depression activate the hypothalamic-pituitary-adrenal (HPA) axis and sympathetic nervous system, elevating cortisol and catecholamines,

provoking endothelial dysfunction, low-grade inflammation, and blood-pressure dysregulation, which are the canonical atherogenic pathways that plausibly accelerate plaque maturation and mineralization (Durham et al., 2018; Levine et al., 2021; Marwaha, 2022; Waclawovsky et al., 2021). Recent American Heart Association (AHA) statements and contemporary reviews synthesize this epidemiology and biology, including notable vulnerability among women in midlife and younger age groups (Ebong et al., 2024; Levine et al., 2021; Osborne et al., 2020; Sara et al., 2022).

Mechanistically, repeated stress reactivity, characterized by increased cortisol and catecholamine levels, impairs nitric-oxide-mediated vasodilation and increases oxidative and inflammatory signaling; mental-stress-induced endothelial dysfunction predicts future cardiovascular events in cohort data. In parallel, depression is linked to heightened platelet reactivity (a prothrombotic, "thrombo-inflammatory" milieu). Downstream, inflammatory and oxidative cues drive vascular smooth-muscle cells toward an osteogenic phenotype via BMP-2/SMAD and RUNX2 programs, the same calcifying biology that carotid calcifications on imaging reflect (Dhar & Barton, 2016; Lima et al., 2019).

Evidence spans structure, function, and hard imaging endpoints. Depressive symptoms independently predict progression of coronary artery calcium (CAC) in midlife women (SWAN), dovetailing with the sex-specific narrative above. A 2024 meta-analysis shows higher carotid intima–media thickness (cIMT) in people with depression, supporting a broader stress–atherosclerosis link. Biomarker work adds biological plausibility: chronic stress indexed by hair cortisol relates to adverse cardiometabolic profiles and prior CVD (Faresjö et al., 2024; Janssen et al., 2011; Saleh et al., 2024).

2.2.5.6. Sleep duration, continuity, and regularity:

Objective cohorts with device-measured sleep show that short or fragmented sleep and irregular sleep timing associate with greater subclinical atherosclerosis across multiple vascular territories (3D carotid/femoral ultrasound and CT), and that sleep irregularity prospectively predicts incident cardiovascular events, independent of average sleep hours (Domínguez et al., 2019; Full et al., 2023; Huang et al., 2020). In parallel, prospective imaging data link shorter sleep to incident coronary artery calcium (CAC) (a calcific phenotype of atherosclerosis) strengthening biological plausibility for sleep-atherosclerosis pathways (King et al., 2008). Mechanistically, fragmentation appears to increase inflammatory leukocytes that track with higher CAC burden, mapping a credible route from choppy sleep to calcific plaque (Vallat et al., 2020).

2.2.5.6. Dietary pattern and food processing:

Prospective cohorts consistently link higher ultra-processed food (UPF) intake “defined by the NOVA system” to increased risk of total, coronary, and cerebrovascular disease. A large BMJ cohort (NutriNet-Santé) found dose-response associations of UPFs with incident CVD, and an updated BMJ umbrella review synthesized dozens of meta-analyses showing cardiometabolic harms across outcomes (Lane et al., 2024; Srour et al., 2019).

Biologically, UPF-heavy patterns co-occur with low-grade inflammation: multiple human datasets report higher high-sensitivity C-reactive protein (hs-CRP) with greater UPF consumption, partially independent of adiposity (Lane et al., 2022; Lopes et al., 2019). By contrast, Mediterranean-style diets: rich in vegetables, fruits, legumes, whole grains, nuts, and extra-virgin olive oil, track with less carotid atherosclerosis and better vascular physiology. In the randomized PREDIMED substudy, Mediterranean diets slowed carotid IMT progression and plaque, while independent RCTs and meta-analyses show improved endothelial function and lower major cardiovascular events versus control diets (Davis et al., 2017; Estruch et al., 2013; Sala-Vila et al., 2014).

Observational syntheses likewise conclude that Mediterranean-style patterns are associated with lower cIMT and subclinical atherosclerosis measures, reinforcing plausibility for imaging endpoints (Petersen et al., 2014).

2.2.5.4. Environmental noise:

Environmental noise, defined as persistent or recurrent unwanted sound in one’s surroundings, is increasingly recognized as a cardiovascular stressor that contributes to hypertension, ischemic heart disease, and stroke in population studies and guideline syntheses (Blanes et al., 2017; Münzel et al., 2014). Recurrent unwanted sound activates the sympathetic nervous system and the hypothalamic-pituitary-adrenal axis, elevating blood pressure and triggering vascular oxidative stress and inflammation (Münzel & Sørensen, 2017).

Night-time exposure is especially consequential because it fragments sleep and blunts normal nocturnal blood-pressure “dipping,” a pathway emphasized in health-based recommendations (van Kempen et al., 2018). Human field experiments with realistic nighttime aircraft noise show that even a single night can impair endothelial function (reduced flow-mediated dilation) and raise stress hormones (F. Schmidt et al., 2014; F. P. Schmidt et al., 2013). In translational models, transportation-noise exposure induces NOX2-dependent oxidative stress, endothelial dysfunction, and eNOS uncoupling; genetic or

pharmacologic suppression of NOX2 attenuates these injuries (Kröller-Schön et al., 2018; Münzel & Sørensen, 2017). Oxidative stress, in turn, promotes osteogenic reprogramming of vascular smooth-muscle cells via RUNX2/BMP-2 signaling and matrix-vesicle pathways, providing a biologically coherent route from noise-triggered vascular stress to calcification (Chang et al., 2008; Liberman et al., 2011). At the population level, European surveillance attributes tens of thousands of ischemic heart-disease cases and thousands of premature deaths annually to chronic environmental noise, showing its public-health relevance (Clark & Paunovic, 2018; Y. Liu et al., 2022). Accordingly, environmental noise is a plausible upstream amplifier of calcific plaque burden, including carotid calcifications that can be visualized on panoramic radiographs, with certain morphologies carrying higher vascular risk (Brar et al., 2024; Garoff et al., 2019).

2.2.5.5. Air pollution:

Long-term exposure to fine particulate matter with an aerodynamic diameter ≤2.5 μm (PM2.5) and to coarser fractions is associated with greater carotid intima–media thickness (CIMT) and more carotid plaque, indexing higher subclinical atherosclerosis burden in pooled observational data (X. Liu et al., 2015; Provost et al., 2015). Prospective imaging from MESA shows that higher residential PM2.5 levels track with faster CIMT progression, and reductions in PM2.5 relate to slower progression, supporting a causal link (Adar et al., 2013). In the same research program, long-term ambient air pollution exposure was associated with progression of coronary artery calcium (CAC), the calcific expression of atherosclerosis, aligning biologically with what panoramic radiographs may capture at the carotid bifurcation (Kaufman et al., 2016). Mechanistically, AHA scientific statements summarize how PM2.5 promotes oxidative stress, endothelial dysfunction, autonomic imbalance, and inflammation, pathways that accelerate atherogenesis and plaque calcification (Brook et al., 2010; Kaufman et al., 2020). WHO's 2021 Air Quality Guidelines show that the cardiovascular harms at lower concentrations than previously thought, reinforcing the relevance of particulate exposure even in "low-pollution" settings (Organización Mundial de la Salud (OMS), 2021).

2.2.5.6. Tobacco use:

Cigarette smoking causes endothelial injury by reducing nitric-oxide bioavailability through oxidative stress and inflammatory signaling, while simultaneously increasing adhesion molecules, platelet activation, and lipid oxidation core processes that accelerate atherogenesis (Förstermann et al., 2017; Klein et al., 2023; Messner & Bernhard, 2014). These smoke-driven pathways link biologically to vascular calcification because oxidative stress and inflammatory cues promote an osteogenic switch in vascular smooth-muscle cells

via RUNX2/BMP-2 signaling and matrix-vesicle pathways (Chang et al., 2008; Leopold, 2014).

Endothelial dysfunction from smoking is reversible to a degree, with cessation improving flow-mediated dilation in clinical studies and reviews of vascular function (Higashi, 2023). Longitudinal imaging demonstrates that continued smoking is associated with greater carotid plaque progression, whereas smoking cessation is associated with less plaque progression even when changes in common-carotid IMT are modest (Stein et al., 2020). Earlier prospective work similarly showed higher 3-year cIMT progression in active smokers, supporting a dose-time relationship between exposure and arterial wall thickening (Howard et al., 1998).

Dose-response evidence indicates that pack-years relate to thicker carotid walls and higher cIMT across cohorts, reinforcing cumulative toxicity (Baldassarre et al., 2009; Saito et al., 2024). Contemporary observational studies continue to detect thicker cIMT and altered carotid ultrasound parameters among smokers versus non-smokers, consistent with persistent structural effects on the arterial wall (Alsiddig & Ali, 2024). Secondhand smoke also carries vascular consequences: population and experimental evidence links SHS to endothelial dysfunction, inflammatory activation, and thicker carotid intima-media, extending risk beyond active smokers (Barnoya & Glantz, 2005; Jefferis et al., 2010; Shu et al., 2022). Taken together, mechanistic and longitudinal imaging data converge to show that tobacco exposure, active and passive, drives endothelial injury, oxidative/inflammatory remodeling, and progression of carotid atherosclerosis, providing a coherent biological bridge to calcific plaque phenotypes captured by vascular imaging.

2.2.5.7. Drinking-water source/quality (tap vs bottled/mineral) as an exposure proxy:

Using primary drinking-water source as a coarse exposure proxy is defensible because contaminant and mineral profiles vary systematically across supplies and delivery systems, tap water quality can be altered by plumbing corrosion and service lines, while bottled/mineral waters differ by source geology and processing, so source choice plausibly tracks long-term metal intake (World Health Organization, 2017). Contemporary analyses of bottled/mineral waters show detectable, and sometimes elevated, trace metals including lead, cadmium, and arsenic, showing between-brand variability that a simple “tap vs bottled/mineral” distinction can partially capture (Hadiani et al., 2015; Krachler & Shotyk, 2008).

Among toxic metals, lead exposure has been linked to subclinical atherosclerosis: in a large Swedish cohort, higher blood lead associated with the prevalence of carotid atherosclerotic plaque, with supportive signals in newer population studies at low exposure levels (Guldbrand et al., 2024; Harari et al., 2019). Cadmium shows robust associations with carotid disease across designs, higher blood/urine cadmium tracks with carotid plaque presence, multi-territory plaque burden, and future plaque growth, including mechanistic ties to plaque inflammation (Bergström et al., 2015; Fagerberg et al., 2012). Arsenic exposure from drinking water relates to greater carotid intima–media thickness and higher plaque scores in prospective community data from the Strong Heart Study, aligning exposure gradients with subclinical vascular injury (Mateen et al., 2017). Recent reviews synthesize these metal-atherosclerosis links across carotid and other vascular beds, reinforcing biological plausibility and the cardiovascular relevance of low-to-moderate exposures (Grau-Perez et al., 2022). Accordingly, where biospecimens or local water testing are unavailable, coding water source/quality (tap vs bottled/mineral) provides a pragmatic proxy exposure for toxic metals and other contaminants, with transparent acknowledgment of potential misclassification from brand- and system-level variability (World Health Organization, 2017).

2.2.5.7. Medication exposures that influence vascular mineralization (Vitamin-K axis):

Matrix Gla protein (MGP) is a vitamin-K–dependent inhibitor of soft-tissue mineralization, and genetic loss of Mgp in mice causes fulminant arterial calcification establishing the pathway's causal relevance (Luo et al., 1997; Schurgers et al., 2013). When MGP is under-carboxylated (dp-ucMGP), reflecting poor vitamin-K status or antagonism of the vitamin-K cycle, vascular beds show greater calcification and higher cardiometabolic risk in observational and translational studies (Barrett et al., 2018; Jespersen et al., 2020). Vitamin-K antagonists (VKAs) such as warfarin block γ-carboxylation of MGP, and across animal models and human cohorts VKA exposure associates with increased vascular and valvular calcification, including longitudinal evidence of faster coronary artery calcium (CAC) progression (Andrews et al., 2018; Kosciuszek et al., 2022; Palaniswamy et al., 2011). Complementarily, dp-ucMGP levels rise with vascular calcification burden and adverse outcomes in several patient groups, supporting its use as a circulating readout of the vitamin-K/MGP axis (Jespersen et al., 2020; Liabeuf et al., 2014). On the interventional side, randomized trials show that vitamin-K supplementation lowers dp-ucMGP and, in some settings, slows CAC progression, for example, phylloquinone (vitamin K_1) attenuated CAC advancement in older adults with pre-existing calcification, and meta-analytic pooling reports modest slowing of CAC alongside robust dp-ucMGP reduction (Li et al., 2023; Shea et al., 2009). Not all trials are uniformly positive, with heterogeneity across populations and outcomes, but the weight of evidence from reviews and RCT syntheses places the vitamin-K/MGP axis as a pharmacologically modifiable contributor to vascular mineralization biology (Vlasschaert et al., 2020).

2.2.5.9. Health literacy, awareness, and access to care:

Health literacy is foundational to cardiovascular prevention and outcomes, as emphasized by the American Heart Association's scientific statement on integrating health literacy across primary and secondary prevention (Magnani et al., 2018). Low health literacy is associated with worse clinical trajectories, including higher mortality and hospital readmission, among patients with cardiovascular conditions, showing its direct relevance to risk-factor control and self-management (Kanejima et al., 2022). Irregular care patterns and reliance on emergency departments, rather than routine primary care, consistently correlate with lower awareness, treatment, and control of major cardiovascular risk factors such as hypertension (Egan et al., 2014; Nguyen et al., 2011). Not having any healthcare visit in the prior year is among the strongest predictors of uncontrolled blood pressure in population analyses, highlighting the role of stable access points for chronic disease management (Akinyelure et al., 2021). Frameworks that track the "hypertension control cascade" show sizable drop-offs at awareness and treatment stages even among people with a usual source of care, indicating that communication quality and system continuity are integral to closing prevention gaps (Wozniak et al., 2015). Together, this section positions health literacy and reliable access to longitudinal, non-emergent care as structural determinants of cardiovascular risk control, providing a clear rationale to account for these domains when interpreting vascular imaging phenotypes and downstream outcomes (Havranek et al., 2015).

2.2.5.10. Core cardiometabolic confounders (must adjust for):

Age, hypertension, diabetes, dyslipidemia, adiposity, and chronic kidney disease are dominant determinants of carotid atherosclerosis, with meta-analyses and imaging cohorts showing consistent associations with greater carotid intima-media thickness (cIMT) and higher plaque burden (Ji et al., 2019; Ren et al., 2015). Age and blood pressure in particular display the strongest population-level relationships to cIMT, showing their central confounding potential in vascular imaging studies (AlGhibiwi et al., 2023; Ren et al., 2015). Hypertension relates to both thicker cIMT and more plaques, including in analyses that capture pulsatile load (e.g., pulse pressure) among older adults with uncontrolled blood pressure (Ji et al., 2019; Yu et al., 2024). Diabetes mellitus is linked to increased cIMT and more severe carotid disease across reviews and meta-analytic summaries (Katsiki & Mikhailidis, 2020; Theofilis et al., 2022). Atherogenic lipids track with carotid plaque presence and incidence, with higher LDL-centric measures (e.g., LDL-C/HDL-C ratio, small dense LDL) predicting plaque development and vulnerability (Ma et al., 2024; Wu et al., 2022). Adiposity (particularly higher BMI) associates with thicker cIMT in observational datasets and reviews, aligning cumulative metabolic load with structural arterial change (Bažadona et al., 2023; Ren et al., 2015). Chronic kidney disease is linked to more advanced

and calcified atherosclerotic plaque phenotypes in the carotid and coronary beds, reinforcing its role as a high-impact confounder (Beddhu et al., 2021; Valdivielso et al., 2019). Consequently, any model relating carotid calcifications on panoramic radiographs to biomarkers or outcomes should adjust “at minimum” for these cardiometabolic drivers to reduce bias from confounding by underlying atherosclerotic burden (Naqvi & Lee, 2014).

2.2.5.11. Sedentary behavior (daily sitting time):

Sedentary behavior is not merely the absence of exercise; it carries an independent cardiometabolic signature linked to adverse outcomes (Biswas et al., 2015; Wilmot et al., 2012). Large meta-analyses show that greater daily sitting time is associated with higher risks of cardiovascular disease, type 2 diabetes, 21ospitalization, and all-cause mortality, even after adjusting for leisure-time physical activity (Biswas et al., 2015). Device-based consortia using accelerometers further indicate that accumulating about 30–40 minutes/day of moderate-to-vigorous physical activity substantially attenuates, but does not fully erase, the elevated mortality risk associated with high sedentary time, showing sitting time as a distinct exposure (Ekelund et al., 2019, 2020). Patterns matter as well: accruing sedentary time in long, uninterrupted bouts is independently associated with higher mortality, beyond total sedentary volume (Diaz et al., 2017). Together, these findings support measuring daily sitting time (and, where possible, sitting patterns) alongside physical activity in cardiometabolic studies and risk models.

2.2.5.12. Physical activity and exercise modalities (aerobic, resistance, balance):

Global guidelines converge that any activity is better than none, with adults advised to accumulate 150–300 min/week of moderate-intensity aerobic activity or 75–150 min/week of vigorous activity, plus muscle-strengthening on ≥2 days/week; older adults are additionally advised to include multicomponent work with balance (Bull et al., 2020; Piercy et al., 2018). Beyond these general benefits, activity relates specifically to carotid vascular health: an 8-year prospective cohort found that higher habitual physical activity predicted slower increase in carotid intima-media thickness (cIMT), consistent with a preventive effect on atherosclerosis (Pae et al., 2023). Interventional evidence aligns with this: exercise training reduces cIMT on average across adult samples in systematic reviews and meta-analyses, with signals that aerobic modalities tend to produce larger cIMT reductions than other modes (while resistance training also improves vascular indices, but typically to a lesser magnitude) (Wang et al., 2022). Complementary trials show that combined aerobic-resistance programs over ~24 weeks can decrease cIMT and improve hemodynamic markers, reinforcing modality-inclusive prescriptions (Park et al., 2017). Taken together, convergent guidelines and imaging-based evidence support treating aerobic activity as the primary

driver for cIMT regression with added value from resistance and balance work to meet functional and age-specific goals

Overall, this expanded profile of modifiable and contextual factors (e.g., stress and depressive symptoms, sleep health, diet quality, environmental noise and air pollution, tobacco exposure, drinking-water source, selected medication-related exposures, health literacy and access to care, sedentary time, and physical activity) provides the context needed to interpret calcification-related imaging patterns as more than isolated radiographic findings. In this thesis, these questionnaire domains are used to contextualize and triangulate the imaging-derived clustering risk groups by (i) describing and comparing participant profiles across derived risk strata, (ii) examining whether higher self-reported cardiometabolic and behavioral risk tends to align with the inferred high-risk imaging cluster, and (iii) evaluating the discriminative ability of questionnaire features to predict the derived risk classification using a Random Forest model. This multimodal framing supports risk-aware, referral-oriented interpretation of opportunistic panoramic radiograph findings rather than treating PR-visible calcifications as a standalone diagnosis.

2.3. Artificial Intelligence in Panoramic Dental Radiography

Artificial intelligence (AI) has become an integral part of medical imaging and is rapidly reshaping dental radiography, including panoramic radiographs (PRs) (Ding et al., 2023; Katsumata, 2023). Deep learning models, particularly convolutional neural networks (CNNs) and vision transformers, have shown the ability to automate complex image-interpretation tasks that once required extensive human expertise (Gao et al., 2024; Litjens et al., 2017). Within panoramic imaging, AI applications have expanded from early proof-of-concept models to clinically oriented systems capable of performing detection, localization, segmentation, classification, and even predictive analysis (Ding et al., 2023; Vashisht et al., 2024). Panoramic radiography provides a rich and structured visual field that captures teeth, jaws, and parts of the craniofacial anatomy in a single image, making it an ideal target for scalable AI development (Ameli et al., 2025; Turosz et al., 2023). Over the past few years, numerous studies have demonstrated the capability of AI to identify and classify dental structures and pathologies with near-expert accuracy, confirming that panoramic images contain sufficient diagnostic signal for high-performing computer vision systems (Bonfanti-Gris et al., 2022; Leite et al., 2021; Vashisht et al., 2024).

Table 2.1: Key studies linking CACs on panoramic radiographs to cardiovascular outcomes.

Author, Year	Sample size	Study type	Key findings
Moshfeghi et al., 2014	n=200 (women >50)	Cross-sectional (Iran J Radiol)	PR-detected CACs significantly associated with hypertension and prior myocardial infarction in women over 50.
Brar et al., 2024	n=314 CAC-positive + 276 matched controls	Retrospective cross-sectional (Dentistry Journal)	CAC associated with higher odds of CVA (aOR≈2.2) and CAD (aOR≈2.1) after adjustment; many CAC-positive patients were not medically referred, showing implementation gaps.
Wallin Bengtsson et al., 2019	635 cohort participants n=635 without prior events (baseline PRs) (~10-13 yr follow-up)	Prospective cohort (Clin Oral Investig)	PR-detected CAC predicted future stroke and/or IHD after risk-factor adjustment; shorter event-free survival in CAC-positive individuals.
Garoff et al. (2019)	117 CAC patients; 121 controls	Prospective cohort with morphology	Bilateral vessel-outlining CACs had higher annual vascular event risk (7.0%) vs other CAC shapes (4.4%) and controls (2.6%); BVO an independent risk marker.
Garoff et al., 2024/2025	n=212 with CAC (mean follow-up 7 yr)	Prospective cohort (Dentomaxillofac Radiol)	BVO remained a strong predictor of MACE (HR≈2.4–2.5) even when accounting for carotid plaque area on ultrasound; links PR morphology to hard outcomes.
Bladh et al., 2024	n=414 participants (802 neck sides)	Cross-sectional with US correlation (OSOMOPOR)	Defined CAC shapes on PR correlated with ultrasound signs of CVD; vessel-outlining shape showed largest plaque area and greatest lumen reduction.
Lim et al., 2021	Systematic review of 5 studies	Systematic review (Clin Oral Investig)	Patients with CACs on PRs more likely to experience stroke/TIA/MI and revascularisation; BVO CACs highlighted as independent risk marker; heterogeneity noted.
Prados-Privado et al., 2022	23 studies (systematic review)	Systematic review (Diagnostics)	Concluded PR can aid in detecting calcified carotid atheroma; emphasized heterogeneity, potential biases, and the need for prospective multicenter standards.

AI systems trained on PRs can detect, number, and segment teeth, identify common restorations and prosthetics, and distinguish between permanent and deciduous dentition(Başaran et al., 2022; Beser et al., 2024; Leite et al., 2021). Deep-learning detectors such as YOLO, Mask R-CNN, and U-Net architectures have achieved excellent sensitivity, precision, and F1-scores in multi-tooth detection, tooth numbering, and segmentation of restorations and implants (Bonfanti-Gris et al., 2025; Tuzoff et al., 2019). These automated pipelines significantly reduce manual charting time, improve record completeness, and

enhance diagnostic reproducibility, particularly in routine dental practice (Başaran et al., 2022; Ding et al., 2023). In addition, panoramic AI has been successfully applied to identify anomalies and pathologies such as alveolar bone loss, vertical root fractures, mesiodens, ectopic eruption, and idiopathic osteosclerosis, achieving strong performance in most studies (Fukuda et al., 2020; Ha et al., 2021; KURT et al., 2020; Tassoker et al., 2024). Anatomical mapping tasks, such as mandibular canal segmentation or classification of root morphology, have also benefited from AI, supporting safer surgical and endodontic planning by improving anatomical localization and standardizing reporting (Aung et al., 2024; Hiraiwa et al., 2019).

Beyond diagnosis, panoramic radiographs have also been used in AI-driven predictive and planning applications, including estimation of dental age, prediction of third molar eruption potential, and opportunistic osteoporosis screening, highlighting how PRs can capture latent health information beyond oral disease alone (Aljameel et al., 2023; Tarighatnia et al., 2025; Vranckx et al., 2020). Recent developments have also addressed practical and methodological aspects such as automated image-quality control and standardization across devices, ensuring reliable AI performance in clinical workflows (Ameli et al., 2025). Studies have demonstrated that deep-learning systems can grade PR image quality, detect artifacts, and assess patient positioning accuracy, supporting consistency and minimizing repeat exposures (Ameli et al., 2025; Kim, 2024). Meanwhile, newer model architectures such as vision transformers have introduced global context modeling and improved generalization, although the field remains in the early stages of exploring hybrid CNN-transformer frameworks for dental imaging (Gao et al., 2024).

Systematic reviews consistently highlight the need for multicenter datasets, transparent reporting, external validation, and standardized reference benchmarks to address challenges such as domain shift and dataset bias, which remain key obstacles to real-world clinical deployment (Ding et al., 2023; Katsumata, 2023; Vashisht et al., 2024). Collectively, this broad literature confirms that AI applied to panoramic radiography is not only technically feasible but also clinically promising, capable of supporting automated diagnosis, charting, screening, and even opportunistic health assessments from images already captured in routine dental care.

Within this context, panoramic imaging offers a valuable foundation for exploring vascular findings such as CACs. The proven ability of AI systems to detect and classify diverse radiographic features, standardize terminology, and enhance diagnostic reproducibility establishes the methodological and technical groundwork for CAC-focused pipelines. These systems can be adapted to localize the carotid region, characterize calcification patterns, and integrate imaging cues with patient-level information to support cardiovascular risk assessment.

2.4. Panoramic Dental Radiographs and Cardiovascular Disease: Revealing the Link

Panoramic dental radiographs (PRs) can display radiopaque foci in the soft-tissue region of the neck that correspond to carotid artery calcifications (CACs), which are surrogates of atherosclerotic plaque and potential markers of elevated cardiovascular risk (Janiszewska-Olszowska et al., 2022; Wadia, 2021). Across routine dental populations, CACs are not rare; cohort studies report measurable prevalence on PRs and consistent associations with traditional cardiovascular risk factors such as age, hypertension, diabetes, and dyslipidemia (Möst et al., 2023). Beyond epidemiology, PR-detected CACs have been linked with carotid ultrasound findings of higher intima-media thickness and plaque burden, supporting a pathophysiologic bridge between what dentists see on PRs and vascular disease in the carotids (Karlsson et al., 2025; J. S. Lee et al., 2014). Emerging longitudinal data suggest that specific PR phenotypes (e.g., bilateral vessel-outlining calcifications) may predict future vascular events, reinforcing the clinical relevance of CACs observed on dental imaging (Garoff et al., 2025). Opportunistic signals on dental imaging also correlate with extra-carotid atherosclerosis; for example, CAC on PR has been associated with coronary artery calcium on chest CT, hinting at a broader systemic risk profile (Carasso et al., 2020).

From a practical standpoint, PR-identified calcifications frequently uncover previously unrecognized atherosclerosis, highlighting the value of dental settings as entry points for risk detection and counseling (Mai et al., 2024).These strengths come with caveats: PR is a 2D projection with superimposition, and its sensitivity for carotid disease is limited compared with duplex ultrasound, so PR findings should be treated as risk markers rather than definitive diagnoses (Alves et al., 2014; Madden et al., 2007). Accordingly, reviews and professional commentaries encourage dental clinicians to recognize CACs on PRs and to refer patients for medical evaluation, usually with carotid ultrasound within clear communication pathways (Kadyan et al., 2024; Wadia, 2021).

Convergent evidence from prevalence cohorts, ultrasound-correlation studies, and longitudinal analyses demonstrates a clinically meaningful link between PR-visible carotid calcifications and cardiovascular disease, positioning PR as an opportunistic risk marker that should prompt cardiovascular assessment and confirmatory vascular imaging when present.

2.4.1. Early signals and conceptual groundwork:

Friedlander and Lande (1981) investigated whether routine panoramic radiographs could incidentally reveal calcified atherosclerotic plaques at the carotid bifurcation and thus flag patients who might merit vascular evaluation. In a cross-sectional review of 1,000 radiographs taken for dental indications in adults aged 50–75 years, they scrutinized the soft-

tissue region posterior–inferior to the mandibular angle for nodular radiopacities consistent with vascular calcification; soft-tissue calcifications were present on about 2% of images, and roughly 88% of those were judged to lie in the carotid bifurcation region, with the remainder attributed to nonvascular entities such as salivary calculi, phleboliths, or calcified lymph nodes. On this basis, the authors proposed panoramic imaging as an opportunistic aid for identifying patients at potential risk of cerebrovascular disease.

The study's contribution was foundational, large for its time, with explicit anatomic criteria that established an early prevalence benchmark and catalyzed later validation work, yet it was limited by the absence of a gold-standard comparator (e.g., Doppler/angiography), the possibility of misclassifying nonvascular calcifications, a sample restricted to older dental outpatients, and the technical constraints of film-based panoramic systems that may have reduced sensitivity. Overall, it remains a seminal proof-of-concept that panoramic radiographs can depict calcified carotid plaques and justify medical referral when suspected (Friedlander & Lande, 1981).

Building on that idea in a modern dental setting, Madden et al. (2007) set out to test whether routine panoramic radiographs can meaningfully detect extracranial calcified carotid atheroma and related carotid luminal stenosis when benchmarked against duplex ultrasonography. In 52 adults who had undergone carotid ultrasound, a trained and calibrated oral and maxillofacial radiologist reviewed new panoramic radiographs for calcifications at the carotid bifurcation, while a cardiologist's ultrasound report served as the reference; analyses used two diagnostic schemes: "any" carotid change versus "moderate–severe" change, and generalized estimating equations to account for side-level clustering. Sensitivity of panoramic radiography was low for both carotid calcifications (31.1% and 25.0% under schemes 1 and 2) and stenoses (22.7% and 21.4%), leading the authors to conclude that panoramic radiography is not a reliable detector of carotid calcification or stenosis relative to ultrasound. As contributions, the study used a clinical gold standard, explicit diagnostic thresholds, a calibrated reader, and appropriate statistics; however, its small sample (n=52), single-reader design, probable spectrum bias (patients already selected for ultrasound), and the known anatomic/image-quality confounders in the mandibular angle–C3–C4 region limit generalizability and likely depress sensitivity estimates. The take-home for literature synthesis is that PR may incidentally flag suspicion but lacks sufficient stand-alone diagnostic performance for carotid disease detection (Madden et al., 2007).

A narrative review by Borba et al. (2016) was conducted to appraise whether routine panoramic radiographs could contribute to earlier recognition of atherosclerotic disease by revealing calcified carotid artery lesions. Using PubMed with the terms "atherosclerosis" and "panoramic" filtered to "last 5 years" and "humans," they identified 20 records and synthesized the six studies available in open access, highlighting reports in which incidental

carotid calcifications on dental panoramics prompted medical evaluation. Across the selected literature, the authors argue that panoramic imaging given its ubiquity and low cost in dental practice can support earlier intervention by flagging patients who merit vascular assessment; at the same time, the narrow time window, restriction to open-access papers, small number of studies, and narrative (non-quantitative) synthesis confine the breadth and precision of the conclusions, and the possibility of confusing nonvascular soft-tissue calcifications showss the need to treat panoramic findings as a trigger for referral rather than a stand-alone diagnostic decision. Overall, the review advances a pragmatic message for clinicians: consciously inspect the carotid region on every panoramic study and, when suspicious opacities are encountered, coordinate prompt medical work-up (Borba et al., 2016).

2.4.2. Prevalence and risk-factor correlates (who has PR-visible CAC, and what does it track with?):

Alves et al. (2014) synthesized evidence on how often CAC appear on panoramic radiographs and how dependable PR-based identification is across study designs and reference standards. From 253 records, they retained 31 studies (35,110 panoramic images) for prevalence and 7 studies for diagnostic performance, showing wide prevalence variation in general dental cohorts (≈0.43%–9.4%) and substantially higher yields in medically high-risk cohorts (up to ≈38.8%). Across included studies, women were often more frequently affected, and calcifications were reported as unilateral or bilateral without a consistent side preference. Diagnostic performance also varied markedly by reference method and sampling, with modest sensitivity (≈22%–74%) and typically higher specificity (near 90% in a CT-referenced series), highlighting that PR is more reliable for ruling in suspicious findings than ruling them out. The review emphasizes interpretive pitfalls from look-alike soft-tissue calcifications and argues that while PR can incidentally flag clinically relevant CAC and prompt referral, confirmation with vascular imaging remains necessary to define disease extent and guide management (Alves et al., 2014).

In a large Brazilian cohort, Santos et al. (2018) provided a routine-care prevalence snapshot by reviewing 2,500 digital panoramic radiographs from a single imaging center in Northeast Brazil using calibrated examiners ($\kappa \approx 0.86$). CAC-like opacities were observed in 96 patients (4.0%), with a sizable fraction bilateral (40.4%) and higher occurrence in women and older age bands, especially 50–70 years. The study supports the practicality of standardized PR reading for opportunistic CAC suspicion but, given the single-center design and the absence of vascular confirmation or clinical covariates, its estimates are best interpreted as radiographic yield rather than diagnostic accuracy or direct cardiovascular risk quantification (Santos et al., 2018). Helmi et al. (2020) extended prevalence and correlates into a Yemeni dental setting by pairing interview-based risk profiling with PR inspection of the C3–C4 region. CAC prevalence was 15.6%, with higher proportions in women (not

statistically significant) and higher occurrence in middle-aged adults and those with higher income. Several clinical-history variables tracked strongly with CAC presence, including prior medical consultation, cardiovascular medication use, and family history, whereas multiple lifestyle items were not statistically associated. While limited by single-center sampling and no ultrasound confirmation, the study's value lies in linking PR-visible CAC to practical referral messaging within a local context (Helmi et al., 2020).

Sinjab et al. (2021) audited 1,781 DPRs but found that field-of-view limitations were a major practical constraint: 1,623 were excluded due to inadequate C3–C4 coverage, leaving 158 analyzable images. They identified CAC in 20 radiographs, yielding an overall prevalence of 1.12% (20/1,781), and most findings were unilateral. Age was associated with calcification frequency, whereas sex and documented cardiovascular diagnoses were not significantly related, though inference is limited by the small analyzable subset and the lack of ultrasound confirmation. The study usefully highlights that real-world PR-based opportunistic screening depends heavily on consistent cervical-region capture and standardized reading protocols (Sinjab et al., 2021).

A nationwide snapshot from Egypt by Professor A. Ibrahim Mousa and colleagues (2025) offered an Egyptian cohort snapshot (Planmeca ProMax 2D; July 2023–June 2024) with balanced sex sampling and consensus expert readings, reporting CAC prevalence of 23.05% (118/512). They described distributions by laterality and side and classified appearance using Garoff's scheme, with "single" patterns most frequent, followed by scattered and "parallel" vessel-outlining configurations. The work strengthens generalizability in a Middle-East/North-Africa context and illustrates how structured reporting can describe PR-visible CAC beyond simple presence/absence, while still remaining limited by the lack of vascular confirmation and sparse clinical covariates. Practically, their data support treating suspicious PR findings as triggers for referral rather than as a stand-alone diagnosis (Professor et al., 2025).

Targeted cohorts deepen the risk picture: Abreu et al. (2017) examined a targeted obese cohort and reported a high yield of cervical-region calcifications on PRs (45/63; 71.4%) under calibrated reading with strong reliability. However, because the endpoint was broad "cervical calcification" rather than definitively verified carotid plaque and because there was no vascular confirmation, the findings primarily indicate the potential screening yield when imaging the C3–C4 region in high-risk groups. The clinical implication remains referral-oriented: careful scrutiny of the carotid region on PRs in high-risk patients may surface candidates who warrant definitive vascular evaluation (Abreu et al., 2017).

Aghazadehsanai et al. (2017) focused on perimenopausal and postmenopausal African American women and reported that 24% had CAC on panoramic imaging, with higher frequency among older participants and higher prevalence of diabetes and dyslipidemia in CAC-positive patients. The strength of this study lies in linking PR findings with extracted cardiometabolic covariates from medical records, reinforcing that PR-visible calcifications tend to cluster with established vascular-risk profiles. Nevertheless, without vascular confirmation, the PR finding should be interpreted as a risk marker prompting follow-up rather than proof of carotid disease severity (Aghazadehsanai et al., 2017).

Azimi et al. (2016) provided one of the largest clinic-based prevalence estimates (n=4,847 adults ≥35 years) using predefined criteria and adjudication by a senior radiologist. CACs were identified in 7.7% of radiographs (373/4,847), more often unilateral than bilateral, and prevalence increased with age. CAC occurrence was higher among individuals with self-reported systemic conditions and smoking history, supporting a consistent clinical picture in which PR-visible CAC tends to co-travel with traditional cardiometabolic risks. While still limited by single-center sampling and lack of vascular confirmation, the study supports using PR findings as triage cues in older or higher-risk patients (Azimi et al., 2016).

Çetin et al. (2020) assessed whether CAC visible on digital panoramic radiographs is associated with periodontal status or standard cardiovascular risk factors in a cross-sectional sample of 1,101 dental-clinic patients. They identified CAC in 34 patients, i.e., 3.1% (34/1,101) prevalence. In their multivariable analysis, age was the only consistent correlate: compared with patients <40, the odds of CAC were higher in 40–55 (OR≈4.5) and >55 (OR≈4.4), while periodontal category and several traditional risk factors (sex, smoking, hypertension, diabetes, hyperlipidemia) were not significant in the adjusted model. Overall, the study suggests DPR-visible CAC in this setting is mainly age-patterned and should prompt medical evaluation rather than be treated as evidence of carotid stenosis or as a surrogate for periodontal disease (Çetin et al., 2020).

Ibraheem et al. (2023) independently linked CAC on PR with periodontitis in a Saudi cohort, they examined whether carotid artery calcifications (CAC) visible on panoramic radiographs among periodontitis patients track with periodontal severity and common cardiometabolic risks and evaluated a periodontitis-enriched sample (n=500 adults ≥40 years) and identified CAC in 5% (25/500), with a notable association between CAC presence and greater alveolar bone loss and higher periodontal risk indices. Their results support the idea that PR-visible CAC can appear in dental patients with substantial inflammatory burden and may align with certain oral-health severity measures, even when some traditional risk factors were not significant in their analyses. As in other studies, the lack of vascular confirmation means PR findings should be used to trigger referral rather than to establish disease diagnosis or severity (Ibraheem et al., 2023).

Gustafsson et al. (2022) examined whether calcified carotid artery atheromas (CACs) visible on panoramic radiographs align with higher estimated cardiovascular risk and with diabetes in participants from the Swedish PAROKRANK cohort, emphasizing individuals without prior myocardial infarction, they linked PR-visible CAC with estimated cardiovascular risk in a large case–control dataset (PAROKRANK), showing that higher Framingham Risk Score related to CAC in both MI cases and controls, and SCORE related to CAC among controls, with stronger signals in men. This design strengthens the conceptual bridge between a radiographic marker and global risk estimation, supporting risk-aware referral logic when CAC is seen on PRs, even though uniform vascular imaging confirmation was not the study's framework (Gustafsson et al., 2018).

Widening the lens to soft-tissue calcifications, Icoz and Akgunlu (2019) set out to quantify how often soft-tissue calcifications are visible on digital panoramic radiographs and how their occurrence relates to age and sex, they broadened the view to soft-tissue calcifications in general (n=4,263 DPRs), reporting an overall calcification frequency of 6.4% and identifying carotid artery calcifications in 2.3% of the cohort. Calcification prevalence rose strongly with age, and while overall presence did not differ by sex, the distribution of specific calcification types did. This study is useful for emphasizing that the cervical region on PRs commonly contains multiple calcification entities, showing why standardized criteria and careful localization are essential to avoid misclassification when CAC is suspected (Icoz & Akgunlu, 2019).

Moshfeghi et al. (2014) examined older women (>50 years; n=200) and reported CAC in 11%, with significantly higher prevalence among those with hypertension and among those reporting prior MI. Despite limitations from self-reported MI and absence of ultrasound confirmation, the study supports a consistent clinical narrative that PR-visible CAC tends to cluster with major vascular risk markers in older populations and should trigger cardiovascular evaluation rather than be treated as a definitive carotid diagnosis (Moshfeghi et al., 2014).

Janiszewska-Olszowska et al. (2022) offered a large Polish series derived from archived PRs with explicit anatomic-field criteria, identifying CAC in 21.68% of eligible images, with unilateral findings more common than bilateral and a clear age gradient across sexes. The study highlights a recurring practical limitation: a substantial proportion of panoramics may not adequately capture the carotid region, which affects real-world feasibility of opportunistic screening. Without vascular confirmation, their results remain prevalence-yield signals, reinforcing that suspicious findings should prompt medical work-up (Janiszewska-Olszowska et al., 2022).

Finally, Möst et al. (2023) directly addressed diagnostic performance by comparing PR against CBCT in older adults (≥60 years; n=607), reporting high specificity (99.5%) with modest sensitivity (67.5%) and overall accuracy 90.6%. They also demonstrated consistent associations between CAC presence and common cardiometabolic risks (age, male sex, hypertension, hypercholesterolemia, other heart disease, COPD), reinforcing that PR-visible CAC behaves like a risk-linked marker even when PR is not a comprehensive vascular test. Collectively, this head-to-head evidence supports the practical framing used across prevalence cohorts: PR is well-suited for opportunistic, high-specificity risk flagging, but positive findings should be interpreted as referral triggers for confirmatory vascular imaging and broader cardiovascular risk assessment (Möst et al., 2023).

2.4.3. Concordance with vascular imaging (do PR findings align with ultrasound/CT?):

Lee et al. (2014) investigated whether calcified carotid lesions seen on panoramic radiographs (PR) correspond to sonographic markers of carotid atherosclerosis when both tests are performed in the same people. In a cross-sectional cohort of 4,050 adults aged ≥50 years, PRs were read for carotid artery calcification (CAC), and duplex ultrasonography quantified common-carotid intima–media thickness (CCA-IMT), carotid-bulb IMT (CB-IMT), carotid plaques, and CCA diameter. CAC on PR aligned with atherosclerotic burden on ultrasound: men with CAC had greater CB-IMT and higher odds of plaque (OR ≈ 2.14; 95% CI 1.01–3.36), and in both sexes CAC was associated with larger CCA diameter; CCA-IMT did not differ overall. By pairing PR interpretation with ultrasound metrics in the same participants and reporting sex-stratified effects, the study builds a practical bridge from an incidental dental finding to arterial disease biology, while its single-country, cross-sectional design and sex-specific signals caution against treating PR alone as definitive for stenosis or event risk; the clinical upshot is that a PR-visible CAC should nudge medical evaluation rather than substitute for it (J. S. Lee et al., 2014).

Atalay et al. (2015) examined an older population with PR plus Doppler ultrasonography to test whether incidental calcified carotid atheroma (CCA) on dental panoramics maps to sonographic disease and common risk indicators. In a retrospective screen of 1,650 adults ≥45 years imaged for routine care in Turkey (2013–2014), 93 patients (5.63%) showed CCA-like opacities on PR; all 93 underwent duplex, which confirmed CCA in 59 and ruled it out in 34, yielding a confirmation rate of 63.4% for PR-positive cases. Age and sex distributions were similar between duplex-confirmed and -negative subgroups, whereas hypertension was enriched among those with duplex-verified CCA (P=0.004); diabetes, smoking, and BMI did not differ. The design ties every positive PR directly to a vascular reference and reports prevalence in a broad dental cohort, while the lack of duplex testing in PR-negative patients and the inherent look-alike problem in the C3–C4 region mean PR remains an opportunistic

flag rather than a stand-alone diagnostic test; clinically, a PR-visible CCA especially in hypertensive patients should trigger medical evaluation (Atalay et al., 2015).

Carasso et al. (2020) extended the concordance beyond the neck by correlating PR-detected CAC with coronary artery calcium (CAC) scores on chest CT. In 177 consecutive candidates for cardiac valve replacement (Oct 2016–Oct 2017), panoramic radiographs were quantified for carotid calcification using ImageJ, while non-gated chest CT provided Agatston CAC, dichotomized at ≥100 as clinically important; multivariable logistic regression adjusted for age, sex, and risk factors. Non-zero carotid calcium on PR occurred in 33% overall and in nearly half of those with high CAC, about twice the prevalence seen in the low-CAC group; in adjusted models, any PR-visible carotid calcium independently aligned with CAC ≥ 100 (OR≈2.2, 95%CI 1.01–4.8), alongside age ≥ 65 (OR≈3.9), male sex (OR≈2.8), and hypertension (OR≈3.6). The authors also derived a simple 4-item score (age, hypertension, sex, PR-calcium) with AUC ~0.80 in training and ~0.78 in validation, suggesting pragmatic triage value. Interpretation is sharpened by paired PR–CT within days and blinded quantitative PR assessment, yet tempered by the high-risk, pre-procedural cohort (not routine dental patients), a single PR reader, absence of vascular ultrasound confirmation, and the plausible role of age as a confounder highlighted in subsequent correspondence; accordingly, a PR-visible carotid opacity should prompt medical evaluation rather than be treated as proof of coronary disease (Carasso et al., 2020).

Explicitly paired PR interpretation with carotid ultrasound in the same patients, Bladh et al. (2024) defined specific PR calcification shapes: single, scattered, vessel-width defining, and vessel-outlining, and explicitly paired PR interpretation with carotid ultrasound in the same participants from the Malmö Offspring Dental Study to test whether these image phenotypes map to vascular disease on ultrasound. In 414 individuals (802 neck sides), readers categorized CAC on panoramic radiographs and sonographers quantified plaque presence, largest plaque area, number of plaques, and lumen-narrowing; across categories, any CAC corresponded to greater ultrasound-evident disease than no CAC, with the most pronounced signal for vessel-outlining lesions (mean largest plaque area ~17.9 vs 2.3 mm², mean plaque count 1.6 vs 0.2, and mean lumen reduction 24.1% vs 3.5%; all $P<0.001$). The one-to-one pairing of PR and ultrasound, the standardized shape taxonomy, and reporting on multiple ultrasound endpoints sharpen the clinical meaning of what dentists see at C3–C4, while the single-region cohort and reliance on ultrasound (rather than angiography) mean the findings index atherosclerotic burden rather than stenosis per se; taken together, the study operationalizes how to read CAC beyond a simple present/absent call and found that these phenotypes correlate with particular ultrasound signs of cardiovascular disease, indicating that how a calcification looks may matter as much as whether it exists (Bladh et al., 2024).

Karlsson et al. (2025) evaluated whether PR-visible CAC and its morphology track with carotid ultrasound disease severity in the VIPVIZA cohort, using the same four-type morphology scheme (single, scattered, vessel-width-defining, vessel-outlining). In a retrospective dental sub-study (n=135; PR within ±18 months of carotid ultrasound among adults with at least one CVD risk factor), any CAC on PR aligned with more ultrasound disease (plaque in 80.9% vs 43.2% without CAC and higher multiview cIMT, mean 0.83 vs 0.77 mm), with vessel-outlining showing the strongest burden signal (cIMT ≈0.88 mm; plaque 87.5%). Using ultrasound plaque as the reference, PR findings were highly specific (≈84.7% overall; ≈96.2% for vessel-outlining) but only moderately to weakly sensitive (≈50% overall; ≈26.9% for vessel-outlining), reinforcing PR as a precise "flag" rather than a screening replacement. Overall, the paired design plus morphology grading supports using structured PR descriptions to strengthen referral decisions while keeping vascular imaging as the confirmatory step (Karlsson et al., 2025).

2.4.4. Clinical outcomes (does a PR finding predict events and established disease?):

Bengtsson et al. (2019) followed patients longitudinally to test whether calcified carotid artery atheroma (CCA) visible on baseline panoramic radiographs predicts future vascular events, moving the evidence from cross-sectional association to prognostic signal. In a population sample aged 60–96 years with no prior stroke or ischemic heart disease, baseline PRs from 2001–2004 were scored for CCA and linked to medical records for ICD-10 outcomes through 2014. CCA was present in 238/635 individuals (37.5%) and associated with subsequent stroke and/or ischemic heart disease overall (χ^2=9.1; OR 1.6, 95% CI 1.2–2.2; p<0.002), with a stronger signal in those aged 60–72 years (crude OR 2.4, 95% CI 1.5–4.0; adjusted for high blood pressure, type 2 diabetes, and BMI: OR 1.9, 95% CI 1.1–3.5; p=0.03). Kaplan-Meier curves showed shorter event-free survival in the 60–72 group when CCA was present (mean 12.1 vs 13.0 years; log-rank χ^2=10.7; p=0.001). Men displayed more baseline CCA, and when the oldest stratum (78–96) was analyzed separately, vascular events were driven mainly by antecedent hypertension rather than CCA status. The design leverages standardized PR reads, long follow-up, and record-verified endpoints; interpretation is tempered by the absence of vascular imaging confirmation, reliance on administrative diagnoses and survival differences without cause-of-death data, and the inherent risk of mistaking look-alike cervical calcifications, yet the data clearly indicate that a PR-visible calcification in late midlife carries prognostic weight for major vascular events (Bengtsson et al., 2019).

In a case-control framework, Gustafsson et al. (2018) reported that patients with a first myocardial infarction had a higher prevalence of calcified carotid artery atheromas (CACs) on panoramic radiographs than age-, sex-, and residence-matched controls, leveraging the multicenter PAROKRANK cohort (696 cases vs 696 controls). All participants underwent standardized PR, and readers scored the C3–C4 region for CAC; prevalence was 33.8% in

cases versus 27.6% in controls (odds ratio 1.24; 95% CI 1.04–1.44; p=0.012), with a similar pattern in men (32.7% vs 26.5%; OR 1.24; 95% CI 1.03–1.48) and a clear excess of bilateral findings among cases (p=0.002). The matched design, large sample, and single imaging protocol strengthen internal validity, while the absence of angiographic confirmation and the inherent limits of case–control inference mean the PR finding should be viewed as a vascular risk indicator rather than proof of stenosis. Together, these data indicate that individuals presenting with a first myocardial infarction more often had CACs visible on prior PRs, aligning opportunistic dental imaging with major cardiac events (Gustafsson et al., 2018).

Garoff et al. (2019) identified a distinctive bilateral vessel-outlining (BVO) pattern on panoramic radiographs and asked whether calcification shape (not just presence) forecasts vascular events. In a prospectively followed cohort drawn from dental imaging (Umeå, Sweden), 117 consecutive patients with PR-detected carotid calcifications and 121 age- and sex-matched controls without calcifications (all <75 years; no prior stroke/TIA) were classified by two blinded oral and maxillofacial radiologists into BVO versus other shapes and tracked for a composite endpoint (stroke/TIA, myocardial infarction, new-onset angina or heart failure, symptomatic claudication, arterial revascularization, and vascular death) over a mean of 9.5 years. Annual risk differed by phenotype about 7.0% for BVO, 4.4% for other shapes, and 2.6% for controls and BVO remained independently associated with events after multivariable adjustment (HR 2.2, 95% CI 1.1–4.5), with an even stronger signal among participants not already on comprehensive preventive medications (adjusted HR ≈3.1). The long follow-up, matched comparison group, standardized shape taxonomy, and blinded readings sharpen the clinical meaning of what dentists see at C3–C4, while interpretation should consider the single-region setting, modest numbers within the BVO category, baseline differences (BVO patients were slightly older and had more prior vascular disease), and the absence of imaging confirmation of stenosis features that point to BVO as a high-risk marker rather than a diagnostic test (Garoff et al., 2019).

In an updated analysis, Garoff et al. (2025) confirmed that PR-visible CACs predict vascular risk at follow-up, reinforcing clinical relevance beyond descriptive epidemiology. Working from a prospectively assembled cohort of 212 consecutive adults in whom panoramic radiographs performed for dental care already showed CAC, the team paired baseline carotid ultrasound (measuring plaque area) with a prespecified panoramic phenotype taxonomy and then tracked major adverse cardiovascular events over a mean of 7.0 years. Vessel-outlining morphology especially when present bilaterally was associated with larger ultrasound plaque area at baseline, and, critically, it remained robustly linked to subsequent events in multivariable Cox models (hazard ratio ≈2.4) even after adjusting for ultrasound total plaque area, which itself lost significance in the joint model. The use of one-to-one PR-ultrasound pairing, a clear image phenotype scheme, and hard clinical endpoints bolsters interpretability; at the same time, enrollment restricted to PR-positive individuals, a moderate sample drawn from a single region, and reliance on ultrasound rather than

angiography mean the findings sharpen risk stratification within CAC-positive patients rather than establish population-level diagnostic accuracy (Garoff et al., 2025).

Brar et al. (2024) reviewed institutional records in a ten-year retrospective cross-sectional analysis to test whether carotid artery calcifications (CAC) detected on panoramic radiographs relate to cerebrovascular accident (CVA), coronary artery disease (CAD), and oral health status. From 2014–2023, 314 adults with PR-identified CAC (confirmed by multiple readers) were assembled and exactly age- and sex-matched to 276 controls without CAC; comorbidities (hypertension, hyperlipidemia, diabetes), histories of CVA and CAD, and the decayed–missing–filled teeth (DMFT) index were abstracted, and multivariable logistic regression adjusted for cardiometabolic risks. CAC-positive patients showed heavier vascular burden and poorer dentition: hypertension 86.2% vs 57.6%, hyperlipidemia 57.6% vs 33.7%, diabetes 30.7% vs 22.1%, CVA 14.9% vs 5.1%, CAD 26.1% vs 9.8%, and higher mean DMFT (26.3 vs 23.7; all $p \leq 0.007$). In adjusted models, CAC remained associated with hypertension (aOR 3.20, 95% CI 2.06–5.07), hyperlipidemia (1.70, 1.14–2.50), CVA (2.20, 1.13–4.30), and CAD (2.10, 1.28–3.60); unilateral and bilateral CAC did not differ across outcomes, and only 41.7% of CAC-positive patients had documented medical referral. The design's age/sex matching, reader confirmation, and inclusion of a quantitative oral-health metric sharpen interpretation, whereas one center, retrospective records, lack of vascular imaging confirmation, and case selection from PR-positive patients bound generalizability and preclude causal claims. Still, the signal is clinically useful: a CAC finding on PR aligns with major vascular disease and worse oral status and should trigger coordinated medical evaluation (Brar et al., 2024).

Historical clinical observations by Almog et al. (2004) anticipated these findings by arguing that PR-identified carotid calcifications flag patients at risk for stroke, a message that has since matured into referral algorithms. In this invited narrative for the New York State Dental Journal, the authors synthesized case reports and early prevalence studies to outline how to recognize carotid-region calcifications on panoramic radiographs (classically nodular or linear opacities inferior–posterior to the mandibular angle around C3–C4), how to distinguish them from common mimickers (triticeous or thyroid cartilage calcifications, sialoliths, phleboliths, calcified lymph nodes), and when to recommend medical work-up typically duplex ultrasonography for older patients or those with cardiometabolic risks. The paper's influence lay in codifying practical image-reading cues and a clear communication pathway from the dental clinic to primary care or vascular services, but it stopped short of providing prospective diagnostic accuracy, angiographic confirmation, or population-level risk estimates, reflecting its era and purpose as pragmatic guidance rather than a controlled study (Almog DM, 2004).

2.4.5. Diagnostic utility, reliability, and practice pathways (can clinicians use PR signals consistently and safely?):

Yoon et al. (2014) measured interobserver agreement for diagnosing CAC on PRs by having two oral and maxillofacial radiologists independently read 1,008 carotid sides (after excluding nondiagnostic sides) from 634 male dental patients aged ≥50 years, classifying calcifications in the standard C3–C4 window and calculating concordance statistics; they reported agreement on 92.4% of sides with a Cohen's κ of 0.688 ($p<0.001$), indicating substantial consistency between readers and supporting the feasibility of routine, reproducible CAC recognition on panoramic images. The focused protocol, explicit anatomic window, and side-level analysis make the reliability estimate clinically useful for standardizing training and audit, while the male-only, single-center sample, use of only two observers, and lack of linkage to a vascular reference (e.g., duplex ultrasound) mean the findings speak to interpretive consistency rather than diagnostic accuracy (Yoon et al., 2014).

Lim et al. (2021) conducted a systematic review asking whether CAC on dental radiographs predicts adverse vascular events and concluded that the signal is real but should be treated as a risk marker that triggers duplex ultrasound rather than as a stand-alone diagnosis. Screening PubMed, Embase, Scopus, Cochrane, and grey literature, they distilled 1,011 records down to five prognostic studies and assessed quality with the Newcastle-Ottawa Scale; outcomes included stroke, TIA, myocardial infarction, revascularization, heart failure, and death. Across heterogeneous designs, individuals with PR-visible CAC were more likely to experience future cerebrovascular or cardiovascular events, though not every endpoint reached statistical significance, and a specific morphology (bilateral vessel-outlining) showed the clearest independent association with subsequent events. The review's breadth across databases, prespecified outcomes, and formal bias appraisal strengthen its message, while the small number of eligible studies, variability in how CAC and endpoints were defined, and reliance on ultrasound or records (rather than angiography) argue for using PR findings to prompt medical evaluation rather than to diagnose disease (Lim et al., 2021).

Prados-Privado et al. (2022) performed a complementary systematic review focused on whether panoramic dental radiographs can reliably detect calcified carotid atheroma and how such findings should be handled clinically. Using PRISMA methods, they searched MEDLINE/PubMed, IEEE Xplore, and ScienceDirect through 15 September 2022, screened 507 records, and included 15 observational studies spanning 2002–2022 that linked PR-visible calcifications with vascular endpoints or cardiometabolic profiles. Most studies were rated at moderate risk of bias, a minority low, and results were heterogeneous, but the overall pattern showed that patients with PR-visible carotid calcification, especially in the presence of risk factors like obesity, diabetes, hypertension, or smoking, had higher prevalence of cerebrovascular or cardiovascular disease than those without such findings. The review emphasizes practical implementation: standardize how the C3–C4 window is read, minimize

false positives by differentiating look-alikes (e.g., triticeous cartilage, sialoliths, phleboliths), and embed clear referral pathways so a suspicious PR triggers duplex ultrasound rather than being treated as a stand-alone diagnosis. The breadth of databases and prespecified outcomes strengthen the message, while variability in definitions, limited prospective data, and reliance on ultrasound or records (not angiography) constrain precision leading to a balanced conclusion that panoramic imaging is a useful opportunistic risk flag that should initiate medical evaluation and risk modification (Prados-Privado et al., 2022).

In day-to-day practice, Madden et al. (2007) showed that PRs can surface previously unrecognized vascular risk, justifying a referral while keeping dental care on track, by explicitly benchmarking panoramic findings against duplex ultrasonography in the same patients. In a cross-sectional diagnostic study of 52 adults who had undergone carotid ultrasound, a calibrated oral and maxillofacial radiologist reviewed new panoramic radiographs for calcifications at the carotid bifurcation, and analyses used two diagnostic schemes ("any" carotid change vs "moderate–severe" change) with side-level clustering handled via generalized estimating equations. Detection performance was modest: sensitivities were ~31% and ~25% for calcifications under the two schemes and ~23% and ~21% for stenoses, indicating many ultrasound-positive cases were missed on PR, but positive calls on PR carried clinical weight and reasonably reflected vascular disease. The reliance on a gold-standard comparator, explicit thresholds, a calibrated single reader, and appropriate statistics supports the internal logic of the findings, whereas the small sample, spectrum bias from recruiting patients already imaged with ultrasound, and anatomic confounders around the mandibular angle temper generalizability; taken together, the study argues that a CAC finding on PR should trigger medical evaluation rather than serve as a stand-alone diagnosis (Madden et al., 2007).

Wadia (2021) offered a concise clinical note on how to word the referral and avoid patient alarm, a small but useful piece in real clinics. Framed as an "Other journals in brief" item in the British Dental Journal, the note showss two practical moves: first, that dentists should deliberately inspect the C3–C4 window on every panoramic radiograph and recognize the typical nodular or linear opacities that suggest carotid calcification; second, that any suspicious finding should be communicated in measured language, flagging an incidental calcification near the carotid bifurcation and recommending medical evaluation, typically with duplex ultrasound, rather than implying a diagnosis. The piece links its advice to contemporary evidence syntheses on prognosis (e.g., systematic reviews associating PR-visible CAC with adverse vascular outcomes), translating them into chairside action: calm, precise wording in the referral, coordination with the patient's physician, and documentation that differentiates likely vascular calcifications from common mimics. As a brief commentary rather than a primary study, it does not present new data, but it crystallizes a referral pathway that fits day-to-day dental workflows and reduces the risk of either over-reassurance or unnecessary alarm (Wadia, 2021).

Mai et al. (2024) framed the topic as preventive cardiology, arguing that standard dental radiographs are a low-cost public-health touchpoint for CV risk reduction if paired with equitable access to confirmatory imaging and follow-up. They retrospectively reviewed charts from a university dental clinic to estimate how often calcified carotid artery atheroma (CAC) appears on routine panoramic radiographs and how often that finding would newly qualify a patient for lipid-lowering therapy under contemporary statin-indication criteria. Among 921 adults with a panoramic radiograph and medical history on file (2019–2021), only 548 images were of sufficient diagnostic quality for CAC assessment; of these, 116 patients (21.2%) had CAC. Just 25.9% of CAC-positive patients were already on lipid-lowering therapy, and another 20.7% had a pre-existing statin-indicated condition but were not treated, so in 53.4% of CAC-positive cases the dental image effectively surfaced a new, untreated diagnosis of atherosclerosis (amounting to 6.7% of the entire clinic population and 11.3% of diagnostically adequate images). Predictors of CAC included dyslipidemia, hypertension, coronary disease, diabetes, atrial fibrillation, stroke/TIA, older age, and male sex. The work's practical value lies in translating a ubiquitous dental image into a trigger for cardiovascular risk modification and an explicit dentist–physician referral pathway, while its single-center design, retrospective charting, and the large fraction of nondiagnostic panoramics emphasize that dental images should prompt medical evaluation rather than substitute for it (Mai et al., 2024).

Case reports collected by Zaghden et al. (2023) illustrated how clearly documented PR findings can move patients into timely vascular evaluation, making the pathway tangible from a chairside discovery to medical action. They presented three incidental discoveries on routine panoramic radiographs, two women in their seventies and an older patient with TMJ/rehabilitation complaints, and combined these with a focused literature review to outline practical handling. In Case 1, bilateral C3-region opacities on PR, clarified with targeted positioning and CT, strongly suggested carotid calcifications but the patient was lost to follow-up, showing real-world attrition. In Case 2, a unilateral C2–C3 calcific pattern on PR was localized with CBCT and then confirmed by Doppler ultrasound as plaque at the carotid bulb; stenosis was non-obstructive and the patient entered cardiology management, exemplifying how PR can trigger appropriate medical care without derailing dental treatment. In Case 3, initial PR suggested stylohyoid ligament ossification (a classic mimic), but CT plus careful rereading showed concurrent carotid-bulb calcification an instructive reminder that shape, level (C3–C5), and relation to adjacent anatomy must be weighed to avoid false positives. The review portion synthesizes why detection performance varies (overlap with surrounding structures, small/early calcifications, bifurcation height outside the PR field, positioning errors) and notes that examiner training improves recognition; they advocate a simple workflow: deliberate inspection of the latero-cervical window on every PR, differentiation from common mimics, and prompt referral for duplex ultrasound when suspicion persists, ideally within a multidisciplinary loop with cardiology/vascular teams (Zaghden et al., 2023).

Taken together, these subsections show a consistent trajectory from early proof of concept to clinically relevant, referral oriented evidence: panoramic radiographs can depict calcified carotid findings in the laterocervical C3 to C4 region and therefore can surface otherwise unrecognized atherosclerotic risk during routine dental care (Friedlander & Lande, 1981; Borba et al., 2016). Across general and targeted cohorts, PR visible CAC is reported with measurable prevalence and it tends to cluster with established cardiometabolic risk patterns, especially increasing age and other common vascular risk profiles, supporting its role as an opportunistic risk cue rather than a random incidental artifact (Alves et al., 2014; Santos et al., 2018; Azimi et al., 2016; Moshfeghi et al., 2014; Möst et al., 2023). Concordance studies add biological plausibility by showing that when CAC is seen on PR it often aligns with ultrasound or CT markers of atherosclerotic burden, including plaque presence and related vascular changes, and it can also correlate with coronary calcification in higher risk populations, strengthening the interpretation that a dental image signal can reflect systemic disease (J. S. Lee et al., 2014; Atalay et al., 2015; Carasso et al., 2020; Bladh et al., 2024; Karlsson et al., 2025).

Prognostic studies further suggest that PR visible carotid calcifications can be linked to future cardiovascular and cerebrovascular outcomes and to established disease, indicating potential clinical value for prevention pathways when the finding is acted upon (Bengtsson et al., 2019; Gustafsson et al., 2018; Garoff et al., 2019; Garoff et al., 2025; Brar et al., 2024). At the same time, the evidence base repeatedly highlights important limitations that define how PR findings should be used: PR is a two dimensional projection with overlap and common mimickers, cervical coverage is not always adequate, sensitivity can be modest even when specificity is high, and many studies are retrospective, single center, and variably confirmed against vascular reference standards, so PR cannot be treated as a stand-alone diagnostic test for carotid stenosis or disease severity (Madden et al., 2007; Alves et al., 2014; Janiszewska Olszowska et al., 2022; Möst et al., 2023). For safe translation into practice, the literature therefore converges on the same operational message: CAC recognition on PR can be reasonably reproducible with standardized reading and training, but the correct clinical action is structured documentation and a clear referral pathway for medical assessment and confirmatory vascular imaging, rather than reassurance or definitive diagnosis within dentistry (Yoon et al., 2014; Wadia, 2021; Prados Privado et al., 2022; Lim et al., 2021; Kadyan et al., 2024; Mai et al., 2024; Zaghden et al., 2023).

2.5. Utilizing Artificial Intelligence to Detect Carotid Artery Calcifications from Panoramic Dental Radiographs

Panoramic dental radiographs (PRs) can incidentally depict calcified atheroma at the carotid bifurcation, offering a low-cost window into vascular disease during routine dental care (Yoo et al., 2024). Recent deep-learning systems aim to automate this recognition on PRs, moving beyond expert-only visual reading toward scalable detection, localization, and lesion

outlining (Kats et al., 2019; Yoo et al., 2024). Early proof-of-concept work showed feasibility with convolutional neural networks (CNNs) trained to flag carotid plaques on PRs, establishing the task and reporting encouraging accuracy on small datasets (Kats et al., 2019). Larger cohorts followed: a CNN classifier trained on 500 PRs achieved patient-level recall ~0.87 and specificity ~0.97, demonstrating that PR-based algorithms can screen for carotid calcifications with near-expert performance (Amitay et al., 2023). Reader-study designs also tested clinical utility; one investigation found that AI assistance improved general dentists' accuracy for carotid calcification on PRs and reduced specialist reading time, supporting workflow integration (Song et al., 2022).

Architecturally, the field now spans cascaded classifier-segmenter networks that jointly label images and delineate calcifications, reporting AUCs near 0.996 and reasonable Dice/Jaccard scores for morphology-aware outputs (Yoo et al., 2024). Transformer-augmented detectors (e.g., Swin Transformer with Faster R-CNN) further raise detection precision/recall on curated PR sets, suggesting gains over CNN-only baselines (Vinayahalingam et al., 2024). Method studies increasingly show that adding explicit region-of-interest detection improves person-level classification compared with whole-image models, a practical point for real-world deployments (Kuwada et al., 2025). Synthesis across primary studies indicates high pooled accuracy: a 2025 systematic review and meta-analysis reports overall sensitivity around 0.92 and specificity around 0.96 for AI detection of carotid calcifications on dental radiographs (Arzani et al., 2025). At the same time, authors flag recurring challenges: variable lesion shapes and overlap with normal anatomy, limited multi-center diversity, and look-alike calcifications, so systems are best positioned as opportunistic screening/triage that triggers confirmatory vascular imaging rather than definitive diagnosis (Amitay et al., 2023; S. W. Yoo et al., 2024).

Although the literature on AI for detecting CACs from panoramic dental radiographs remains relatively small, a coherent set of studies ranging from early proof-of-concept detectors to cascaded classify-then-segment models and a recent systematic review/meta-analysis shows that automated PR-based screening is feasible and increasingly robust across datasets and architectures (Amitay et al., 2023; Arzani et al., 2025; Kats et al., 2019; Song et al., 2022; Vinayahalingam et al., 2024; S. W. Yoo et al., 2024).

Early work established that neural networks can "see" carotid-level soft-tissue calcifications on panoramic radiographs and return a screening signal that mirrors expert judgment. Kats et al. (2019) trained a Faster R-CNN detector (ResNet-101 backbone) on a deliberately small, expert-annotated dataset of 65 panoramic images from two systems (Carestream CS-8100 and Planmeca ProMax 2D), with two oral medicine/maxillofacial radiology specialists providing the ground truth. They cropped standardized left/right cervical regions of interest and used data augmentation (brightness changes, flips, rotations) with a 70/10/20

train/validation/test split; the dataset was challenging and intentionally heterogeneous, and about two-thirds of images contained pathology. Performance reached sensitivity 75%, specificity 80%, accuracy 83%, and ROC-AUC ~0.83, evidence that routine dental images can be converted into an automated "triage ping" to cue duplex ultrasound without interrupting dental care. The clear annotation protocol, clinically interpretable bounding boxes, and cross-device training lend credibility, whereas the tiny single-center sample, absence of external validation, lack of vascular confirmation, and probable class/spectrum imbalance mean the result is a proof-of-concept rather than a deployable tool. Still, it put the task on the dental informatics map, motivating larger multi-site cohorts, standardized PR reading windows, and phenotype-aware labeling that later studies have begun to develop (Kats et al., 2019).

Building on that feasibility step, Song et al. (2022) benchmarked AI across multiple soft-tissue calcification classes on panoramic radiographs, including the carotid region, and compared detector performance under realistic class imbalance, showing that automated localization can be achieved on heterogeneous clinic images while also flagging look-alike structures that challenge readers and models alike. They trained a Fast R-CNN with a ResNet backbone on 20,000 panoramics and then ran a two-session observer study in which two oral and maxillofacial radiologists and two general dentists each interpreted 176 images per session (352 total), with the test set mixing normal studies and three target entities (carotid artery calcification, lymph-node calcification, sialolith); for AI testing they randomly sampled 60 carotid cases and 60 sialolith cases and included all 26 lymph-node cases, reflecting real scarcity. AI's standalone performance was strongest for carotid findings (sensitivity 0.77, specificity 0.71), but noticeably weaker for lymph-node calcifications and sialoliths (sensitivities 0.25 and 0.19), mirroring the thin data for those classes; when used as decision support, accuracy rose for general dentists and their confidence scores improved, while radiologists traded a small sensitivity drop for higher specificity and shorter reading time. The single-center design, rare-class scarcity, and a now-dated detector architecture temper generalization, yet the study demonstrates a workable path: PR-based AI can reliably "ping" carotid-region calcifications to cue vascular referral, while reminding readers where false positives and misses are most likely (Song et al., 2022).

With broader cohorts, Amitay et al. (2023) trained a deep convolutional neural network to screen for carotid calcification at the patient level, reporting high discrimination on held-out data and demonstrating that PR-based screening can be operationalized with standard dental archives rather than bespoke research scans. Using 500 routine panoramics from Poriya Medical Center (2016–2021), each radiograph was side-labeled at C3–C4 and modeled with transfer learning (InceptionResNetV2 features followed by an XGBoost classifier) under 7-fold cross-validation tuned to class imbalance; performance reached recall 0.82 and specificity 0.97 per artery, and recall 0.87 and specificity 0.97 per patient, indicating a strong triage signal that could trigger duplex ultrasound without derailing dental care. The work

benefits from per-patient aggregation, explicit side-level labeling, and a workflow built from ordinary clinical archives; interpretation is bounded by a single-center dataset, no external validation, and the absence of a vascular gold standard, so the output should cue medical evaluation rather than substitute for it (Amitay et al., 2023).

Around the same time, Vinayahalingam et al. (2024) developed a deep-learning pipeline to detect carotid plaque directly on routine panoramic radiographs and evaluated it on real clinic archives, positioning PR as a practical trigger for vascular work-up rather than a bespoke research tool. From 6,404 PRs sourced at a hospital, an oral radiologist and three senior clinicians produced consensus bounding-box annotations; a class-balanced subset (185 CAC, 185 non-CAC) trained and tested a hybrid detector that coupled Faster R-CNN with a Swin Vision Transformer, and performance was benchmarked against published CNN baselines. The transformer-augmented model delivered strong discrimination (precision 0.895, recall 0.881, F1 0.888, AUC 0.950, AP 0.942), exceeding prior CNN-only approaches and showing that automated localization can ride on everyday dental images without interrupting care. The work benefits from expert consensus labels, explicit comparison to earlier models, and pragmatic sourcing from routine archives; interpretability is bounded by a single-center dataset, a curated class-balanced evaluation set from the wider archive, and the absence of external validation or vascular gold standards so outputs should cue duplex ultrasound and risk management rather than function as a diagnosis (Vinayahalingam et al., 2024).

For cross-modality context, one recent study evaluated external carotid calcifications on CBCT rather than PR, showing that territory-aware labeling and modality differences limit direct comparison with PR-based AI, Nelson et al. (2024) extended the target anatomically and asked whether convolutional models can identify external carotid artery calcifications (ECACs), clarifying that territory-specific labeling and careful attention to neck anatomy are needed when moving beyond the internal carotid bifurcation signal typically captured on PRs. Using 427 cone-beam CT scans labeled by a board-certified oral radiologist as the reference, they trained a TensorFlow CNN with an 80:20 train–validation split and evaluated performance with k-fold cross-validation, reporting ~76% accuracy, recall ~66%, precision ~79%, F1≈0.72, and a Matthews correlation coefficient of ~0.53. The study shows that ECACs can be automatically recognized on routine CBCT despite heterogeneous image quality, while also revealing where confusion with nearby structures can erode sensitivity, an argument for precise anatomical ROI definition and phenotype-aware labeling if models are to generalize to varied cervical territories. In practical terms, their pipeline supports the idea that dental imaging can surface vascular risk signals outside the classic PR window, but outputs should cue duplex ultrasound and cardiovascular risk management rather than substitute for diagnosis (Nelson et al., 2024).

Architecture has also evolved from single-head classifiers to pipelines that both classify and draw the lesion. Yoo et al. (2024) introduced CACSNet, a cascaded network that first flags a panoramic radiograph as normal/abnormal and then segments carotid artery calcification (CAC) only in the abnormal images, with ground-truth labels anchored to same-patient CT to handle overlap with the hyoid, thyroid cartilage, and cervical spine. In 400 retrospectively collected PRs from Seoul National University Dental Hospital (2009–2022; half CAC-positive by CT), the classification stage (tested across VGG16, MobileNetV2, ResNet101, DenseNet121, and EfficientNet-B4 backbones) reached its best performance with EfficientNet-B4 (AUC 0.996, accuracy 0.985, sensitivity 0.980, specificity 0.988), while the segmentation stage (encoder–decoder with Tversky loss tuned to α=0.6, β=0.4) achieved Dice ≈0.72 and Jaccard ≈0.60, producing morphology-aware masks rather than black-box labels. Heat-map analyses showed the model focusing on true carotid-level opacities despite size/shape variability, yet false positives clustered near the hyoid/thyroid cartilage and false negatives occurred when calcifications overlapped the cervical spine or posterior pharyngeal wall, showing the need for phenotype-aware labeling and clinical confirmation. Taken together, the work demonstrates a practical two-step workflow that aligns better with referral and documentation than classification alone, while reminding readers that results were derived from a single center with a modest dataset even if CT-referenced labels and explicit ablations strengthen confidence (Yoo et al., 2024).

Method papers now test that intuition directly: Kuwada et al. (2025) showed that adding an explicit area-detection stage before person-level classification improves the overall decision on whether a patient "has CAC," arguing for two-stage, ROI-guided pipelines over whole-image classifiers in real clinics with device and positioning variability. Using 580 panoramic radiographs from 290 CAC-positive patients and 290 matched controls, they compared three systems: (1) direct whole-image classification, (2) preceding region-of-interest (ROI) detection followed by classification, and (3) simultaneous ROI detection and classification (GoogLeNet for classification; YOLOv7 for detection). Person-based AUCs were significantly higher for the ROI-guided systems (0.86 and 0.90 for systems 2 and 3) than for direct whole-image classification (DeLong test, $P<0.001$), and side-based AUCs for the ROI systems were 0.89 and 0.84, respectively, with no meaningful difference between preceding vs simultaneous detection. The design makes a clear methodological point: focusing the model on carotid-level windows stabilizes the patient-level call; nonetheless, a single-center dataset, PR-based labels without vascular confirmation, and lack of external validation mean the output should cue duplex ultrasound rather than substitute for it (Kuwada et al., 2025).

Across these primary studies, a consistent picture emerges: convolutional detectors can flag carotid-territory calcifications on standard PRs with accuracy that is clinically useful for screening/triage, and pipelines that localize the suspected focus (either via dedicated ROI detectors or segmentation heads) tend to yield more stable person-level decisions and more

interpretable outputs for dentists and referrers (Amitay et al., 2023; Kats et al., 2019; Kuwada et al., 2025; Song et al., 2022; Vinayahalingam et al., 2024; S. W. Yoo et al., 2024).

A contemporary synthesis pulls these strands together: Arzani et al. (2025) conducted a systematic review and meta-analysis to quantify how accurately AI detects carotid calcifications on dental radiographs and, while finding high pooled accuracy, emphasized that a positive PR/AI "ping" should still route patients to confirmatory vascular imaging. Searching PubMed, Embase, Scopus, Cochrane, and Web of Science through 11 Nov 2024 under a PROSPERO-registered protocol, they included nine studies qualitatively (CBCT = 3; panoramic = 6) and five in the meta-analysis, most using convolutional-network classifiers or detectors with radiologist readouts or ultrasound as references. A random-effects model (one AI method per paper) yielded pooled sensitivity 0.92 (95% CI 0.81–0.97) and specificity 0.96 (95% CI 0.92–0.97), supporting AI as a useful opportunistic screening aid on routine dental images. At the same time, heterogeneity in datasets and label definitions (e.g., inclusion/exclusion of look-alike soft-tissue calcifications), mixed reference standards, and limited external validation argued for standardizing reading windows and workflows and for treating AI-flagged CAC as a referral trigger typically duplex ultrasound rather than a stand-alone diagnosis (Arzani et al., 2025).

Taken together, **Table 2.2** provides a compact snapshot of a still-small but growing evidence base on AI-driven detection of carotid artery calcifications from panoramic dental radiographs, plus one CBCT comparator, spanning feasibility detectors, reader-aid designs, ROI-guided/cascaded pipelines, transformer backbones, and a recent meta-analysis (Amitay et al., 2023; Arzani et al., 2025; Kats et al., 2019; Kuwada et al., 2025; Nelson et al., 2024; Song et al., 2022; Vinayahalingam et al., 2024; Yoo et al., 2024). As shown in the table, ROI-first or cascaded pipelines generally outperform whole-image classifiers, transformer-based detectors edge past plain CNNs, and reader-aid designs improve usability, collectively supporting PR-based AI as a screening/triage cue that should trigger confirmatory vascular imaging rather than serve as a stand-alone diagnostic.

Table 2.2: Comparison of methodologies and performance metrics across reviewed studies (2019–2025)

Study (Year)	Modality & data/setting	AI type & task	Aim	Key findings & remarks
Kats et al., 2019	PRs; n≈65, single-center; expert boxes	Faster R-CNN; object detection (ROI)	Feasibility of detecting carotid plaque on PRs	Sens 0.75, Spec 0.80, Acc 0.83. Early proof-of-concept showing ROI-level detection on routine PRs; very small dataset, but established the task.
Song et al., 2022	PRs; ~20k train; 352-image reader test; OMRs & GPs	Fast R-CNN detector; AI-assisted reading	Detect soft-issue calcifications (CAC, lymph node, sialolith); measure AI + human effects	AI for CAC ≈ Sens 0.77 / Spec 0.71; assistance improved general-dentist accuracy and reduced specialist time. Multi-class setting highlights look-alike pitfalls and class imbalance.
Amitay et al., 2023	PRs; 500 pts (left/right sides); expert PR labels	Transfer-earning CNN; image-level classification (side- and person-level)	Screen for CAC on routine PRs	Side: Recall 0.82, Spec 0.97; Person: Recall 0.87, Spec 0.97. Operates on standard archives; no ultrasound/CT reference (PR is the ground truth), single-center.
Vinayahalingam et al., 2024	PRs; 6,404 screened; 185 CAC + 185 controls with consensus boxes	Hybrid detector-classifier (Faster R-CNN + Swin ision Transformer); ROI detection	Detect CAC on PRs; compare to CNN baselines	AUC 0.95; Precision 0.895, Recall 0.881, F1 0.888, AP 0.942. Transformer-backed detector outperformed CNN baseline; curated expert annotations; single-center.
Nelson et al., 2024*	CBCT external carotid); 427 scans; single-center	CNN; image-level classification	Identify external carotid artery calcifications on CBCT	Acc 0.76; Precision 0.79; Recall 0.66; F1 0.72 (k-fold). Different modality/territory than PR internal carotid; showss need for territory-aware labels and anatomy.
Yoo et al., 2024	PRs; CT-referenced CAC locations	Cascaded network (EfficientNet-B4 classifier → segmentation net, Tversky loss); classification + segmentation	Robustly classify PRs (normal vs CAC) and segment CAC morphology	Classif: AUC 0.996, Acc 0.985, Sens 0.980, Spec 0.988; Seg: Dice 0.722, Jaccard 0.595. CT-anchored labels boost trust; masks aid reporting/referral beyond a binary flag.
Kuwada et al., 2025	PRs; 580 PRs (290 CAC / 290 controls); side & person analyses	ROI-guided pipelines(YOLOv7 for area detection) + GoogLeNet classifier; compare 3 systems	Test whether adding area detection boosts person-level classification	Person-AUC 0.86–0.90 and Side-AUC 0.84–0.89, both > whole-image classifier ($p<0.001$). Clear take-home: crop/detect first, then classify for stability across devices/positions.
Arzani et al. (2025)	PR/CBCT across 9 studies (5 meta-analyzed)	Mixed AI (CNN/detector/segmenter)	Summarize diagnostic accuracy of AI for CAC on dental images	Pooled Sens 0.92 (0.81–0.97), Spec 0.96 (0.92–0.97). Confirms screening-grade performance is achievable; notes heterogeneity and calls for multi-center external validation.

**Note: Nelson et al., 2024 used CBCT and targeted external carotid calcifications; included as a cross-modality comparator. Metrics are not directly comparable to PR studies*

2.6. Unsupervised Representation Learning and Deep Clustering for CAC Risk Stratification

Although most published AI studies that address carotid artery calcification on panoramic dental radiographs focus on supervised classification, detection, or detection plus segmentation pipelines, the recent evidence syntheses show that the field is still dominated by label-driven models (typically CNN-based) rather than unsupervised, structure-discovering approaches. In settings where labels are scarce, reader-dependent, or difficult to guarantee at scale, unsupervised representation learning offers a complementary route: instead of learning predefined classes, the model learns a compact feature space and then groups images (or ROIs) by shared latent structure (Caron et al., 2018; Xie et al., 2016).

Deep clustering represents a key family of such methods. In Deep Embedded Clustering (DEC), the model simultaneously learns feature representations and cluster assignments, mapping inputs into a lower-dimensional embedding where a clustering objective is optimized iteratively (Xie et al., 2016). Related frameworks such as Deep Cluster follow a similar principle, coupling representation learning with iterative clustering, typically via k-means, so that the resulting pseudo-labels serve as supervision to refine the learned representation (Caron et al., 2018).

This rationale is particularly relevant for panoramic analysis of the carotid region, where confident annotation of CAC can be hindered by projection overlap, variable cervical anatomy, and look-alike radiopacities, all of which increase uncertainty and inter-reader variability. Motivated by these considerations, this thesis adopts an anatomically guided, ROI-based deep-clustering approach to support patient-level pattern discovery from carotid-region ROIs without requiring pixel-level annotations (e.g., segmentation masks). Cluster structure is then evaluated for clinical coherence by examining enrichment of the clinically documented high-risk subset and by contextualizing cluster membership against questionnaire-derived cardiovascular risk profiles captured in this study. In other words, the clustering analysis functions as a label-light, structure-discovering complement to supervised CAC detection pipelines reported in prior work, supporting the broader aim of organizing carotid-region image information into clinically interpretable risk strata.

Because clustering assignments are not anchored to manual class labels, interpretability checks are essential for clinical plausibility. Accordingly, gradient-based explanation maps such as Grad-CAM++ can be used within the autoencoder–DEC pathway to verify that cluster-defining signals arise from anatomically credible carotid-region cues rather than unrelated image artefacts (Chattopadhyay et al., 2018).

2.7. Research Gap and Rationale

Across three converging literatures, a coherent but incomplete picture emerges. First, AI on panoramic radiographs already performs strongly for multiple dental tasks (e.g., tooth detection/numbering, restoration mapping, anatomy segmentation, anomaly detection, and selected predictive workflows), particularly when models localize regions of interest and use workflow-aware designs. Methodological reviews nevertheless emphasize that translation depends less on novelty and more on robust study design: diverse datasets, transparent reference standards, explicit external validation, and clinically meaningful endpoints (Abdalla-Aslan et al., 2020; Başaran et al., 2022; Beser et al., 2024; Bonfanti-Gris et al., 2022; Ding et al., 2023; Litjens et al., 2017; Turosz et al., 2023; Vashisht et al., 2024). However, for many opportunistic screening use-cases in dentistry, large-scale lesion-level labels and vascular reference imaging are not routinely available, which constrains the feasibility of fully supervised, morphology-rich pipelines in low-resource settings.

Second, the cardiovascular literature indicates that carotid calcifications visible on PRs are not incidental artefacts. They co-vary with established cardiometabolic risks, align with carotid ultrasound and coronary calcium on CT in paired studies, and in several cohorts are associated with future stroke, myocardial infarction, and broader cardiovascular events. Importantly, morphology, particularly bilateral vessel-outlining patterns, appears to sharpen risk stratification beyond a simple present/absent label (Bengtsson et al., 2019; Bladh et al., 2024; Carasso et al., 2020; Garoff et al., 2019, 2025; Karlsson et al., 2025; Lim et al., 2021; Möst et al., 2023). At the same time, diagnostic comparisons against ultrasound and CT underline that PR is often a high-specificity but modest-sensitivity indicator; suspicious calcifications should prompt confirmatory vascular imaging rather than be treated as diagnostic in their own right (Alves et al., 2014; Atalay et al., 2015; J. S. Lee et al., 2014; Madden et al., 2007; Prados-Privado et al., 2022). This positioning (risk flag to confirmatory imaging) creates a practical need for systems that are not only accurate, but also interpretable and workflow-ready for dental settings.

Third, dedicated AI systems for detecting carotid calcifications on dental images remain relatively few but report promising performance, ranging from early proof-of-concept detectors to transformer-backed, ROI-guided cascaded classification-segmentation pipelines, and a recent meta-analysis showing screening-grade pooled sensitivity and specificity (Amitay et al., 2023; Arzani et al., 2025; Kats et al., 2019; Kuwada et al., 2025; Song et al., 2022; Vinayahalingam et al., 2024; S. W. Yoo et al., 2024). Yet many models are trained within single centers, often rely on expert PR labels without vascular confirmation, frequently emit predominantly binary outputs rather than standardized morphology-aware descriptors, and are commonly evaluated without explicit linkage to concise patient-level risk profiles or clearly specified referral pathways. In addition, many pipelines focus on “detection” as the primary endpoint, while the real-world dental screening value often

depends on consistent patient-level triage and explainable localization within the carotid region.

Despite these advances, cross-cutting limitations remain. Many AI studies define carotid calcification purely from expert readings of panoramic radiographs, with limited duplex ultrasound or CT confirmation and only sparse linkage to longitudinal outcomes, which limits clinical interpretability beyond internal cross-validation (Amitay et al., 2023; Arzani et al., 2025; Lim et al., 2021; Prados-Privado et al., 2022). Morphology is often reduced to a binary present/absent label even though observational and ultrasound-correlation work shows that patterns such as bilateral vessel-outlining or extensive, vessel-width defining calcification carry higher risk (Bladh et al., 2024; Garoff et al., 2019; Karlsson et al., 2025). External validity is under-tested because many pipelines are trained and evaluated within a single center, device, and demographic slice, leaving uncertainty about performance across different hardware and populations, including under-represented regions such as the Middle East and North Africa (Helmi et al., 2020; Möst et al., 2023; Professor et al., 2025; Vinayahalingam et al., 2024). Finally, while prevalence studies repeatedly show that PR-visible carotid calcifications co-travel with age, hypertension, diabetes, dyslipidemia, obesity, and periodontitis, AI systems less often incorporate brief patient-reported risk domains or operationalize standardized, morphology-aware report wording within a clearly defined referral workflow, leaving opportunistic screening use-cases variably specified (Abreu et al., 2017; Azimi et al., 2016; Gustafsson et al., 2018; Helmi et al., 2020; Mai et al., 2024; Santos et al., 2018). Accordingly, there is a gap for methods that can operate with limited labels, support patient-level stratification, and provide an interpretable rationale that clinicians can trust and act upon.

Against this backdrop, the present thesis targets a narrower and comparatively underexplored direction in dental opportunistic screening. Rather than framing PR-visible carotid calcifications purely as a supervised detection problem, it develops a patient-level, unsupervised risk stratification pipeline that clusters carotid-region imaging patterns using deep embedded clustering (DEC) alongside classical clustering baselines. The study employs anatomically guided ROI extraction and a standardized ROI-focused preprocessing workflow, and evaluates cluster quality, separability, and patient-level grouping of clinically documented high-risk subset. Imaging-derived stratification is then triangulated with a brief questionnaire-based risk profile to support risk-aware interpretation and referral-oriented communication in dental settings. Finally, GradCAM++ explanation maps are used to verify that high-risk assignments are driven by anatomically plausible carotid-region cues, moving toward a practical pathway for opportunistic cardiovascular risk flagging that can be validated and integrated within broader clinical workflows. Importantly, this thesis frames the output as an opportunistic risk signal intended to support referral decisions rather than as a stand-alone diagnostic assessment of carotid stenosis or plaque burden. By evaluating clustering structure using internal validation indices and patient-level enrichment of a

predefined high-risk reference subset, the study aims to provide an evidence-aligned and deployable foundation for screening-oriented decision support in resource-limited dental environments.

Chapter Three

3.1. Methodology

This methodology outlines an unsupervised deep learning pipeline designed to stratify carotid calcification-related cardiovascular risk from routine panoramic radiographs at the patient level. The workflow integrates standardized image preprocessing, anatomically guided region of interest (ROI) extraction, and complementary feature representations that combine hand-crafted radiographic descriptors with deep latent features learned by a convolutional autoencoder. These features are then used as input to several clustering algorithms, including both classical methods and a deep embedded clustering framework, to partition patients into two clusters and map them to low- and high-risk strata using a high-risk validation subset. The following subsections describe each component of the pipeline in detail: the composition of the dataset and the patient-level validation strategy; preprocessing and ROI definition; feature extraction; clustering approaches; patient-level evaluation and visualization; the use of GradCAM++ for model explainability; and implementation details of the computational framework.

3.2. Dataset and Study Population

This single-center retrospective cross-sectional observational study analyzed a clinic-based consecutive (non-probability) sample of 1,107 panoramic radiographs acquired between February 2025 and August 2025 during routine dental examinations at Abraj Dental Clinics, affiliated with Al-Quds University, in collaboration with the Faculty of Dentistry. The study

population included 48% male and 52% female participants, aged 18–85 years (mean age: 40 years). All images were obtained using standardized panoramic radiography systems under consistent acquisition protocols. Within this cohort, 21 patients were selected for model validation based on confirmed cardiovascular disease history or documented carotid calcifications in their clinical records. In addition, a cross-sectional cardiovascular risk assessment questionnaire sub-study was prospectively administered to a subset of 438 participants and used to support validation and complementary non-imaging analyses. The study was conducted in accordance with institutional ethical guidelines and received approval from the Al-Quds University Research Ethics Committee (Ref. No. 427/REC/2024). All patient data were anonymized prior to analysis.

Each panoramic radiograph provides bilateral visualization of the cervical region, allowing assessment of both left and right carotid arteries. Accordingly, a patient-level validation strategy was adopted: a case was considered correctly classified if at least one carotid artery (left or right) clustered with the majority of high-risk cases. This criterion reflects clinical practice, where unilateral carotid calcification is sufficient to indicate elevated cardiovascular risk.

3.3. Image Preprocessing and ROI Extraction

The preprocessing pipeline consisted of four sequential stages designed to enhance the visibility of calcifications while preserving key anatomical structures.

Stage 1: DICOM Loading and Normalization

Stage 1 involved loading and preparing the panoramic radiographs. DICOM files were imported using the *pydicom* library (Mason, 2011), which allowed direct access to the raw pixel data and metadata. Because radiographs were acquired under varying exposure and equipment settings, intensity ranges differed across images. To address this, min–max normalization was applied to rescale all pixel values to a standard 0–255 range. This ensured consistent contrast across the dataset and provided a stable input for the clustering and feature extraction stages that followed.

Stage 2: Region of Interest (ROI) Extraction

Carotid arteries lie in the lateral neck region at approximately the C3–C4 vertebral level. Based on established anatomical guidelines (Yoon et al., 2008), bilateral ROIs were defined as rectangular areas located in the lower lateral zones of each panoramic radiograph.

- Each ROI was derived from the bottom 35% of the image height.
- The left ROI spanned the leftmost 25% of the image width, while the right ROI covered the rightmost 25%.

This strategy effectively isolates the region's most likely to contain carotid calcifications while excluding dental structures and the cervical spine.

Stage 3: Contrast Enhancement

To improve the visibility of subtle calcification patterns, the images underwent contrast enhancement using Contrast Limited Adaptive Histogram Equalization (CLAHE) (Pizer et al., 1987). CLAHE was applied with a clip limit of 3.0 and a tile grid size of 8×8 pixels, parameters chosen to balance detail enhancement with noise control. Unlike global histogram equalization, which adjusts contrast uniformly across the entire image, CLAHE operates on small local regions, allowing fine structures, such as early-stage or low-density carotid calcifications, to become more distinguishable from surrounding soft tissue and overlapping anatomical features.

The use of a clip limit prevents excessive amplification of noise, a common issue in panoramic radiographs where image quality can vary due to differences in acquisition settings, patient positioning, or hardware. By constraining the contrast enhancement in this way, CLAHE sharpens diagnostically relevant boundaries while avoiding artefacts that could mislead downstream feature extraction or clustering. This step therefore ensures that calcifications, which often present with low contrast on raw radiographs, are highlighted in a consistent and clinically meaningful manner before entering the deep learning pipeline.

Stage 4: Noise Reduction

Following contrast enhancement, we applied bilateral filtering (Tomasi & Manduchi, 1998) configured with a 9-pixel filter diameter, sigma color of 75, and sigma space of 75. This smoothing technique reduces noise while preserving important edges, which is critical for distinguishing calcified regions from surrounding soft tissue. The final preprocessed images were resized to 128×128 pixels and used for feature extraction and clustering. All 2,214 ROI images (1,107 patients × 2 carotid regions) underwent identical preprocessing to maintain consistency throughout the analysis workflow.

3.4. Feature Extraction

To ensure detailed characterization of carotid artery calcifications, two complementary groups of features were extracted: (1) hand-crafted radiographic descriptors derived from established image-processing techniques, and (2) deep learned features obtained from a convolutional autoencoder. Together, these feature sets capture both interpretable radiographic markers and higher-order visual patterns learned directly from the images.

3.4.1. Hand-Crafted Radiographic Features:

We computed 16 radiographic features designed to quantify key visual characteristics associated with calcifications:

- **Intensity-based features:**

These features quantify the distribution of bright, high-density pixels that commonly represent calcified tissue. They include the mean intensity, standard deviation, ratios of pixels exceeding the 90th and 95th intensity percentiles, and the intensity values at the 90th, 95th, and 99th percentile thresholds. Together, they provide a detailed profile of localized brightness patterns within the region of interest.

- **Morphological features:**

These descriptors capture the shape and spatial extent of potential calcified structures. They include the number of connected components larger than five pixels, the average size of detected components, and the maximum component size within each image. These metrics help identify clustered, discrete, or large calcification-like regions.

- **Edge features:**

Calcifications often exhibit sharp boundaries compared to surrounding soft tissue. To capture this property, edge density (via the Canny detector), mean gradient magnitude, and maximum gradient magnitude were computed. These features highlight abrupt intensity transitions that are characteristic of mineralized plaques.

- **Texture features:**

Local variance in a 3×3 neighborhood and Shannon entropy were extracted to capture the textural heterogeneity of the region. Higher variance or entropy may indicate irregular structures consistent with calcified deposits.

- **Composite calcification score:**

A combined score was generated using weighted contributions from high-intensity ratios, connected component metrics, and edge density. This integrated measure provides a single interpretable indicator reflecting the likelihood of calcification.

All hand-crafted features were standardized using RobustScaler to reduce sensitivity to extreme values and preserve stability in the presence of imaging artifacts.

3.4.2. Deep Learned Features via CNN Autoencoder:

A convolutional autoencoder was developed to extract higher-level, data-driven representations from the radiographs. The encoder progressively reduces spatial resolution through stacked convolutional and pooling layers, allowing the network to learn increasingly abstract visual patterns relevant to calcification. This compressed representation is encoded in a low-dimensional latent space, which forces the model to retain only the most informative characteristics of the input. The decoder then reconstructs the image by reversing the encoding process using up sampling and convolutional layers that restore spatial detail. This symmetrical design ensures that the latent features remain tied to meaningful anatomical structures. The autoencoder was pretrained for 300 epochs using mean squared error as the reconstruction objective and optimized with Adam (learning rate = 0.001, batch size = 32; 10% validation split).

3.5. Clustering Methods

To categorize patients into low, and high calcification risk groups, we implemented and compared four clustering techniques. Each method offers a different perspective on how patterns emerge from radiographic and learned features, allowing us to evaluate which approach best captures clinically meaningful groupings.

1. K-Means Clustering

K-Means remains one of the most widely used clustering algorithms due to its simplicity and effectiveness. It groups data points by minimizing the distance between each point and its assigned cluster center. In this study, we ran K-Means 10 times using different random seeds (n_init = 25, max_iter = 500). Because cluster quality can vary depending on the initialization, we selected the run with the highest silhouette score, ensuring that the chosen solution provided well-separated and cohesive clusters.

2. Hierarchical Clustering

Agglomerative hierarchical clustering offers a more intuitive, tree-like view of how data points merge to form clusters. We used Ward's linkage method, which emphasizes forming clusters that minimize internal variance. This method gradually merges the closest clusters until the full hierarchy is built. We then cut the dendrogram to obtain two clusters, corresponding to the desired risk categories. This approach allows visual inspection of cluster formation, which can be helpful for interpreting patient stratification.

3. Gaussian Mixture Models (GMM)

Gaussian Mixture Models introduce a probabilistic view of clustering by assuming that the data arise from a combination of several Gaussian distributions. Unlike K-Means, which assigns each point to a single cluster, GMM provides soft assignments, reflecting the probability that a point belongs to each cluster. We used full covariance matrices (covariance_type = "full") to allow flexible cluster shapes. As with K-Means, we ran GMM 10 times with different initializations and selected the solution with the highest silhouette score. This helped ensure that we identified the most stable and informative clustering structure.

4. Deep Embedded Clustering (DEC)

DEC represents the most advanced method in our pipeline, integrating deep feature learning and clustering into a unified framework. It improves upon traditional approaches by continually refining both the feature representation and the cluster boundaries during training. The DEC process consists of two main phases:

Phase 1: Cluster Initialization

After training the autoencoder, we extracted latent representations from the encoder and used K-Means to initialize the cluster centers (two clusters, 20 initializations). This provided a strong starting point for DEC by anchoring the clustering process in high-quality deep features.

Phase 2: Joint Optimization

DEC introduces a specialized clustering layer that computes soft assignment probabilities for each image, based on its distance to the cluster centers in the latent space. These soft probabilities reflect how strongly each sample aligns with each cluster. To refine the clustering process, we computed an auxiliary target distribution, which is designed to emphasize high-confidence assignments and normalize the size of the clusters. This target distribution takes into account the soft cluster frequencies and adjusts the focus on more certain cluster assignments. The model then minimizes the Kullback-Leibler divergence (KL) between the current soft assignments and the target distribution. This ensures that the soft assignments approach the target values, leading to better clustering performance.

The DEC model was fine-tuned for up to 200 epochs using stochastic gradient descent (SGD) with a learning rate of 0.01, momentum 0.9, and batch size 32. Convergence was evaluated every 140 iterations by monitoring changes in cluster label assignments. Training was stopped when the proportion of samples that changed labels fell below 0.1% (tolerance = 0.001). In our dataset, this convergence criterion was met at the first scheduled evaluation point (after 140 iterations), indicating that the pretrained autoencoder embeddings already provided a strong initial separation of clusters.

3.6. Patient-Level Validation Methodology

Unlike conventional image-level evaluation, our validation accounts for the bilateral nature of carotid assessment and operates at the patient level, the clinically relevant unit of analysis.

3.6.1. Patient-Level Cluster Assignment

For each patient p, we obtained cluster labels for both carotid arteries:

- c_p^{left} = cluster assignment for left carotid

- c_p^{right} = cluster assignment for right carotid

A patient contributes to cluster j if either carotid is assigned to that cluster: $p \in C_j$ if $c_p^{left} = j$ OR $c_p^{Right} = j$.

3.6.2. Accuracy Calculation:

Given a set of high-risk patients $\mathcal{H}$,we:

1. Identified the cluster distribution: $\left|C_j \in \mathcal{H}\right|$ for each cluster j
2. Designated the largest cluster as the "high-risk cluster": $j^* = argmax_j \left|C_j \in \mathcal{H}\right|$
3. Computed patient-level accuracy:

$$Accuracy = \frac{\left|C_j \in \mathcal{H}\right|}{|\mathcal{H}|}$$

This metric reflects the proportion of high-risk patients correctly grouped together in the dominant cluster.

3.6.3. Visualization Strategy

For visualization on 2D PCA projections, each patient is represented by a single marker:

- **Correctly classified patients** (in largest cluster): Red circle outline
- **Incorrectly classified patients** (not in largest cluster): Solid red X with black edge

We selected one representative sample per patient (preferentially the carotid assigned to the largest cluster) to avoid duplicate markers.

3.7. Clustering Quality Metrics

To assess how well each clustering method grouped patients into meaningful risk categories, we evaluated the results using three widely used internal validation metrics. Each metric captures a different aspect of clustering quality, allowing for a more complete assessment of how well the models separated low- and high-risk cases.

1. **Silhouette Score**

The silhouette score measures how similar each sample is to its own cluster compared to other clusters. It evaluates both cohesion (how tightly points are grouped within a cluster) and separation (how far clusters are from one another). Scores range from –1 to 1, with higher values indicating well-separated, compact clusters. A high silhouette score suggests that the algorithm is identifying clear, meaningful group boundaries.

2. **Davies-Bouldin Index**

This index quantifies the ratio between within-cluster variation and between-cluster separation. A lower value indicates that clusters are compact internally yet well separated from one another. Because it penalizes overlapping or poorly defined clusters, the Davies-Bouldin Index is particularly useful for identifying whether certain risk categories are ambiguously defined.

3. **Calinski-Harabasz Index**

Also known as the Variance Ratio Criterion, this index compares the degree of dispersion between clusters to the dispersion within clusters. Higher values indicate that clusters are dense, distinct, and well-structured. This metric tends to favor clustering results where samples within a group are highly similar to each other but clearly different from samples in other groups.

Together, these three metrics provide a multi-angle evaluation of clustering performance, balancing considerations of compactness, separation, and overall structure.

3.8. Explainability via GradCAM++

Deep clustering methods such as DEC can produce highly accurate groupings but are often criticized for being opaque. To address this limitation, we incorporated **GradCAM++**, an explainability technique that reveals which regions in an image had the strongest influence on the model's decisions. By generating intuitive heatmaps, we aimed to help clinicians and researchers visually understand why the model assigned certain images as high risk. For each high-risk patient scan, the GradCAM++ process unfolded in several steps:

1. **Forward Pass**

The image was first fed through the DEC model, and feature maps from the final convolutional layer were captured. These maps highlight spatial patterns the network considers most relevant.

2. **Gradient Computation**

We then computed gradients of the cluster assignment scores with respect to each feature map. These gradients identify which parts of the image contribute most strongly to the model's decision.

3. **Weight Calculation**

GradCAM++ refines the weighting process by incorporating not only first derivatives but also second and third derivatives. This produces more precise importance weights, especially when multiple image regions contribute to the classification.

4. **Feature Map Combination**

In this study, the DEC framework operated on learned latent representations extracted by the autoencoder. These representations were used to generate weighted feature maps that were combined into a raw activation map, highlighting regions that influenced the cluster assignment. Areas with higher activation correspond to spatial locations identified as most indicative of calcification-like patterns. In contrast, the classical clustering methods were applied exclusively to hand-crafted features.

5. **Heatmap Generation and Visualization**

The activation map was resized, normalized, and overlaid onto the original image using partial transparency. The resulting heatmap allowed us to see exactly where the model was "looking" and which structures most strongly guided its risk assignment. This pipeline was applied to all 21 high-risk patients (42 carotid ROIs). The resulting

visualizations provided clear evidence that the model focused on anatomically plausible regions associated with carotid calcifications, thereby enhancing trust in the clustering results.

3.9. Implementation Details

All components of the methodology were implemented using Python 3.10. The computational framework integrated several specialized libraries:

- TensorFlow 2.12.0 for training the convolutional autoencoder and DEC model
- scikit-learn 1.3.2 for implementing classical clustering algorithms and computing validation metrics
- OpenCV 4.8.1 for preprocessing, ROI extraction, and image enhancement
- NumPy 1.24.3 and SciPy 1.11.4 for numerical operations and scientific computation

Experiments were executed on an NVIDIA GeForce RTX 3050 Ti GPU (4 GB VRAM) with CUDA 11.2 and cuDNN 8.1. The full DEC training procedure required approximately 4 hours, including autoencoder pretraining and iterative refinement of cluster assignments.

3.10. Validation

3.10.1. Imaging-based validation strategy:

The validation strategy in this study was designed to reflect how carotid-calcification–related risk is assessed at the patient level in clinical practice. Because each panoramic radiograph contains both left and right carotid regions, clustering was first performed at the ROI level and then aggregated to the patient level. For each patient, the two carotid ROIs were assigned to clusters, and a patient-level cluster label was derived by considering whether either side belonged to a given cluster. This approach acknowledges that unilateral calcification can be clinically relevant and avoids underestimating risk in patients with asymmetric findings.

To provide an external reference for validating the clustering structure, a predefined subset of patients with a documented history of cardiovascular disease and/or previously confirmed carotid artery calcifications was used as a high-risk validation group. For each clustering algorithm, the cluster that contained the largest number of these validation patients was designated as the putative high-risk cluster. Patient-level performance for each method was then defined in terms of how many validation patients were assigned to this cluster on at least one side, and how many appeared as anomalies in other clusters.

In addition to this patient-level mapping, internal clustering quality was assessed using standard unsupervised validation indices. The silhouette coefficient, Calinski-Harabasz index, and Davies-Bouldin index were computed for each algorithm to quantify, respectively, within-cluster cohesion, between-cluster separation, and overall cluster compactness versus overlap. Principal component analysis (PCA) was further applied to the learned feature spaces to obtain two-dimensional projections that visually illustrate the relative placement of clusters and the distribution of high-risk validation patients within those spaces. These visualizations were used as a qualitative complement to the numerical indices when judging the plausibility of the clustering structure.

Explainability analysis using GradCAM++ was incorporated as an additional validation layer for the imaging pipeline. For a set of representative ROIs from different clusters, GradCAM++ maps were generated on the encoder-clustering pathway to highlight image regions that contributed most strongly to the model's high-risk assignments. These saliency maps were inspected qualitatively to verify that the model's focus lay within anatomically plausible carotid regions rather than on unrelated dental or skeletal structures.

3.10.2. Questionnaire sub-study and analysis plan:

In parallel with the imaging analysis, a cross-sectional questionnaire sub-study was prospectively administered to characterize cardiovascular risk using non-imaging factors and to support supervised modelling. Data were collected from a subset of patients with both analyzable panoramic radiographs and complete cardiovascular risk questionnaires. Participants were classified into high- and low-risk groups based on a predefined derived risk label informed by questionnaire responses and clinical judgement. The questionnaire captured key cardiovascular risk domains, including socio-demographic and economic characteristics, lifestyle and dietary habits, physical activity, sleep, environmental exposures, medical history, mental health indicators, and self-reported cardiovascular symptoms. Variables were coded using standard epidemiological conventions, with derived features constructed where appropriate.

Analysis comprised two components. First, descriptive statistics and chi-square tests (with Cramér's V) were used to examine associations between individual questionnaire variables and risk status. Second, a supervised Random Forest classifier was trained using questionnaire variables to predict high- versus low-risk status, with performance evaluated on a held-out test set using accuracy, precision, recall, F1-score, and AUC. Feature-importance measures were used to identify the most informative predictors. Questionnaire-based analyses were conducted independently of the imaging-based clustering, with concordance between image-derived clusters and questionnaire-defined risk profiles explored during interpretation.

Chapter Four

4.1. Results

This chapter presents the empirical findings of the study in two main parts that together describe the full analytical pipeline. The first part focuses on image-based analysis: it reports the performance of the preprocessing pipeline, compares four clustering methods using internal validation metrics, evaluates patient level clustering accuracy, inspects cluster separability using two-dimensional PCA projections, and examines model interpretability through GradCAM++ saliency maps in carotid regions. The second part summarizes questionnaire-based results: it describes the socio demographic, lifestyle, environmental, medical, and mental health profiles of high versus low-risk participants, reports univariate associations between these domains and risk status, and presents the performance of a Random Forest classifier trained on questionnaire features to predict high risk classification.

4.2. Image Preprocessing

The preprocessing pipeline was successfully applied to all 1,107 panoramic radiographs, yielding 2,214 carotid regions of interest images (two ROIs per patient, one per side). The standardized workflow included DICOM loading and intensity normalization, anatomically guided ROI cropping, contrast enhancement, and edge preserving smoothing, followed by resizing to a fixed 128 × 128-pixel format. This ensured that all images entering the clustering stage were comparable in scale and focused on the relevant cervical region. Figure 4.1 illustrates the complete preprocessing workflow for a representative high-risk patient, demonstrating visually how each stage progressively enhances the visibility of carotid region structures while suppressing irrelevant background details.

The autoencoder achieved a final reconstruction loss of 0.0078, demonstrating that the latent-space features preserved essential visual information required for downstream clustering.

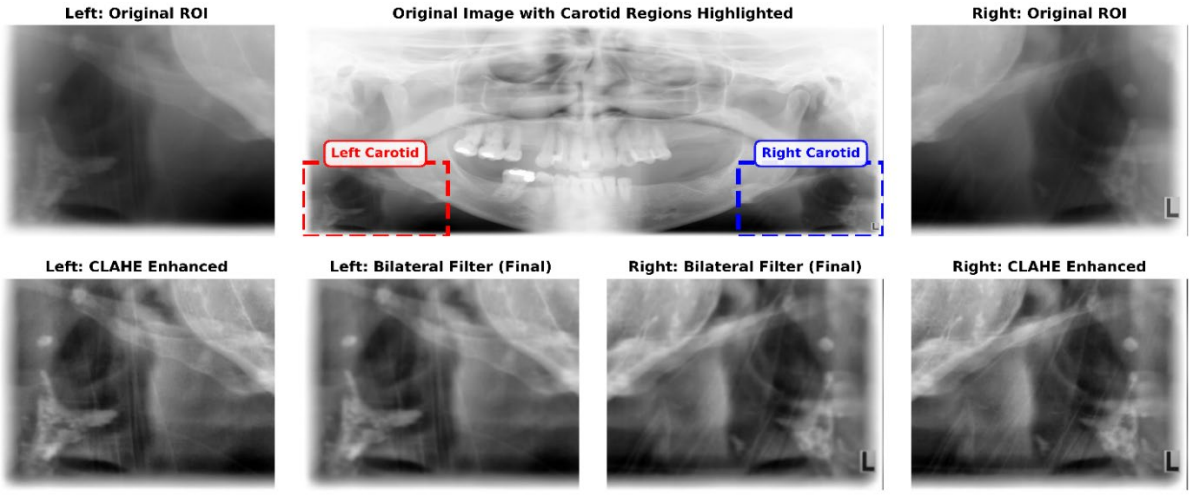

Figure 4.1: *The Complete Preprocessing Pipeline for the Proposed Model*

4.3. Clustering Quality Evaluation

We compared four clustering methods across three internal validation metrics (**Figure 4.2, Table 4.1**). DEC demonstrated very good performance across all metrics, achieving a silhouette score of 0.214, representing a 62% improvement over the second-best method (K-Means: 0.132). The Davies-Bouldin index for DEC (1.752) was 14% lower than K-Means (2.042), indicating better cluster separation. Most notably, DEC achieved a Calinski-Harabasz score of 524, surpassing K-Means (365) by 44%.

Table 4.1: Clustering Quality Metrics Comparison

Method	**Silhouette ↑**	**Davies-Bouldin ↓**	**Calinski-Harabasz ↑**
K-Means	0.132	2.042	365
Hierarchical	0.090	2.536	254
GMM	0.089	2.743	233
DEC	**0.214**	**1.752**	**524**

- ↑ indicates higher is better, ↓ indicates lower is better

Traditional methods (Hierarchical and GMM) performed similarly to each other (silhouette scores: 0.090 and 0.089, respectively) but substantially worse than DEC, highlighting the advantage of learned feature representations over hand-crafted features for this task.

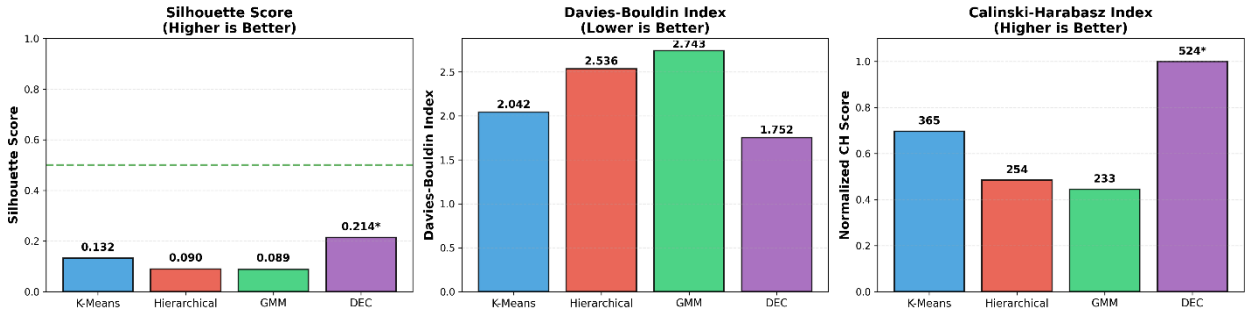

Figure 4.2: Clustering Quality Metrics Comparison

Figure 4.2 compares the performance of the four clustering approaches across three internal validation metrics, and the results consistently show that the Deep Embedded Clustering (DEC) method outperformed the classical algorithms. DEC achieved the highest silhouette score (0.214), indicating better cohesion within clusters and greater separation between them compared with K-Means, Hierarchical Clustering, and GMM, all of which showed relatively weak structural separation. This advantage was reinforced by the Davies-Bouldin Index, where DEC produced the lowest value (1.752), suggesting that its clusters were more compact and more distinct from one another. In contrast, GMM and Hierarchical Clustering generated higher Davies–Bouldin scores, reflecting substantial overlap in their cluster formations.

The Calinski–Harabasz Index further supported the superiority of DEC, as it achieved the highest normalized score (524), indicating dense, well-defined cluster structures. Classical methods showed weaker compactness and poorer inter-cluster separation, with K-Means performing moderately and Hierarchical and GMM yielding the least favorable results. Taken together, these metrics demonstrate that DEC produced the most coherent and clinically promising clustering structure, suggesting that its joint optimization of feature representation and cluster boundaries provides a meaningful advantage for stratifying calcification-related cardiovascular risk from panoramic radiographs.

4.4. Patient-Level Validation Results

4.4.1. High-Risk Patient Accuracy:

Analysis in Figure 4.3 presents the patient-level validation results and demonstrates a clear advantage of the Deep Embedded Clustering (DEC) model over the classical clustering approaches. DEC achieved the highest accuracy in identifying high-risk patients (95%), substantially outperforming K-Means (81%), GMM (76%), and Hierarchical Clustering (62%). This indicates that DEC was better able to capture clinically meaningful patterns associated with carotid artery calcification and cardiovascular risk, even without supervised labels. The strong performance reflects the model's ability to refine latent representations during training, resulting in more coherent groupings of high-risk individuals. The second panel reinforces this outcome by showing how many known high-risk patients were assigned to the dominant risk cluster for each method. DEC grouped 20 out of 21 evaluable high-risk patients into the same cluster, while K-Means and GMM captured 17 and 16 patients, respectively, and Hierarchical Clustering only 13. This concentration of high-risk individuals within a single DEC cluster suggests that its joint feature–clustering optimization created a meaningful separation between patients with and without elevated risk profiles. The patient-level results show the effectiveness of DEC as the most clinically aligned and discriminative clustering method in this study, offering strong potential for supporting opportunistic cardiovascular risk stratification from panoramic radiographs.

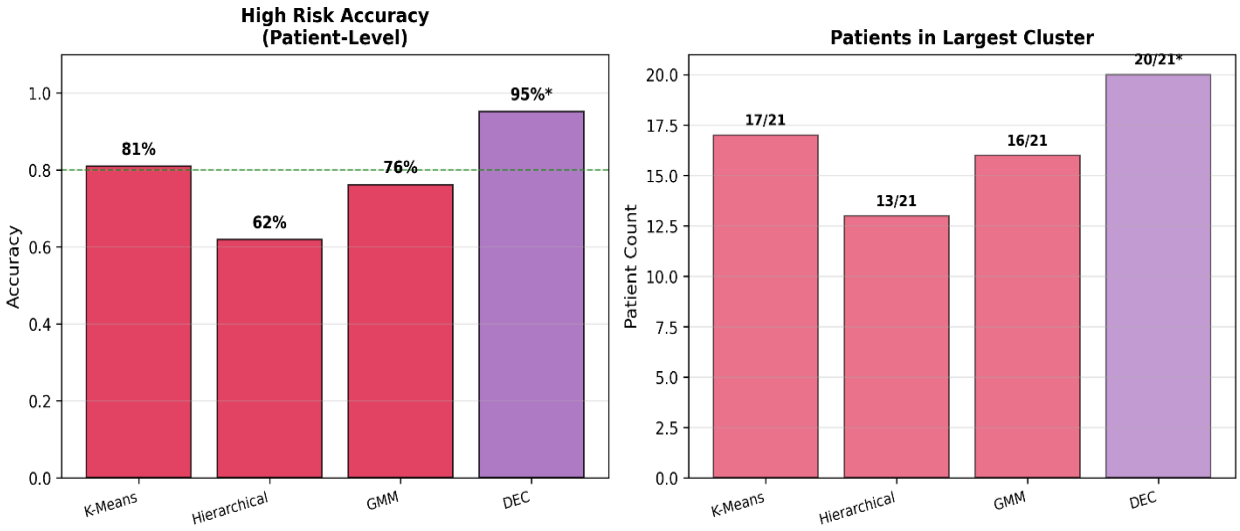

Figure 4.3: Patient-Level Clustering Performance Across Methods

4.4.2. Cluster Distribution Analysis:

Table 4.2 compares the ability of the four clustering methods to correctly group high-risk patients into the appropriate risk cluster. The results show that the Deep Embedded Clustering (DEC) model achieved the strongest performance, correctly identifying 95.2% of high-risk patients and misclassifying only one case. DEC's very low anomaly count suggests that its joint optimization of latent features and cluster boundaries produced well-defined groupings aligned with known cardiovascular risk profiles.

Table 4.2: High-Risk Patient Distribution Across Clusters

Method	Accuracy	Clustered (n)	Anomalies (n)
K-Means	81.0%	17	4
Hierarchical	61.9%	13	8
GMM	76.2%	16	5
DEC	**95.2%**	**20**	**1**

Among the classical clustering algorithms, K-Means performed reasonably well, assigning 17 of 21 high-risk patients to the correct cluster (81.0% accuracy). GMM showed slightly lower performance (76.2% accuracy), while Hierarchical Clustering demonstrated the weakest ability to recover the high-risk group, with only 13 correct assignments (61.9%) and the highest anomaly count. These findings indicate that methods relying solely on distance- or variance-based clustering have difficulty capturing the subtle morphological and intensity patterns associated with carotid calcifications. In contrast, DEC's integration of deep learned representations allowed it to more effectively differentiate high-risk individuals, reinforcing its suitability for opportunistic cardiovascular risk stratification from panoramic radiographs.

4.5. Visual Analysis of Clustering Results

Figure 4.4 provides a statistical visualization of how each clustering method organizes patients in the reduced two-dimensional PCA space. The distribution patterns across the four panels align closely with the corresponding clustering quality metrics and patient-level accuracy results. In the K-Means projection, high-risk patients show moderate grouping, with 17 out of 21 cases positioned within a common region; however, substantial overlap

with neighboring clusters remains evident, supporting the relatively low silhouette score (0.132). Hierarchical clustering displays even weaker statistical separation, with high-risk patients dispersed throughout the feature space and eight cases falling into inconsistent regions, consistent with its lowest accuracy (62%) and limited inter-cluster differentiation.

GMM presents slightly better structural organization, grouping 16 of 21 high-risk patients within a coherent area, though the cluster boundaries remain diffuse, reflecting its modest silhouette and Davies–Bouldin scores. The DEC model shows the strongest statistical coherence: 20 of 21 high-risk patients are positioned within a clearly defined cluster, with minimal overlap across groups. This compact, well-separated spatial distribution corresponds with DEC's superior silhouette score (0.214), lowest Davies–Bouldin index, and highest patient-level accuracy (95%). The PCA projections illustrate that DEC generates the most distinct and clinically meaningful partitioning of the feature space, reinforcing its statistical robustness and suitability for CAC-related cardiovascular risk stratification.

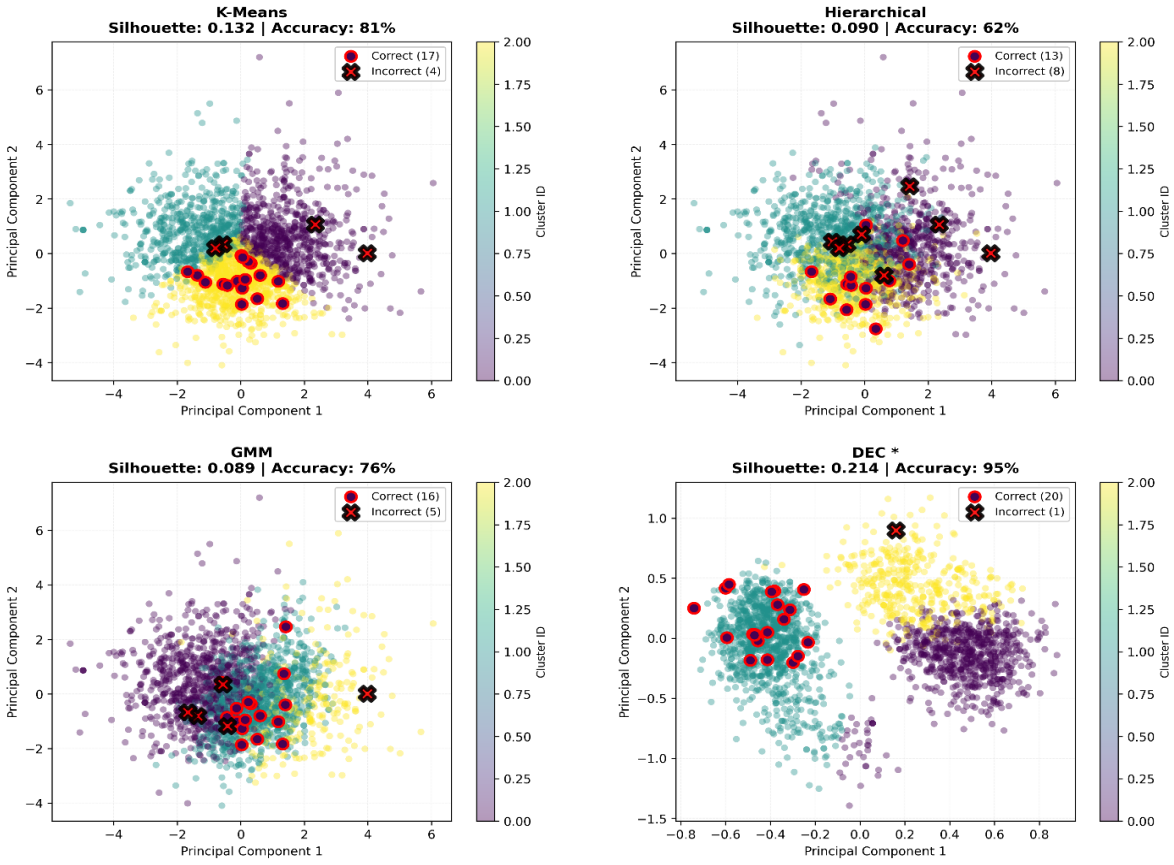

Figure 4.4: PCA Projections of the Feature Spaces for All Clustering Methods

4.6. GradCAM++ Interpretability Analysis

GradCAM++ visualizations for all 21 high-risk patients revealed highly consistent attention patterns across the dataset, demonstrating that the model systematically focused on anatomically plausible regions associated with carotid calcifications. As shown in Figure 4.5, the heatmaps concentrated along the inferior lateral neck region, precisely where calcifications are expected to appear on panoramic radiographs. In the representative example, GradCAM++ highlighted the dense, high-intensity clusters indicated by visual inspection on the original images, confirming that the model's decisions were driven by clinically relevant features rather than spurious artefacts or unrelated structures.

These attention maps provide valuable interpretability for the clustering framework. The spatial coherence across patients suggests that the deep embedded clustering model consistently learned to associate calcification-related patterns with the high-risk cluster. The limited presence of misdirected activations indicates that the model rarely relied on irrelevant radiographic features, supporting the reliability of its latent representations. Overall, the GradCAM++ results strengthen confidence in the model by demonstrating that its internal reasoning aligns with expected anatomical cues and established visual markers of carotid artery calcification.

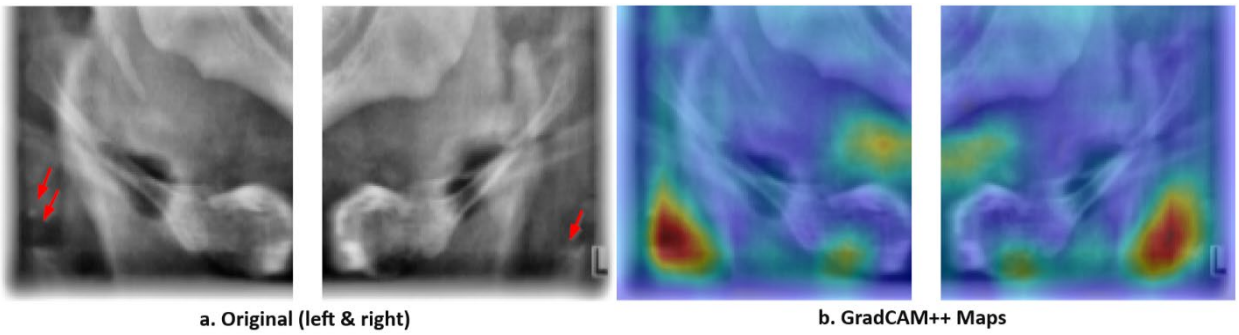

Figure 4.5: GradCAM++ Visualization of Saliency Maps

4.7. Questionnaire Based Descriptive Profiles

The second part of the results focuses on questionnaire findings comparing participants classified as high or low cardiovascular risk. Descriptive statistics for the main sociodemographic variables are reported in Table 4.3. Clear differences emerged between the two groups. High-risk participants tended to be substantially older, with half aged 60 years or above, compared with only 2.8% in the low-risk group, where younger ages were

far more common. Differences in body mass index were also evident: overweight and obesity were more frequent among high-risk individuals, while normal BMI predominated in the low-risk group.

Socioeconomic patterns were equally noticeable. Participants in the high-risk group were more likely to have limited education and lower income, whereas university education and medium income were more common among those classified as low risk. Employment status followed a similar trend, with unemployment clustering in the high-risk group and employment more prevalent among low-risk participants. Smaller differences were observed for gender, marital status, and place of residence. Women and rural residents were somewhat more represented among high-risk participants, although these contrasts were less pronounced than those seen for age, BMI, and socioeconomic indicators.

4.8. Cardiovascular Risk Factors Univariate Analysis

Univariate associations between cardiovascular risk status and questionnaire variables were examined using chi square tests, with Cramer's V used to quantify effect size across sociodemographic, environmental, health awareness, lifestyle and dietary, medical history, mental health, and symptom domains. Full results are presented in Table 4.4. Within the sociodemographic domain, age group, income status, education level, occupation, marital status, gender, and body mass index (BMI) category were significantly associated with risk status ($p < 0.05$). In contrast, place of residence was not significantly associated with risk status ($\chi^2 = 3.71$, $p = 0.157$), although the effect size was small (Cramér's $V \approx 0.09$). Several environmental factors, including primary water source, perceived air quality, noise exposure, and air pollution exposure, were also significantly associated with risk classification, with high-risk participants more likely to report adverse environmental conditions.

Health awareness variables showed consistent associations with risk status. First aid training, response to unconscious individuals, prior cardiovascular education, awareness of sudden cardiac arrest, regular access to healthcare, interest in health-related applications, and frequency of healthcare visits were significantly related to risk classification ($p < 0.05$), whereas knowledge of heart attack versus cardiac arrest was not statistically significant ($p = 0.4107$). Lifestyle and dietary factors exhibited some of the strongest associations. Exercise type and frequency, daily sitting time, sleep duration, dietary habits, intake of snacks and sweets, consumption of fruits and vegetables, smoking status, fast food and high fat food consumption, and meal structure were generally significantly associated with risk status ($p < 0.05$). Daily sleep duration showed a particularly large effect size, with Cramér's V greater than 0.7, indicating a strong relationship between sleep patterns and cardiovascular risk classification in this cohort. In contrast, monthly red meat consumption ($p = 0.0527$), special diet ($p = 0.2786$), and quit-smoking attempts ($p = 0.6704$) were not statistically significant.

Medical history variables, including diagnosed chronic diseases, coronary heart disease, diabetes, family history of stroke, kidney disease, and hypertension, were significantly associated with high-risk status, consistent with established cardiovascular risk factors. In contrast, family history of cardiovascular disease, regular physician visits, and hypercholesterolemia showed weaker or non-significant associations. Mental health indicators were also strongly associated with risk status. While the general "mental health issues" item was not statistically significant ($p = 0.2065$), items reflecting depressive and anxiety symptoms, including depressed mood, feelings of worthlessness, psychomotor changes, sleep disturbance, suicidal ideation, fear and worry, difficulty relaxing, fatigue, appetite changes, and physical anxiety symptoms, differed significantly between high and low risk groups with moderate to large effect sizes. Finally, symptoms such as severe headache, shortness of breath, and chest pain were significantly more frequent among high-risk participants, further supporting the convergent validity of the derived risk classification.

4.9. Random Forest Classification Performance

To move beyond descriptive and univariate analysis and test whether questionnaire features can jointly discriminate between high and low risk participants, a Random Forest classifier was trained using the full set of questionnaire variables. After data cleaning and balancing, the model was evaluated using standard performance metrics.

Table 4.3: Patients risk assessment descriptive analysis

Feature	Category	Risk	
		High	**Low**
Age group	<30	41 (18.6%)	95 (43.6%)
	30-59	69 (31.4%)	117 (53.7%)
	60+	110 (50.0%)	6 (2.8%)
BMI Category	Above	89 (40.5%)	51 (23.4%)
	Bellow	56 (25.5%)	24 (11.0%)
	Normal	75 (34.1%)	143 (65.6%)
Education Level	No Formal Education	49 (22.3%)	23 (10.6%)
	Primary	76 (34.5%)	16 (7.3%)
	Secondary	28 (12.7%)	50 (22.9%)
	University	67 (30.5%)	129 (59.2%)
Gender	Female	153 (69.5%)	119 (54.6%)
	Male	67 (30.5%)	99 (45.4%)
Income Status	High	32 (14.5%)	21 (9.6%)
	Low	113 (51.4%)	21 (9.6%)
	Medium	75 (34.1%)	176 (80.7%)
Marital Status	Married	141 (64.1%)	141 (64.7%)
	Single	79 (35.9%)	77 (35.3%)
Occupation	Employed	80 (36.36%)	128 (58.72%)
	Unemployed	140 (63.64%)	90 (41.28%)
Residence	Refugee Camp	42 (19.1%)	32 (14.7%)
	Rural	114 (51.8%)	105 (48.2%)
	Urban	64 (29.1%)	81 (37.2%)

Table 4.4 - A: Patients risk assessment univariate analysis

Group	Feature	Chi2-Value	P-Value	Cramér's V
Sociodemographic	Age Group	127.06	<0.001	0.5386
	Income Status	106.08	<0.001	0.4921
	Education Level	74.329	<0.001	0.4119
	Occupation	50.99	<0.001	0.3412
	Marital Status	23.882	<0.001	0.2335
	Gender	9.7839	0.0018	0.1495
	Residence	3.7053	0.1566	0.092
	BMI Category	44.317	<0.001	0.3181
Environmental Factors	Primary Water Source	35.975	<0.001	0.2866
	Air Quality	29.752	<0.001	0.2606
	Noise Exposure	17.101	<0.001	0.1976
	Air Pollution Exposure	8.2487	0.0162	0.1372
Health Awareness	First Aid Training	92.716	<0.001	0.4601
	Unconscious Person Response	47.856	<0.001	0.3305
	Cardiovascular Education	41.15	<0.001	0.3065
	Heard of Sudden Cardiac Arrest	18.375	<0.001	0.2048
	Regular Healthcare Access	16.024	<0.001	0.1913
	Health App Interest	13.532	<0.001	0.1758
	Healthcare Visit Frequency	12.04	0.0024	0.1658
	Knows Heart Attack vs Cardiac Arrest	0.6768	0.4107	0.0393
Lifestyle & Diet	Dietary Habits	97.191	<0.001	0.4711
	Daily Sitting Hours	72.825	<0.001	0.4078
	Exercise Type	158.91	<0.001	0.6023
	Daily Main Meals	63.35	<0.001	0.3803
	Weekly Exercise	50.776	<0.001	0.3405
	Daily Snacks	47.144	<0.001	0.3281
	Monthly Sweets/Pastries	51.117	<0.001	0.3416
	Monthly Fresh Vegetables	47.434	<0.001	0.3291
	Daily Mineral Water (Liters)	32.299	<0.001	0.2716
Lifestyle & Diet	Overeats	30.031	<0.001	0.2618
	Smoking Status	29.48	<0.001	0.2594
	Home Food Preparation	27.352	<0.001	0.2499
	Eats Quickly	23.652	<0.001	0.2324
	Fast Food	27.943	<0.001	0.2526
Lifestyle & Diet	High Fat Diet	20.233	<0.001	0.2149
	Physical Activity Level	26.507	<0.001	0.246
	Daily Sleep Hours	226.79	<0.001	0.7196
	Daily Breakfast	16.15	<0.001	0.192
	Monthly Sweetened Beverages	20.112	<0.001	0.2143
	Insomnia	11.382	<0.001	0.1612

Table 4.4 - B: Patients risk assessment univariate analysis

Group	Feature	Chi2-Value	P-Value	Cramér's V
	High Sugar Diet	10.174	0.0014	0.1524
	Monthly Dairy/Cheese	15.119	0.0045	0.1858
	Monthly Fresh Fruits	14.952	0.0048	0.1848
	High Salt Diet	5.0666	0.0244	0.1076
	Monthly Chicken/Fish	11.089	0.0256	0.1591
	Monthly Red Meat	9.3624	0.0527	0.1462
	Special Diet	1.174	0.2786	0.0518
	Quit Smoking Attempt	0.1812	0.6704	0.0203
Medical History	Diagnosed Diseases	40.001	<0.001	0.3022
	Coronary Heart Disease	37.295	<0.001	0.2918
	Diabetes	31.408	<0.001	0.2678
	Family Stroke History	11.633	<0.001	0.163
	Kidney Disease	10.265	0.0014	0.1531
	High Blood Pressure	8.7613	0.0031	0.1414
	Family Cardiovascular Diseases	3.3481	0.0673	0.0874
	Regular Doctor Visits	2.9601	0.0853	0.0822
	High Cholesterol/Triglycerides	1.8019	0.1795	0.0641
Mental Health	Mental Health Issues	1.2323	0.2065	0.0422
	Depression Scale – Worthlessness	81.682	<0.001	0.4318
	Depression Scale - Depressed Mood	66.35	<0.001	0.3892
	Anxiety Scale - Easily Upset	38.89	<0.001	0.298
	Depression Scale - Psychomotor Issues	38.075	<0.001	0.2948
	Anxiety Scale – Anhedonia	36.342	<0.001	0.288
	Depression Scale - Sleep Issues	34.805	<0.001	0.2819
	Depression Scale - Suicidal Thoughts	34.741	<0.001	0.2816
	Anxiety Scale - Unexplained Fear	32.603	<0.001	0.2728
	Anxiety Scale - Relaxation Difficulty	20.023	<0.001	0.2138
	Depression Scale - Lack of Interest	15.158	0.0017	0.186
	Depression Scale – Fatigue	14.424	0.0024	0.1815
	Depression Scale - Appetite Changes	11.356	0.0099	0.161
	Anxiety Scale - Physical Symptoms	11.046	0.0115	0.1588
	Anxiety Scale - Stress Control	9.9498	0.019	0.1507
	Anxiety Scale – Irritability	6.4413	0.092	0.1213
	Depression Scale - Concentration Issues	2.1552	0.5408	0.0701
Symptoms	Severe Headache	8.7689	0.0031	0.1415
	Shortness of Breath	5.6403	0.0176	0.1135
	Chest Pain	5.0097	0.0252	0.1069
	Weakness/Numbness	3.4357	0.0638	0.0886
	Speech Difficulty	1.4696	0.2254	0.0579
	Dizziness	0.3234	0.5695	0.0272

As summarized in Table 4.5, the Random Forest achieved an accuracy of approximately 93% and an area under the ROC curve of about 0.98. For the high-risk class specifically, precision reached about 0.97, recall about 0.89, and the F1 score about 0.93. These values indicate that, within this dataset, the model can distinguish high from low-risk individuals with very high discriminative performance based solely on questionnaire responses.

Feature importance plots (Figure 4.6) indicated that age, body mass index, daily sleep hours, daily sitting time, exercise patterns, and selected medical history variables (such as hypertension and diabetes) contribute most strongly to model decisions. This pattern closely aligns with both global cardiovascular risk literature and the univariate associations described above. At the same time, it is important to interpret these results cautiously: the model is trained and evaluated in a single cohort, the risk label is derived rather than based on hard clinical outcomes such as myocardial infarction or stroke, and some predictors may overlap conceptually with how the label itself was defined.

Table 4.5: Random Forest prediction performance

Metric	Accuracy	ROC-AUC	Precision (High)	Recall (High)	F1-Score (High)
Value	0.931818	0.982094	0.967213	0.893939	0.929134

The feature importance analysis from the Random Forest model highlights which questionnaire-based risk factors contributed most strongly to predicting cardiovascular risk within the study population. Income emerged as the most influential predictor, suggesting that socioeconomic status plays a substantial role in shaping lifestyle patterns, access to care, and overall vulnerability to cardiovascular disease. Feelings of worthlessness ranked second, indicating that psychological or emotional distress may meaningfully interact with cardiovascular risk, an observation consistent with evidence linking mental health and cardiometabolic outcomes.

Several lifestyle-related variables also showed high importance. Exercise type, first-aid knowledge, diet habits, and education contributed prominently, reflecting the influence of health literacy, nutrition, and physical activity on disease risk. Sleep duration and sedentary behavior (sitting hours) also exhibited notable importance, aligning with well-established relationships between sleep quality, sedentary lifestyles, and cardiometabolic health.

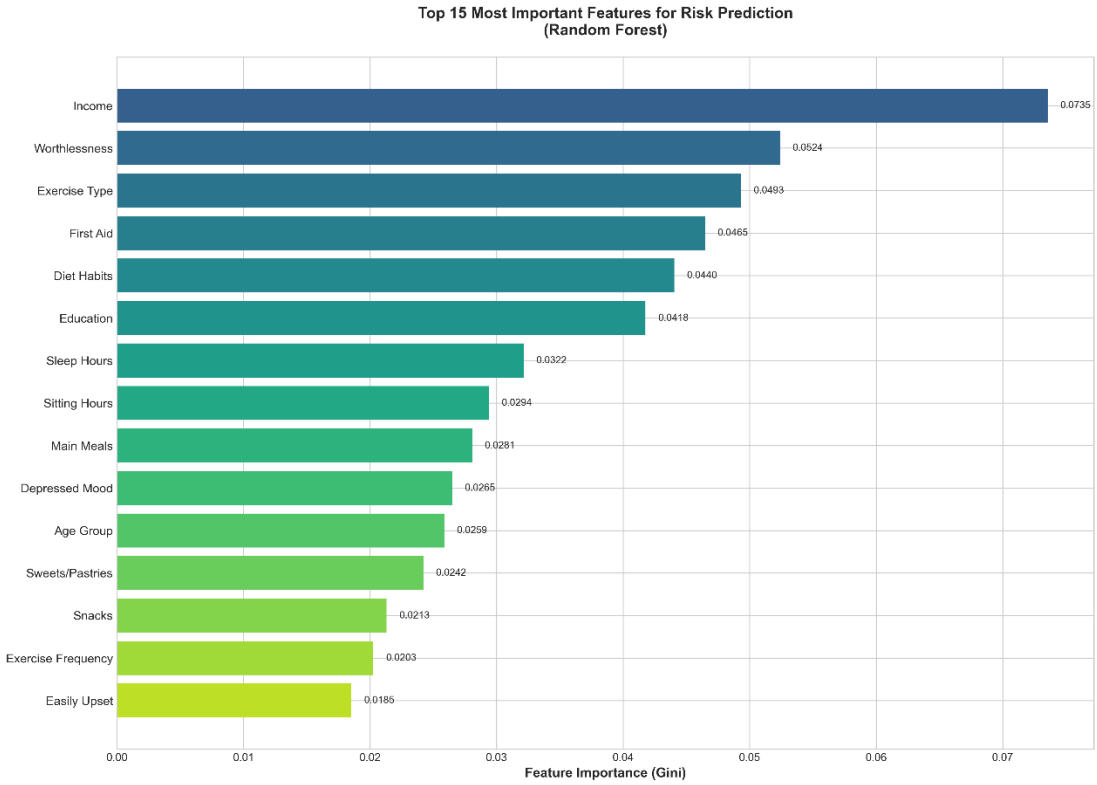

Figure 4.6: Top 15 Most Important Questionnaire-Based Predictors of Cardiovascular Risk (Random Forest Model).

Chapter Five

5.1. Discussion

This chapter provides a critical interpretation of the study's results, drawing out what the imaging-derived clusters and questionnaire findings jointly suggest about carotid calcification and cardiovascular risk in routine dental imaging settings. The study combined unsupervised deep clustering of carotid regions of interest extracted from 1,107 panoramic radiographs with questionnaire-based cardiovascular risk profiling in patient subgroups to examine whether latent image patterns and simple clinical variables can jointly stratify carotid-calcification-related cardiovascular risk.

5.2. Finding Discussion

The results of this study indicate that deep embedded clustering (DEC) is a highly effective method for stratifying carotid-artery-calcification-related cardiovascular risk using panoramic radiographs. DEC consistently outperformed classical clustering methods across all internal validation metrics, supporting the idea that integrating feature learning with cluster optimization produces more clinically coherent representations. The highest silhouette score among the compared methods achieved by DEC suggests improved intra-cluster homogeneity, while its lower Davies–Bouldin index and higher Calinski–Harabasz value indicate more compact and better-separated clusters relative to the classical baselines. Similar findings have been reported in other domains of medical imaging where DEC has shown great performance compared with conventional clustering algorithms, particularly when the underlying patterns are subtle or heterogeneous (Caron et al., 2018; Xie et al., 2016). These results extend previous work by demonstrating that deep clustering can

uncover meaningful latent structures from panoramic radiographs, a modality characterized by low soft-tissue contrast and substantial anatomical overlap.

The patient-level accuracy provides further evidence of the effectiveness of DEC. The method successfully grouped the vast majority of high-risk patients into a single dominant cluster, achieving 95.2 percent accuracy. This level of performance compares favorably with recent supervised deep-learning studies that detected or segmented carotid artery calcifications on panoramic radiographs. For instance, Amitay et al. (2023) and Yoo et al. (2024) reported high diagnostic performance using convolutional networks trained on annotated datasets, whereas the present study achieved encouraging patient-level risk-stratification performance without requiring pixel-level annotations (e.g., bounding boxes or segmentation masks) for training (Amitay et al., 2023; Yoo et al., 2024). This highlights the potential value of unsupervised learning for clinical settings where expert-annotated datasets remain limited. The relatively weaker performance of K-Means, GMM, and hierarchical clustering further shows the difficulty of capturing calcification patterns using distance-based grouping alone, particularly when those patterns present considerable anatomical variability or low-intensity contrast.

The PCA visualizations provide important qualitative insight into the separability achieved by different methods. Classical approaches produced overlapping feature distributions, suggesting that their representations lacked the dimensional structure required to differentiate high-risk from lower-risk individuals. By contrast, DEC created a visibly distinct region for high-risk patients, reflecting the strength of its latent embedding. Comparable spatial separability has been reported in vascular phenotyping studies using computed-tomography-based imaging or ultrasound, where deep representations have been shown to cluster plaque morphology or disease severity more effectively than engineered features (Anderson et al., 2000; Bladh et al., 2024; Carasso et al., 2020; Karlsson et al., 2025). The findings of the current study indicate that these advantages extend to the more challenging context of panoramic radiographs, which are prone to noise, anatomical variation, and superimposition.

Explainability analysis using GradCAM++ reinforces the clinical validity of the model. The consistent activation of regions corresponding to the anatomical course of the carotid artery suggests that DEC learned representations grounded in meaningful pathology rather than relying on artefacts or image noise. This aligns with established biological models of vascular calcification, in which vascular smooth muscle cells undergo osteogenic differentiation and contribute to plaque mineralization through regulated cellular pathways (Demer & Tintut, 2014; Durham et al., 2018). This level of anatomical alignment has also been described in supervised deep-learning models for CAC detection and contributes to trustworthiness and interpretability, which are crucial for clinical adoption (Amitay et al.,

2023; Chattopadhyay et al., 2018; Yoo et al., 2024). The absence of diffuse or misplaced activations implies that the model did not overfit to irrelevant structures, addressing a common concern raised in explainability research. These findings support the feasibility of integrating deep unsupervised clustering into clinical workflows, provided that appropriate visualization tools are employed to guide clinician interpretation.

The questionnaire-based risk-factor analysis showed that socioeconomic, lifestyle, nutritional, and psychological variables were important determinants of cardiovascular risk in this population. This pattern aligns with major cardiovascular guidance emphasizing multi-domain risk assessment and with contemporary evidence linking psychosocial stressors to vascular dysfunction and cardiovascular outcomes (Ebong et al., 2024; Havranek et al., 2015; Levine et al., 2021; Osborne et al., 2020; Sara et al., 2022). In addition, recent evidence from machine-learning analyses of population-health datasets indicates that emotional and behavioral variables can possess predictive value comparable to traditional clinical indicators. The integration of these questionnaire features with imaging-derived latent representations supports a more holistic understanding of cardiovascular risk, reflecting current preventive-cardiology recommendations that emphasize multi-domain assessment (World Health Organization, 2025).

Taken together, the imaging, computational, and behavioral findings of this study indicate that panoramic radiographs represent a viable and under-utilized opportunity for opportunistic cardiovascular risk identification. Prior research has demonstrated that carotid artery calcifications visible on panoramic radiographs are not merely incidental findings but are associated with subsequent cerebrovascular and coronary events, including myocardial infarction and ischemic heart disease, in both case-control and long-term follow-up studies (Arzani et al., 2025; Bengtsson et al., 2019; Garoff et al., 2019, 2025; Gustafsson et al., 2018). The present results extend this evidence by showing that an unsupervised deep-learning framework can extract meaningful risk-related patterns even without manual annotations. This capability is particularly relevant for low-resource healthcare environments, such as Palestine, where access to advanced vascular imaging is limited and dental radiographs are widely performed. Recent public-health-oriented analyses have emphasized that carotid artery calcifications visible on routine dental radiographs represent an underutilized opportunity for cardiovascular risk reduction and early preventive intervention (Mai et al., 2024). By combining morphology-aware latent features with behavioral risk indicators, the proposed system could support earlier identification of high-risk individuals and facilitate more timely referral pathways.

The study supports the potential of Deep Embedded Clustering as a scalable and clinically relevant tool for cardiovascular risk stratification from panoramic radiographs. Future studies should explore external validation across multiple imaging centres, integration with

electronic dental records, and prospective evaluation to assess real-world impact. Nevertheless, the present results establish a strong foundation for the use of unsupervised deep learning as part of a multimodal early-detection strategy.

5.3. Strengths of the Study

Several methodological features strengthen the robustness of the findings. First, a standardized and anatomically guided preprocessing pipeline was applied to panoramic radiographs to extract bilateral carotid regions of interest, enhancing calcification visibility while limiting noise through consistent cropping and contrast enhancement. Second, the use of deep embedded clustering based on convolutional autoencoder features enabled the model to learn nonlinear, data driven representations beyond what hand crafted descriptors alone can capture.

Model performance was evaluated at the patient level, aligning the analysis with clinical decision making. The concentration of high-risk patients within a single DEC cluster supports the clinical relevance of the learned latent features. In parallel, the questionnaire component covered a broad range of cardiovascular risk domains, providing a holistic perspective that extends beyond traditional biomedical factors. Machine learning analysis of these data highlighted the added contribution of behavioral and psychosocial variables. Finally, the focus on a resource limited setting shows the practical value of leveraging routinely acquired dental imaging for cardiovascular risk assessment.

5.4. Practical and Operational Challenges

Practical and operational challenges were primarily related to real-world data acquisition, patient linkage, and resource availability rather than model development alone. First, to the best of our knowledge, there is no clear precedent for applying deep clustering to carotid artery calcification assessment on panoramic radiographs, which constrained direct benchmarking and required a gap-driven methodological rationale. Second, ROI-level specialist review could not be integrated routinely during the data-collection phase because of practical constraints in expert availability within a high-throughput clinical environment. Third, because radiographs were obtained from a busy imaging setting, acquisition was conducted across multiple periods to minimize disruption to routine workflow while maintaining consistent imaging conditions. Finally, linking radiographs to questionnaire-based risk profiles required retrieving contact information from paper-based archives and conducting telephone follow-up, which demanded substantial time and direct financial resources (e.g., communication and repeated follow-up costs) and limited the number of

participants for whom complete questionnaire linkage could be achieved (n = 438) within the overall imaging cohort (n = 1,107).

5.5. Limitations and Potential Sources of Bias

Several limitations should be considered when interpreting these findings. First, the study lacks a direct vascular reference standard, such as duplex ultrasound or CT angiography. Consequently, cluster-associated risk is inferred from clinical records and questionnaire-based profiles rather than from measured carotid stenosis or plaque burden, and should be interpreted as risk enrichment rather than validated outcome prediction. In addition, ROI-level confirmation by an independent specialist was not available during the study period to verify carotid artery calcification and to differentiate common radiographic look-alikes. Accordingly, the imaging component is interpreted in terms of clustering consistency and risk enrichment rather than definitive radiographic confirmation. The number of high-risk patients available for patient-level validation was limited, increasing sensitivity to misclassification and restricting stratified analyses. In addition, the single-center design limits generalizability to other settings with different imaging systems, protocols, and population risk profiles.

The questionnaire component was cross-sectional and relied largely on self-reported data, making it vulnerable to recall, reporting, and selection biases. Moreover, questionnaire-based analyses were limited to the successfully linked and consenting subset (n = 438) rather than the full imaging cohort (n = 1,107), which may introduce non-response and selection effects and should be considered when generalizing questionnaire-based associations to the entire sample. The derived risk label also overlaps conceptually with several predictor variables, introducing potential circularity and inflation of performance estimates. Finally, imaging-based clustering and questionnaire analyses were conducted in parallel rather than within a unified predictive framework, preventing assessment of their incremental or combined predictive value.

5.6. Implications for Clinical Practice and Public Health

Despite these limitations, the findings have relevant implications for clinical practice and public health, particularly in resource constrained settings. The ability of deep embedded clustering to identify a compact and clinically plausible high-risk group from routine panoramic radiographs suggests a potential role for dental imaging in cardiovascular risk screening. When integrated into dental workflows, automated analysis of carotid regions could provide simple risk alerts to dentists, supporting referral decisions without additional imaging or consultation time.

At the population level, the results reinforce a multidimensional view of cardiovascular risk, in which traditional clinical factors interact with lifestyle, sleep, mental health, and environmental exposures. These findings support broader prevention strategies that extend beyond conventional risk factors and highlight the value of integrating simple risk profiling with routinely collected imaging to facilitate earlier identification and referral of high-risk individuals, particularly in low resource settings.

5.7. Future Directions and Outlook

This study represents an initial step in a broader research agenda, with several clear directions for future work. From an imaging perspective, extending beyond unsupervised clustering toward supervised detection and segmentation of carotid artery calcifications will be important once reliable annotations and vascular reference imaging become available. Such models would enable direct characterization of calcification morphology, laterality, and extent, and facilitate closer alignment with established prognostic frameworks. A second priority is prospective validation. Linking imaging features and questionnaire-based profiles to objective cardiovascular outcomes, including stroke and myocardial infarction, would allow calibration against clinical endpoints rather than derived risk labels. External validation across multiple centers and imaging systems will also be essential to assess robustness and generalizability.

Future research should further explore multimodal integration by combining imaging-derived features with questionnaire and basic clinical data within unified predictive models. For practical deployment, these advances should be supported by streamlined questionnaires, clear action thresholds, and interpretable outputs suitable for routine clinical use. This work provides a foundation for leveraging routine panoramic radiography, alongside multi-domain risk profiling, as an opportunistic approach to early cardiovascular risk identification, with particular relevance for resource-limited settings.

Chapter Six

6.1. Conclusion

This chapter brings together the key findings of the thesis and reflects on what they collectively mean for opportunistic cardiovascular risk assessment using dental panoramic radiographs. It summarizes the main results from the imaging-based deep clustering of carotid regions and the questionnaire-based risk profiling, highlights how these strands converge to identify a high-risk subset of patients, and distils the core messages for clinical practice and public health in resource-limited settings. The chapter also revisits the central aim of the work, draws out the broader conceptual implications for repurposing panoramic radiography as part of cardiovascular prevention pathways, and outlines how the insights gained here could guide future research and implementation efforts.

6.2. Summary of the Study

This thesis set out to examine whether routinely acquired dental panoramic radiographs, when analyzed with deep unsupervised learning and interpreted alongside questionnaire-based risk profiling, could contribute to opportunistic cardiovascular risk stratification in a resource-constrained setting. Using standardized carotid regions of interest extracted from 1,107 panoramic radiographs, a deep embedded clustering framework was developed to discover latent image-based groupings potentially related to carotid artery calcification phenotypes. In parallel, a multi-domain questionnaire captured sociodemographic characteristics, lifestyle and dietary habits, environmental exposures, medical history, and mental health indicators in a substantial patient subgroup.

Across these two pillars, the study showed that deep embedded clustering can form compact, well-separated clusters that concentrate the majority of clinically high-risk individuals, and that questionnaire-derived profiles distinguish high- from low-risk patients with high discriminative performance. Together, these strands demonstrate that panoramic radiographs, when paired with structured risk profiling, can provide more than purely dental information and may serve as an additional window onto cardiovascular vulnerability in everyday dental practice.

6.3. Main Conclusions

Several conclusions emerge from this study. First, deep embedded clustering of carotid regions in panoramic radiographs can identify image-based groupings that correspond to cardiovascular risk as inferred from clinical and contextual information. Internal validation, patient-level performance, and GradCAM++ visualizations indicate that the learned representations capture consistent calcification-related patterns in anatomically plausible regions rather than noise or artefacts.

Second, questionnaire-based analyses demonstrate that cardiovascular risk in this cohort is strongly associated with age, adiposity, socioeconomic disadvantage, lifestyle behaviors, sleep disturbance, psychological distress, and environmental exposures. A non-linear machine learning model trained on these variables achieved strong discrimination between high- and low-risk individuals, highlighting the predictive value of low-cost, self-reported data in this setting.

Finally, the observed concordance between image-derived clusters and questionnaire-based risk profiles suggests that panoramic radiographs and simple risk questionnaires provide complementary information. Individuals assigned to adverse imaging clusters tended to exhibit a higher burden of both conventional and non-conventional risk factors, supporting the role of carotid calcifications on panoramic radiographs as a meaningful element within a broader, multidimensional cardiovascular risk framework rather than as incidental findings.

6.4. Implications and Outlook

Although this work remains exploratory and internally validated, its findings support the feasibility of re-purposing existing dental imaging infrastructure to contribute to earlier cardiovascular risk flagging, particularly in low-resource environments where advanced vascular imaging is scarce. In practical terms, the results point toward future systems in

which carotid regions are automatically analyzed whenever a panoramic radiograph is acquired, and the resulting image-based risk signal is interpreted alongside a brief, structured questionnaire to generate a simple, actionable summary for both dentist and patient.

At a broader level, the thesis reinforces a multi-domain view of cardiovascular risk, in which structural arterial changes, metabolic status, lifestyle habits, sleep, psychosocial stress, and environmental burdens interact to shape overall vulnerability. For clinicians and public-health planners, this implies that opportunistic screening strategies built around panoramic radiography and simple questionnaires should be embedded within wider efforts to address modifiable behaviors, improve mental-health support, and mitigate environmental stressors. Moving from proof-of-concept to practice will require prospective studies linking panoramic-radiograph–based phenotypes and questionnaire profiles to vascular imaging and hard cardiovascular outcomes, as well as external validation across centers and devices.

6.5. Final Remarks

In summary, this thesis provides an initial but substantive step toward viewing dental panoramic radiographs as part of a wider cardiovascular-screening ecosystem rather than as narrow, tooth-focused examinations. By showing that unsupervised deep clustering can extract clinically meaningful patterns from carotid regions and that these patterns align with multi-domain cardiovascular risk profiles derived from simple questionnaires, the work opens a pathway for opportunistic, equity-oriented risk assessment in everyday dental settings. With appropriate validation, simplification, and integration into real-world workflows, such approaches have the potential to support earlier and more accessible cardiovascular prevention for populations in which traditional screening resources are limited.

References

Abdalla-Aslan, R., Yeshua, T., Kabla, D., Leichter, I., & Nadler, C. (2020). An artificial intelligence system using machine-learning for automatic detection and classification of dental restorations in panoramic radiography. *Oral Surgery, Oral Medicine, Oral Pathology and Oral Radiology*, *130*(5), 593–602. https://doi.org/10.1016/j.oooo.2020.05.012

Abreu, S. G. de, Simoes, N. M., Zanini, A. P., Girundi, M. G., Silva, A. I. V., & Manzi, F. R. (2017). Use of digital panoramic radiography to detect cervical calcifications in obese individuals. *Journal of Oral Diagnosis*, *2*, 1–6. https://doi.org/10.5935/2525-5711.20170043

Adar, S. D., Sheppard, L., Vedal, S., Polak, J. F., Sampson, P. D., Diez Roux, A. V., Budoff, M., Jacobs, D. R., Barr, R. G., Watson, K., & Kaufman, J. D. (2013). Fine Particulate Air Pollution and the Progression of Carotid Intima-Medial Thickness: A Prospective Cohort Study from the Multi-Ethnic Study of Atherosclerosis and Air Pollution. *PLOS Medicine*, *10*(4), e1001430. https://doi.org/10.1371/JOURNAL.PMED.1001430

Adla, T., & Adlova, R. (2015). Multimodality Imaging of Carotid Stenosis. *The International Journal of Angiology : Official Publication of the International College of Angiology, Inc*, *24*(3), 179. https://doi.org/10.1055/S-0035-1556056

Aghazadehsanai, N., Chang, T. I., Garrett, N. R., & Friedlander, A. H. (2017). Prevalence of calcified carotid artery atheromas on digital panoramic images among perimenopausal and postmenopausal African American women. *Oral Surgery, Oral Medicine, Oral Pathology and Oral Radiology*, *123*(5), 621–625. https://doi.org/10.1016/J.OOOO.2017.01.011

Akinyelure, O. P., Hubbard, D., Sakhuja, S., Hardy, S. T., Oparil, S., Cherrington, A. L., Reynolds, K., Wozniak, G., & Muntner, P. (2021). Factors Associated With Not Having a Healthcare Visit in the Past Year Among US Adults With Hypertension: Data From NHANES 2013–2018. *American Journal of Hypertension*, *35*(2), 132. https://doi.org/10.1093/AJH/HPAB153

AlGhibiwi, H. K., Sarawi, W. S., Alosaimi, M. E., Alhusaini, A. M., Assiri, M. A., & Algarzae, N. K. (2023). The Association between Cardiovascular Risk Factors and Carotid Intima-Media Thickness in 42,726 Adults in UK Biobank: A Cross-Sectional Study. *Journal of Cardiovascular Development and Disease 2023, Vol. 10, Page 358*, *10*(9), 358. https://doi.org/10.3390/JCDD10090358

Aljameel, S. S., Althumairy, L., Albassam, B., Alsheikh, G., Albluwi, L., Althukair, R., Alhareky, M., Alamri, A., Alabdan, A., & Shahin, S. Y. (2023). Predictive Artificial Intelligence Model for Detecting Dental Age Using Panoramic Radiograph Images. *Big Data and Cognitive Computing*, *7*(1), 8. https://doi.org/10.3390/bdcc7010008

Almog, D. M., Illig, K. A., Carter, L. C., Friedlander, A. H., Brooks, S. L., & Grimes, R. M. (2004). Diagnosis of non-dental conditions. Carotid artery calcifications on panoramic radiographs identify patients at risk for stroke. *The New York State Dental Journal*, *70*(8), 20–25.

Almog DM, I. K. C. L. F. A. B. S. G. RM. (2004). Diagnosis of non-dental conditions. Carotid artery calcifications on panoramic radiographs identify patients at risk for stroke. *N Y State Dent J.*, *70(8)*, 20–25.

Alsiddig, A. M., & Ali, I. A. (2024). Effects of Smoking on Intima-Media Thickness of the Common Carotid Artery Using Ultrasonography. *Artery Research*, *30*(1), 1–11. https://doi.org/10.1007/S44200-024-00044-W/TABLES/6

Alsweed, A., Farah, R., Ps, S., & Farah, R. (2019). The Prevalence and Correlation of Carotid Artery Calcifications and Dental Pulp Stones in a Saudi Arabian Population. *Diseases (Basel, Switzerland)*, *7*(3). https://doi.org/10.3390/diseases7030050

Alves, N., Deana, N. F., & Garay, I. (2014). Detection of common carotid artery calcifications on panoramic radiographs: prevalence and reliability. *International Journal of Clinical and Experimental Medicine*, *7*(8), 1931. https://pmc.ncbi.nlm.nih.gov/articles/PMC4161533/

Ameli, N., Moghaddam, M. M., Lai, H., & Pacheco-Pereira, C. (2025). Automated quality evaluation of dental panoramic radiographs using deep learning. *Imaging Science in Dentistry*, *55*(2), 175. https://doi.org/10.5624/ISD.20240232

Amitay, M., Barnett-Itzhaki, Z., Sudri, S., Drori, C., Wase, T., Abu-El-Naaj, I., Ben-Ari, M. K., Rieck, M., Avni, Y., Pogozelich, G., Weiss, E., & Mosseri, M. (2023). Deep convolution neural network for screening carotid calcification in dental panoramic radiographs. *PLOS Digital Health*, *2*(4), e0000081. https://doi.org/10.1371/JOURNAL.PDIG.0000081

Anderson, G. B., Ashforth, R., Steinke, D. E., Ferdinandy, R., & Findlay, J. M. (2000). CT Angiography for the Detection and Characterization of Carotid Artery Bifurcation Disease. *Stroke*, *31*(9), 2168–2174. https://doi.org/10.1161/01.STR.31.9.2168

Andrews, J., Psaltis, P. J., Bayturan, O., Shao, M., Stegman, B., Elshazly, M., Kapadia, S. R., Tuzcu, E. M., Nissen, S. E., Nicholls, S. J., & Puri, R. (2018). Warfarin Use Is Associated With Progressive Coronary Arterial Calcification: Insights From Serial Intravascular Ultrasound. *JACC: Cardiovascular Imaging*, *11*(9), 1315–1323. https://doi.org/10.1016/J.JCMG.2017.04.010

Aoun, G., & Nasseh, I. (2018). Calcified Triticeous Cartilage Detected on Digital Panoramic Radiographs in a Sample of Lebanese Population. *Journal of Clinical Imaging Science*, *8*(1). https://doi.org/10.4103/JCIS.JCIS_11_18

Arzani, S., Soltani, P., Karimi, A., Yazdi, M., Ayoub, A., Khurshid, Z., Galderisi, D., & Devlin, H. (2025). Detection of carotid artery calcifications using artificial intelligence

in dental radiographs: a systematic review and meta-analysis. *BMC Medical Imaging*, *25*(1), 174. https://doi.org/10.1186/S12880-025-01719-9

Atalay, Y., Asutay, F., Agacayak, K. S., Koparal, M., Adali, F., & Gulsun, B. (2015). Evaluation of calcified carotid atheroma on panoramic radiographs and Doppler ultrasonography in an older population. *Clinical Interventions in Aging*, *10*, 1121–1129. https://doi.org/10.2147/CIA.S84683

Aung, M. T. Z., Lim, S. H., Han, J., Yang, S., Kang, J. H., Kim, J. E., Huh, K. H., Yi, W. J., Heo, M. S., & Lee, S. S. (2024). Deep learning-based automatic segmentation of the mandibular canal on panoramic radiographs: A multi-device study. *Imaging Science in Dentistry*, *54*(1), 81–91. https://doi.org/10.5624/ISD.20230245

Azimi, S., Sarlak, H., & Tofangchiha, M. (2016). Determining the Prevalence of Carotid Artery Calcification and Associations with Medical History Using Dental Panoramic Radiographs. *Dental and Medical Problems*, *53*(1), 29–33. https://doi.org/10.17219/DMP/60966

Baldassarre, D., Castelnuovo, S., Frigerio, B., Amato, M., Werba, J. P., De Jong, A., Ravani, A. L., Tremoli, E., & Sirtori, C. R. (2009). Effects of Timing and Extent of Smoking, Type of Cigarettes, and Concomitant Risk Factors on the Association Between Smoking and Subclinical Atherosclerosis. *Stroke*, *40*(6), 1991–1998. https://doi.org/10.1161/STROKEAHA.108.543413

Barnoya, J., & Glantz, S. A. (2005). Cardiovascular Effects of Secondhand Smoke. *Circulation*, *111*(20), 2684–2698. https://doi.org/10.1161/CIRCULATIONAHA.104.492215

Barrett, H., O'Keeffe, M., Kavanagh, E., Walsh, M., & O'Connor, E. M. (2018). Is Matrix Gla Protein Associated with Vascular Calcification? A Systematic Review. *Nutrients*, *10*(4), 415. https://doi.org/10.3390/NU10040415

Başaran, M., Çelik, Ö., Bayrakdar, I. S., Bilgir, E., Orhan, K., Odabaş, A., Aslan, A. F., & Jagtap, R. (2022). Diagnostic charting of panoramic radiography using deep-learning artificial intelligence system. *Oral Radiology*, *38*(3), 363–369. https://doi.org/10.1007/s11282-021-00572-0

Bažadona, D., Matovinović, M., Krbot Skorić, M., Grbavac, H., Belančić, A., & Malojčić, B. (2023). The Interconnection between Carotid Intima–Media Thickness and Obesity: Anthropometric, Clinical and Biochemical Correlations. *Medicina (Lithuania)*, *59*(9), 1512. https://doi.org/10.3390/MEDICINA59091512/S1

Beddhu, S., Boucher, R. E., Sun, J., Balu, N., Chonchol, M., Navaneethan, S., Chertow, G. M., Townsend, R., Haley, W., Cheung, A. K., Conroy, M. B., Raj, D. S., Xu, D., George, T., Yunis, R., Wei, G., Canton, G., Bates, J., Chen, J., … Yuan, C. (2021). Chronic kidney disease, atherosclerotic plaque characteristics on carotid magnetic resonance imaging, and cardiovascular outcomes. *BMC Nephrology*, *22*(1), 1–10. https://doi.org/10.1186/S12882-021-02260-X/FIGURES/3

Bengtsson, V. W., Persson, G. R., Berglund, J., & Renvert, S. (2019). Carotid calcifications in panoramic radiographs are associated with future stroke or ischemic heart diseases: a long-term follow-up study. *Clinical Oral Investigations*, *23*(3), 1171–1179. https://doi.org/10.1007/s00784-018-2533-8

Bergström, G., Fagerberg, B., Sallsten, G., Lundh, T., & Barregard, L. (2015). Is Cadmium Exposure Associated with the Burden, Vulnerability and Rupture of Human Atherosclerotic Plaques? *PLOS ONE*, *10*(3), e0121240. https://doi.org/10.1371/JOURNAL.PONE.0121240

Beser, B., Reis, T., Berber, M. N., Topaloglu, E., Gungor, E., Kılıc, M. C., Duman, S., Çelik, Ö., Kuran, A., & Bayrakdar, I. S. (2024). YOLO-V5 based deep learning approach for tooth detection and segmentation on pediatric panoramic radiographs in mixed dentition. *BMC Medical Imaging*, *24*(1). https://doi.org/10.1186/S12880-024-01338-W

Biswas, A., Oh, P. I., Faulkner, G. E., Bajaj, R. R., Silver, M. A., Mitchell, M. S., & Alter, D. A. (2015). Sedentary Time and Its Association With Risk for Disease Incidence, Mortality, and Hospitalization in Adults. *Https://Doi.Org/10.7326/M14-1651*, *162*(2), 123–132. https://doi.org/10.7326/M14-1651

Bladh, M., Gustafsson, N., Engström, G., Kennbäck, C., Klinge, B., Nilsson, P. M., Jönsson, D., & Levring Jäghagen, E. (2024). Defined shapes of carotid artery calcifications on panoramic radiographs correlate with specific signs of cardiovascular disease on ultrasound examination. *Oral Surgery, Oral Medicine, Oral Pathology and Oral Radiology*, *137*(4), 408–420. https://doi.org/10.1016/j.oooo.2023.12.783

Blanes, N., Houthuijs, D., Swart, W., Sainz de la Maza, M., Ramos, M., Castell, N., & Van Kempen, E. (2017). Noise in Europe 2017: updated assessment ETC/ACM Technical Paper 2016/13. *European Topic Centre on Air Pollution and Climate Change Mitigation*, *13*(6), 200–203.

Bonfanti-Gris, M., Garcia-Cañas, A., Alonso-Calvo, R., Salido Rodriguez-Manzaneque, M. P., & Pradies Ramiro, G. (2022). Evaluation of an Artificial Intelligence web-based software to detect and classify dental structures and treatments in panoramic radiographs. *Journal of Dentistry*, *126*, 104301. https://doi.org/10.1016/j.jdent.2022.104301

Bonfanti-Gris, M., Herrera, A., Salido Rodríguez-Manzaneque, M. P., Martínez-Rus, F., & Pradíes, G. (2025). Deep learning for tooth detection and segmentation in panoramic radiographs: a systematic review and meta-analysis. *BMC Oral Health*, *25*(1), 1–18. https://doi.org/10.1186/S12903-025-06349-9/FIGURES/5

Borba, D. L., Hipólito, U. V., & Pereira, Y. C. L. (2016). Early diagnosis of atherosclerosis with panoramic radiographs: a review. *Jornal Vascular Brasileiro*, *15*(4), 302. https://doi.org/10.1590/1677-5449.002316

Brar, A., DeColibus, K., Rasner, D. S., Haynes, A. R., Pancratz, F., Oladiran, O., Gbadamosi, S. O., & Owosho, A. A. (2024). Carotid Artery Calcification Detected on Panoramic

Radiography Is Significantly Related to Cerebrovascular Accident, Coronary Artery Disease, and Poor Oral Health: A Retrospective Cross-Sectional Study. *Dentistry Journal 2024, Vol. 12, Page 99*, *12*(4), 99. https://doi.org/10.3390/DJ12040099

Brook, R. D., Rajagopalan, S., Pope, C. A., Brook, J. R., Bhatnagar, A., Diez-Roux, A. V., Holguin, F., Hong, Y., Luepker, R. V., Mittleman, M. A., Peters, A., Siscovick, D., Smith, S. C., Whitsel, L., & Kaufman, J. D. (2010). Particulate matter air pollution and cardiovascular disease: An update to the scientific statement from the American Heart Association. *Circulation*, *121*(21), 2331–2378. https://doi.org/10.1161/CIR.0B013E3181DBECE1

Bull, F. C., Al-Ansari, S. S., Biddle, S., Borodulin, K., Buman, M. P., Cardon, G., Carty, C., Chaput, J. P., Chastin, S., Chou, R., Dempsey, P. C., Dipietro, L., Ekelund, U., Firth, J., Friedenreich, C. M., Garcia, L., Gichu, M., Jago, R., Katzmarzyk, P. T., … Willumsen, J. F. (2020). World Health Organization 2020 guidelines on physical activity and sedentary behaviour. *British Journal of Sports Medicine*, *54*(24), 1451. https://doi.org/10.1136/BJSPORTS-2020-102955

Carasso, S., Ben Amy, D. P., Issawy, M., Kusniec, F., Ghanim, D., Sudarsky, D., Elbaz-Greener, G., Kinany, W., Shmuel, C., El-Naaj, I. A., Kachel, E., & Amir, O. (2020). The association between carotid calcium on dental panoramic radiographs and coronary calcium score on chest computerized tomography. *Dentomaxillofacial Radiology*, *50*(2), 20200174. https://doi.org/10.1259/DMFR.20200174

Caron, M., Bojanowski, P., Joulin, A., & Douze, M. (2018). Deep Clustering for Unsupervised Learning of Visual Features. *Lecture Notes in Computer Science (Including Subseries Lecture Notes in Artificial Intelligence and Lecture Notes in Bioinformatics)*, *11218 LNCS*, 139–156. https://doi.org/10.1007/978-3-030-01264-9_9

CEE Noffke, EJ Raubenheimer, & NJ Chabikuli. (2015). *Radiopacities in soft tissue on dental radiographs: diagnostic considerations*. www.sada.co.za

Çetin, M. B., Sezgin, Y., Yilmaz, M. N. N., & Seçgin, C. K. (2020). Assessment of carotid artery calcifications on digital panoramic radiographs and their relationship with periodontal condition and cardiovascular risk factors. *International Dental Journal*, *71*(2), 160–166. https://doi.org/10.1111/IDJ.12618

Chan, H. P., Samala, R. K., Hadjiiski, L. M., & Zhou, C. (2020). Deep Learning in Medical Image Analysis. *Advances in Experimental Medicine and Biology*, *1213*, 3. https://doi.org/10.1007/978-3-030-33128-3_1

Chang, H. B., Javed, A., Dai, Q., Kappes, J. C., Clemens, T. L., Darley-Usmar, V. M., McDonald, J. M., & Chen, Y. (2008). Oxidative Stress Induces Vascular Calcification through Modulation of the Osteogenic Transcription Factor Runx2 by AKT Signaling. *The Journal of Biological Chemistry*, *283*(22), 15319. https://doi.org/10.1074/JBC.M800021200

Chattopadhyay, A., Sarkar, A., Howlader, P., & Balasubramanian, V. N. (2018). Grad-CAM++: Improved Visual Explanations for Deep Convolutional Networks. *Proceedings - 2018 IEEE Winter Conference on Applications of Computer Vision, WACV 2018*, *2018-January*, 839–847. https://doi.org/10.1109/WACV.2018.00097

Clark, C., & Paunovic, K. (2018). WHO Environmental Noise Guidelines for the European Region: A Systematic Review on Environmental Noise and Quality of Life, Wellbeing and Mental Health. *International Journal of Environmental Research and Public Health*, *15*(11), 2400. https://doi.org/10.3390/IJERPH15112400

Davis, C. R., Hodgson, J. M., Woodman, R., Bryan, J., Wilson, C., & Murphy, K. J. (2017). A Mediterranean diet lowers blood pressure and improves endothelial function: Results from the MedLey randomized intervention trial. *American Journal of Clinical Nutrition*, *105*(6), 1305–1313. https://doi.org/10.3945/ajcn.116.146803

Demer, L. L., & Tintut, Y. (2014). Inflammatory, Metabolic, and Genetic Mechanisms of Vascular Calcification. *Arteriosclerosis, Thrombosis, and Vascular Biology*, *34*(4), 715–723. https://doi.org/10.1161/ATVBAHA.113.302070

Dhar, A. K., & Barton, D. A. (2016). Depression and the Link with Cardiovascular Disease. *Frontiers in Psychiatry*, *7*(MAR), 33. https://doi.org/10.3389/FPSYT.2016.00033

Diaz, K. M., Howard, V. J., Hutto, B., Colabianchi, N., Vena, J. E., Safford, M. M., Blair, S. N., & Hooker, S. P. (2017). Patterns of sedentary behavior and mortality in U.S. middle-aged and older adults: A national cohort study. *Annals of Internal Medicine*, *167*(7), 465. https://doi.org/10.7326/M17-0212

Ding, H., Wu, J., Zhao, W., Matinlinna, J. P., Burrow, M. F., & Tsoi, J. K. H. (2023). Artificial intelligence in dentistry—A review. *Frontiers in Dental Medicine*, *4*, 1085251. https://doi.org/10.3389/FDMED.2023.1085251

Domínguez, F., Fuster, V., Fernández-Alvira, J. M., Fernández-Friera, L., López-Melgar, B., Blanco-Rojo, R., Fernández-Ortiz, A., García-Pavía, P., Sanz, J., Mendiguren, J. M., Ibañez, B., Bueno, H., Lara-Pezzi, E., & Ordovás, J. M. (2019). Association of Sleep Duration and Quality With Subclinical Atherosclerosis. *Journal of the American College of Cardiology*, *73*(2), 134–144. https://doi.org/10.1016/J.JACC.2018.10.060

Durham, A. L., Speer, M. Y., Scatena, M., Giachelli, C. M., & Shanahan, C. M. (2018). Role of smooth muscle cells in vascular calcification: implications in atherosclerosis and arterial stiffness. *Cardiovascular Research*, *114*(4), 590–600. https://doi.org/10.1093/CVR/CVY010

Ebong, I. A., Quesada, O., Fonkoue, I. T., Mattina, D., Sullivan, S., Oliveira, G. M. M. de, Spikes, T., Sharma, J., Commodore, Y., Ogunniyi, M. O., Aggarwal, N. R., & Vaccarino, V. (2024). The Role of Psychosocial Stress on Cardiovascular Disease in Women: JACC State-of-the-Art Review. *Journal of the American College of Cardiology*, *84*(3), 298–314. https://doi.org/10.1016/J.JACC.2024.05.016

Egan, B. M., Li, J., Small, J., Nietert, P. J., & Sinopoli, A. (2014). The Growing Gap in Hypertension Control Between Insured and Uninsured Adults: NHANES 1988–2010. *Hypertension*, *64*(5), 997. https://doi.org/10.1161/HYPERTENSIONAHA.114.04276

Ekelund, U., Tarp, J., Fagerland, M. W., Johannessen, J. S., Hansen, B. H., Jefferis, B. J., Whincup, P. H., Diaz, K. M., Hooker, S., Howard, V. J., Chernofsky, A., Larson, M. G., Spartano, N., Vasan, R. S., Dohrn, I. M., Hagströmer, M., Edwardson, C., Yates, T., Shiroma, E. J., … Lee, I. M. (2020). Joint associations of accelero-meter measured physical activity and sedentary time with all-cause mortality: a harmonised meta-analysis in more than 44 000 middle-aged and older individuals. *British Journal of Sports Medicine*, *54*(24), 1499–1506. https://doi.org/10.1136/BJSPORTS-2020-103270

Ekelund, U., Tarp, J., Steene-Johannessen, J., Hansen, B. H., Jefferis, B., Fagerland, M. W., Whincup, P., Diaz, K. M., Hooker, S. P., Chernofsky, A., Larson, M. G., Spartano, N., Vasan, R. S., Dohrn, I. M., Hagströmer, M., Edwardson, C., Yates, T., Shiroma, E., Anderssen, S. A., & Lee, I. M. (2019). Dose-response associations between accelerometry measured physical activity and sedentary time and all cause mortality: systematic review and harmonised meta-analysis. *BMJ*, *366*. https://doi.org/10.1136/BMJ.L4570

Estruch, R., Ros, E., Salas-Salvadó, J., Covas, M.-I., Corella, D., Arós, F., Gómez-Gracia, E., Ruiz-Gutiérrez, V., Fiol, M., Lapetra, J., Lamuela-Raventos, R. M., Serra-Majem, L., Pintó, X., Basora, J., Muñoz, M. A., Sorlí, J. V., Martínez, J. A., & Martínez-González, M. A. (2013). Primary Prevention of Cardiovascular Disease with a Mediterranean Diet. *Zeitschrift Fur Gefassmedizin*, *10*(2), 28. https://doi.org/10.1056/NEJMOA1200303

Fagerberg, B., Bergström, G., Borén, J., & Barregard, L. (2012). Cadmium exposure is accompanied by increased prevalence and future growth of atherosclerotic plaques in 64-year-old women. *Journal of Internal Medicine*, *272*(6), 601–610. https://doi.org/10.1111/J.1365-2796.2012.02578.X

Faresjö, Å., Theodorsson, E., Stomby, A., Quist, H., Jones, M. P., Östgren, C. J., Dahlqvist, P., & Faresjö, T. (2024). Higher hair cortisol levels associated with previous cardiovascular events and cardiovascular risks in a large cross-sectional population study. *BMC Cardiovascular Disorders*, *24*(1), 1–10. https://doi.org/10.1186/S12872-024-04221-2/TABLES/6

Förstermann, U., Xia, N., & Li, H. (2017). Roles of Vascular Oxidative Stress and Nitric Oxide in the Pathogenesis of Atherosclerosis. *Circulation Research*, *120*(4), 713–735. https://doi.org/10.1161/CIRCRESAHA.116.309326

Friedlander, A. H., & Lande, A. (1981). Panoramic radiographic identification of carotid arterial plaques. *Oral Surgery, Oral Medicine, Oral Pathology*, *52*(1), 102–104. https://doi.org/10.1016/0030-4220(81)90181-X

Fukuda, M., Inamoto, K., Shibata, N., Ariji, Y., Yanashita, Y., Kutsuna, S., Nakata, K., Katsumata, A., Fujita, H., & Ariji, E. (2020). Evaluation of an artificial intelligence system for detecting vertical root fracture on panoramic radiography. *Oral Radiology*, *36*(4), 337–343. https://doi.org/10.1007/s11282-019-00409-x

Full, K. M., Huang, T., Shah, N. A., Allison, M. A., Michos, E. D., Duprez, D. A., Redline, S., & Lutsey, P. L. (2023). Sleep Irregularity and Subclinical Markers of Cardiovascular Disease: The Multi-Ethnic Study of Atherosclerosis. *Journal of the American Heart Association*, *12*(4), 27361. https://doi.org/10.1161/JAHA.122.027361

Gao, Y., Zhang, P., Xie, Y., Han, J., Zeng, L., Ning, N., Zheng, Q., Li, H., Chen, X., & Chen, Z. (2024). Application of transformers in stomatological imaging: A review. *Digital Medicine*, *10*(3). https://doi.org/10.1097/DM-2024-00001

Garoff, M., Ahlqvist, J., Edin, L. T., Jensen, S., Levring Jäghagen, E., Petäjäniemi, F., Wester, P., & Johansson, E. (2019). Bilateral vessel-outlining carotid artery calcifications in panoramic radiographs: an independent risk marker for vascular events. *BMC Cardiovascular Disorders*, *19*(1). https://doi.org/10.1186/S12872-019-1211-3

Garoff, M., Ahlqvist, J., Levring Jäghagen, E., Wester, P., & Johansson, E. (2025). Carotid calcifications in panoramic radiographs can predict vascular risk. *Dento Maxillo Facial Radiology*, *54*(1), 28–34. https://doi.org/10.1093/DMFR/TWAE057

Grau-Perez, M., Caballero-Mateos, M. J., Domingo-Relloso, A., Navas-Acien, A., Gomez-Ariza, J. L., Garcia-Barrera, T., Leon-Latre, M., Soriano-Gil, Z., Jarauta, E., Cenarro, A., Moreno-Franco, B., Laclaustra, M., Civeira, F., Casasnovas, J. A., Guallar, E., & Tellez-Plaza, M. (2022). Toxic Metals and Subclinical Atherosclerosis in Carotid, Femoral, and Coronary Vascular Territories: The Aragon Workers Health Study. *Arteriosclerosis, Thrombosis, and Vascular Biology*, *42*(1), 87–99. https://doi.org/10.1161/ATVBAHA.121.316358

Guldbrand, C., Barregard, L., Sallsten, G., Forsgard, N., Lundh, T., Borné, Y., Fagerberg, B., Engström, G., Bergström, G., & Harari, F. (2024). Low-level exposure to lead and atherosclerosis in the carotid arteries: Results from the Swedish population-based cohort SCAPIS. *Environmental Research*, *244*, 117900. https://doi.org/10.1016/J.ENVRES.2023.117900

Guo, X., Gao, L., Liu, X., & Yin, J. (2017). *Improved Deep Embedded Clustering with Local Structure Preservation*.

Gustafsson, N., Ahlqvist, J. B., Näslund, U., Wester, P., Buhlin, K., Gustafsson, A., & Levring Jäghagen, E. (2018). Calcified carotid artery atheromas in panoramic radiographs are associated with a first myocardial infarction: a case-control study. *Oral Surgery, Oral Medicine, Oral Pathology and Oral Radiology*, *125*(2), 199-204.e1. https://doi.org/10.1016/J.OOOO.2017.10.009

Ha, E. G., Jeon, K. J., Kim, Y. H., Kim, J. Y., & Han, S. S. (2021). Automatic detection of mesiodens on panoramic radiographs using artificial intelligence. *Scientific Reports 2021 11:1*, *11*(1), 1–8. https://doi.org/10.1038/s41598-021-02571-x

Hadiani, M. R., Dezfooli-manesh, S., Shoeibi, S., Ziarati, P., & Mousavi Khaneghah, A. (2015). Trace elements and heavy metals in mineral and bottled drinking waters on the Iranian market. *Food Additives & Contaminants. Part B, Surveillance*, *8*(1), 18–24. https://doi.org/10.1080/19393210.2014.947526

Harari, F., Barregard, L., Östling, G., Sallsten, G., Hedblad, B., Forsgard, N., Borné, Y., Fagerberg, B., & Engström, G. (2019). Blood Lead Levels and Risk of Atherosclerosis in the Carotid Artery: Results from a Swedish Cohort. *Environmental Health Perspectives*, *127*(12). https://doi.org/10.1289/EHP5057

Havranek, E. P., Mujahid, M. S., Barr, D. A., Blair, I. V., Cohen, M. S., Cruz-Flores, S., Davey-Smith, G., Dennison-Himmelfarb, C. R., Lauer, M. S., Lockwood, D. W., Rosal, M., & Yancy, C. W. (2015). Social Determinants of Risk and Outcomes for Cardiovascular Disease. *Circulation*, *132*(9), 873–898. https://doi.org/10.1161/CIR.0000000000000228

Helmi, J., Alhariri, Z., Al-Jawfi, K., & Shamala, A. (2020). Prevalence of carotid artery calcification detected by digital panoramic radiographs in a sample of yemeni dental patients. *Journal of Oral Research*, *8*(6), 510–516. https://doi.org/10.17126/JORALRES.2019.076

Higashi, Y. (2023). Smoking cessation and vascular endothelial function. *Hypertension Research*, *46*(12), 2670–2678. https://doi.org/10.1038/S41440-023-01455-Z;KWRD

Hiraiwa, T., Ariji, Y., Fukuda, M., Kise, Y., Nakata, K., Katsumata, A., Fujita, H., & Ariji, E. (2019). A deep-learning artificial intelligence system for assessment of root morphology of the mandibular first molar on panoramic radiography. *Dentomaxillofacial Radiology*, *48*(3), 20180218. https://doi.org/10.1259/dmfr.20180218

Howard, G., Wagenknecht, L. E., Burke, G. L., Diez-Roux, A., Evans, G. W., McGovern, P., Nieto, F. J., & Tell, G. S. (1998). Cigarette Smoking and Progression of Atherosclerosis: The Atherosclerosis Risk in Communities (ARIC) Study. *JAMA*, *279*(2), 119–124. https://doi.org/10.1001/JAMA.279.2.119

Huang, T., Mariani, S., & Redline, S. (2020). Sleep Irregularity and Risk of Cardiovascular Events: The Multi-Ethnic Study of Atherosclerosis. *Journal of the American College of Cardiology*, *75*(9), 991–999. https://doi.org/10.1016/J.JACC.2019.12.054

Ibraheem, W. I., Bhati, A. K., Alhomood, M. A., Allayl, O. A., Qsadi, A. A., Mohammed, T. I. M., & Aljabri, Y. S. (2023). Relationship between Carotid Artery Calcification and Periodontitis in the Saudi Population: A Retrospective Study. *Applied Sciences 2023, Vol. 13, Page 12370*, *13*(22), 12370. https://doi.org/10.3390/APP132212370

Icoz, D., & Akgunlu, F. (2019). Prevalence of detected soft tissue calcifications on digital panoramic radiographs. *SRM Journal of Research in Dental Sciences*, *10*(1), 21. https://doi.org/10.4103/SRMJRDS.SRMJRDS_60_18

Janiszewska-Olszowska, J., Jakubowska, A., Gieruszczak, E., Jakubowski, K., Wawrzyniak, P., & Grocholewicz, K. (2022). Carotid Artery Calcifications on Panoramic Radiographs. *International Journal of Environmental Research and Public Health*, *19*(21), 14056. https://doi.org/10.3390/IJERPH192114056

Janssen, I., Powell, L. H., Matthews, K. A., Cursio, J. F., Hollenberg, S. M., Sutton-Tyrrell, K., Bromberger, J. T., & Everson-Rose, S. A. (2011). Depressive Symptoms are Related to Progression of Coronary Calcium in Midlife Women: The Study of Women's Health Across the Nation (SWAN) Heart Study. *American Heart Journal*, *161*(6), 1186. https://doi.org/10.1016/J.AHJ.2011.03.017

Jebari-Benslaiman, S., Galicia-García, U., Larrea-Sebal, A., Olaetxea, J. R., Alloza, I., Vandenbroeck, K., Benito-Vicente, A., & Martín, C. (2022). Pathophysiology of Atherosclerosis. *International Journal of Molecular Sciences*, *23*(6), 3346. https://doi.org/10.3390/IJMS23063346

Jefferis, B. J., Lowe, G. D. O., Welsh, P., Rumley, A., Lawlor, D. A., Ebrahim, S., Carson, C., Doig, M., Feyerabend, C., McMeekin, L., Wannamethee, S. G., Cook, D. G., & Whincup, P. H. (2010). Secondhand smoke (SHS) exposure is associated with circulating markers of inflammation and endothelial function in adult men and women. *Atherosclerosis*, *208*(2), 550–556. https://doi.org/10.1016/j.atherosclerosis.2009.07.044

Jespersen, T., Møllehave, L. T., Thuesen, B. H., Skaaby, T., Rossing, P., Toft, U., Jørgensen, N. R., Corfixen, B. L., Jakobsen, J., Frimodt-Møller, M., & Linneberg, A. (2020). Uncarboxylated matrix Gla-protein: A biomarker of vitamin K status and cardiovascular risk. *Clinical Biochemistry*, *83*, 49–56. https://doi.org/10.1016/J.CLINBIOCHEM.2020.05.005

Ji, X., Leng, X.-Y., Dong, Y., Ma, Y.-H., Xu, W., Cao, X.-P., Hou, X.-H., Dong, Q., Tan, L., & Yu, J.-T. (2019). Modifiable risk factors for carotid atherosclerosis: a meta-analysis and systematic review. *Annals of Translational Medicine*, *7*(22), 632. https://doi.org/10.21037/ATM.2019.10.115

Kadyan, V., Vaddi, A., Nagpal, A., Molina, M. R., Lurie, A. G., & Tadinada, A. (2024). Evaluation of Cone-Beam Computed Tomography Scans to Develop a Staging Method of External Carotid Artery Calcification. *Journal of Clinical Medicine 2024, Vol. 13, Page 3189*, *13*(11), 3189. https://doi.org/10.3390/JCM13113189

Kanejima, Y., Shimogai, T., Kitamura, M., Ishihara, K., & Izawa, K. P. (2022). Impact of health literacy in patients with cardiovascular diseases: A systematic review and meta-analysis. *Patient Education and Counseling*, *105*(7), 1793–1800. https://doi.org/10.1016/J.PEC.2021.11.021

Karlsson, A., Gustafsson, N., Wester, P., Zamure-Damberga, L., & Levring Jäghagen, E. (2025). Carotid artery calcifications on panoramic radiographs are associated with vascular disease severity on carotid ultrasound. *Dento Maxillo Facial Radiology*. https://doi.org/10.1093/DMFR/TWAF061

Kats, L., Vered, M., Zlotogorski-Hurvitz, A., & Harpaz, I. (2019). Atherosclerotic carotid plaque on panoramic radiographs: neural network detection. *International Journal of Computerized Dentistry*, *22*(2), 163–169. https://europepmc.org/article/med/31134222

Katsiki, N., & Mikhailidis, D. P. (2020). Diabetes and carotid artery disease: a narrative review. *Annals of Translational Medicine*, *8*(19), 1280. https://doi.org/10.21037/ATM.2019.12.153

Katsumata, A. (2023). Deep learning and artificial intelligence in dental diagnostic imaging. *Japanese Dental Science Review*, *59*, 329–333. https://doi.org/10.1016/J.JDSR.2023.09.004

Kaufman, J. D., Adar, S. D., Barr, R. G., Budoff, M., Burke, G. L., Curl, C. L., Daviglus, M. L., Roux, A. V. D., Gassett, A. J., Jacobs, D. R., Kronmal, R., Larson, T. V., Navas-Acien, A., Olives, C., Sampson, P. D., Sheppard, L., Siscovick, D. S., Stein, J. H., Szpiro, A. A., & Watson, K. E. (2016). Association between air pollution and coronary artery calcification within six metropolitan areas in the USA (the Multi-Ethnic Study of Atherosclerosis and Air Pollution): a longitudinal cohort study. *Lancet (London, England)*, *388*(10045), 696–704. https://doi.org/10.1016/S0140-6736(16)00378-0

Kaufman, J. D., Elkind, M. S. V., Bhatnagar, A., Koehler, K., Balmes, J. R., Sidney, S., Burroughs Peña, M. S., Dockery, D. W., Hou, L., Brook, R. D., Laden, F., Rajagopalan, S., Kendrick, K. B., Turner, J. R., Cohen, A. J., Mittleman, M. A., Siscovick, D., & Thurston, G. D. (2020). Guidance to Reduce the Cardiovascular Burden of Ambient Air Pollutants: A Policy Statement From the American Heart Association. *Circulation*, *142*(23), E432–E447. https://doi.org/10.1161/CIR.0000000000000930

Kim, H. (2024). *Deep Learning in Dental Radiographic Imaging*. https://doi.org/10.5933/JKAPD.2024.51.1.1

King, C. R., Knutson, K. L., Rathouz, P. J., Sidney, S., Liu, K., & Lauderdale, D. S. (2008). Short Sleep Duration and Incident Coronary Artery Calcification. *JAMA*, *300*(24), 2859–2866. https://doi.org/10.1001/JAMA.2008.867

Klein, J., Diaba-Nuhoho, P., Giebe, S., Brunssen, C., & Morawietz, H. (2023). Regulation of endothelial function by cigarette smoke and next-generation tobacco and nicotine products. *Pflugers Archiv*, *475*(7), 835. https://doi.org/10.1007/S00424-023-02824-W

Kosciuszek, N. D., Kalta, D., Singh, M., & Savinova, O. V. (2022). Vitamin K antagonists and cardiovascular calcification: A systematic review and meta-analysis. *Frontiers in Cardiovascular Medicine*, *9*, 938567. https://doi.org/10.3389/FCVM.2022.938567/FULL

Krachler, M., & Shotyk, W. (2008). *Author's personal copy Trace and ultratrace metals in bottled waters: Survey of sources worldwide and comparison with refillable metal bottles*. https://doi.org/10.1016/j.scitotenv.2008.10.014

Kröller-Schön, S., Daiber, A., Steven, S., Oelze, M., Frenis, K., Kalinovic, S., Heimann, A., Schmidt, F. P., Pinto, A., Kvandova, M., Vujacic-Mirski, K., Filippou, K., Dudek, M., Bosmann, M., Klein, M., Bopp, T., Hahad, O., Wild, P. S., Frauenknecht, K., … Münzel, T. (2018). Crucial role for Nox2 and sleep deprivation in aircraft noise-induced vascular and cerebral oxidative stress, inflammation, and gene regulation. *European Heart Journal*, *39*(38), 3528. https://doi.org/10.1093/EURHEARTJ/EHY333

KURT, S., ÇELİK, Ö., BAYRAKDAR, İ. Ş., ORHAN, K., BİLGİR, E., ODABAS, A., & ASLAN, A. F. (2020). SUCCESS OF ARTIFICIAL INTELLIGENCE SYSTEM IN DETERMINING ALVEOLAR BONE LOSS FROM DENTAL PANORAMIC RADIOGRAPHY IMAGES. *Cumhuriyet Dental Journal*, *23*(4), 318–324. https://doi.org/10.7126/cumudj.777057

Kuwada, C., Mitsuya, Y., Fukuda, M., Yang, S., Kise, Y., Mori, M., Naitoh, M., Ariji, Y., & Ariji, E. (2025). Area detection improves the person-based performance of a deep learning system for classifying the presence of carotid artery calcifications on panoramic radiographs. *Oral Radiology*, 1–10. https://doi.org/10.1007/S11282-025-00843-0/METRICS

Lane, M. M., Gamage, E., Du, S., Ashtree, D. N., McGuinness, A. J., Gauci, S., Baker, P., Lawrence, M., Rebholz, C. M., Srour, B., Touvier, M., Jacka, F. N., O'Neil, A., Segasby, T., & Marx, W. (2024). Ultra-processed food exposure and adverse health outcomes: umbrella review of epidemiological meta-analyses. *BMJ*, *384*. https://doi.org/10.1136/BMJ-2023-077310

Lane, M. M., Lotfaliany, M., Forbes, M., Loughman, A., Rocks, T., O'Neil, A., Machado, P., Jacka, F. N., Hodge, A., & Marx, W. (2022). Higher Ultra-Processed Food Consumption Is Associated with Greater High-Sensitivity C-Reactive Protein Concentration in Adults: Cross-Sectional Results from the Melbourne Collaborative Cohort Study. *Nutrients*, *14*(16). https://doi.org/10.3390/NU14163309

Lee, J. S., Kim, O. S., Chung, H. J., Kim, Y. J., Kweon, S. S., Lee, Y. H., Shin, M. H., & Yoon, S. J. (2014). The correlation of carotid artery calcification on panoramic radiographs and determination of carotid artery atherosclerosis with ultrasonography. *Oral Surgery, Oral Medicine, Oral Pathology and Oral Radiology*, *118*(6), 739–745. https://doi.org/10.1016/J.OOOO.2014.09.011

Lee, S. J., Lee, I. K., & Jeon, J. H. (2020). Vascular Calcification—New Insights into Its Mechanism. *International Journal of Molecular Sciences*, *21*(8), 2685. https://doi.org/10.3390/IJMS21082685

Leite, A. F., Gerven, A. Van, Willems, H., Beznik, T., Lahoud, P., Gaêta-Araujo, H., Vranckx, M., & Jacobs, R. (2021). Artificial intelligence-driven novel tool for tooth detection and

segmentation on panoramic radiographs. *Clinical Oral Investigations*, *25*(4), 2257–2267. https://doi.org/10.1007/s00784-020-03544-6

Leopold, J. A. (2014). Vascular Calcification: Mechanisms of Vascular Smooth Muscle Cell Calcification. *Trends in Cardiovascular Medicine*, *25*(4), 267. https://doi.org/10.1016/J.TCM.2014.10.021

Levine, G. N., Cohen, B. E., Commodore-Mensah, Y., Fleury, J., Huffman, J. C., Khalid, U., Labarthe, D. R., Lavretsky, H., Michos, E. D., Spatz, E. S., Kubzansky, L. D., Boehm, J. K., Carney, R. M., & Smith, S. C. (2021). Psychological Health, Well-Being, and the Mind-Heart-Body Connection: A Scientific Statement From the American Heart Association. *Circulation*, *143*(10), E763–E783. https://doi.org/10.1161/CIR.0000000000000947

Li, T., Wang, Y., & Tu, W. P. (2023). Vitamin K supplementation and vascular calcification: a systematic review and meta-analysis of randomized controlled trials. *Frontiers in Nutrition*, *10*, 1115069. https://doi.org/10.3389/FNUT.2023.1115069/FULL

Liabeuf, S., Olivier, B., Vemeer, C., Theuwissen, E., Magdeleyns, E., Aubert, C. E., Brazier, M., Mentaverri, R., Hartemann, A., & Massy, Z. A. (2014). Vascular calcification in patients with type 2 diabetes: The involvement of matrix Gla protein. *Cardiovascular Diabetology*, *13*(1), 1–8. https://doi.org/10.1186/1475-2840-13-85/TABLES/4

Libby, P., Buring, J. E., Badimon, L., Hansson, G. K., Deanfield, J., Bittencourt, M. S., Tokgözoğlu, L., & Lewis, E. F. (2019). Atherosclerosis. *Nature Reviews Disease Primers*, *5*(1), 1–18. https://doi.org/10.1038/S41572-019-0106-Z;SUBJMETA

Liberman, M., Johnson, R. C., Handy, D. E., Loscalzo, J., & Leopold, J. A. (2011). Bone Morphogenetic Protein-2 Activates NADPH Oxidase to Increase Endoplasmic Reticulum Stress and Human Coronary Artery Smooth Muscle Cell Calcification. *Biochemical and Biophysical Research Communications*, *413*(3), 436. https://doi.org/10.1016/J.BBRC.2011.08.114

Lim, L. Z., Koh, P. S. F., Cao, S., & Wong, R. C. W. (2021). Can carotid artery calcifications on dental radiographs predict adverse vascular events? A systematic review. *Clinical Oral Investigations*, *25*(1), 37–53. https://doi.org/10.1007/S00784-020-03696-5

Lima, B. B., Hammadah, M., Kim, J. H., Uphoff, I., Shah, A., Levantsevych, O., Almuwaqqat, Z., Moazzami, K., Sullivan, S., Ward, L., Kutner, M., Ko, Y. A., Sheps, D. S., Bremner, J. D., Quyyumi, A. A., & Vaccarino, V. (2019). Association of Transient Endothelial Dysfunction Induced by Mental Stress With Major Adverse Cardiovascular Events in Men and Women With Coronary Artery Disease. *JAMA Cardiology*, *4*(10), 988–996. https://doi.org/10.1001/JAMACARDIO.2019.3252

Litjens, G., Kooi, T., Bejnordi, B. E., Setio, A. A. A., Ciompi, F., Ghafoorian, M., van der Laak, J. A. W. M., van Ginneken, B., & Sánchez, C. I. (2017). A survey on deep learning in medical image analysis. *Medical Image Analysis*, *42*, 60–88. https://doi.org/10.1016/J.MEDIA.2017.07.005

Liu, X., Lian, H., Ruan, Y., Liang, R., Zhao, X., Routledge, M., & Fan, Z. (2015). Association of Exposure to Particular Matter and Carotid Intima-Media Thickness: A Systematic Review and Meta-Analysis. *International Journal of Environmental Research and Public Health*, *12*(10), 12924. https://doi.org/10.3390/IJERPH121012924

Liu, Y., Yan, S., Zou, L., Wen, J., & Fu, W. (2022). Noise exposure and risk of myocardial infarction incidence and mortality: a dose–response meta-analysis. *Environmental Science and Pollution Research*, *29*(31), 46458–46470. https://doi.org/10.1007/S11356-022-20377-W)

Lopes, A. E. da S. C., Araújo, L. F., Levy, R. B., Barreto, S. M., & Giatti, L. (2019). Association between consumption of ultra-processed foods and serum C-reactive protein levels: cross-sectional results from the ELSA-Brasil study. *São Paulo Medical Journal*, *137*(2), 169. https://doi.org/10.1590/1516-3180.2018.0363070219

Luo, G., Ducy, P., McKee, M. D., Pinero, G. J., Loyer, E., Behringer, R. R., & Karsenty, G. (1997). Spontaneous calcification of arteries and cartilage in mice lacking matrix GLA protein. *Nature*, *386*(6620), 78–81. https://doi.org/10.1038/386078A0

Ma, X., Wang, Q., Hu, X., Wang, X., Zhao, Y., Liu, X., Li, J., Du, Y., Wang, M., Qiu, C., & Sun, Q. (2024). Association of sdLDL-C With Incident Carotid Plaques With Stable and Vulnerable Morphology: A Prospective Cohort Study. *Stroke*, *55*(3), 576–585. https://doi.org/10.1161/STROKEAHA.123.045601

Madden, R. P., Hodges, J. S., Salmen, C. W., Rindal, D. B., Tunio, J., Michalowicz, B. S., & Ahmad, M. (2007). Utility of panoramic radiographs in detecting cervical calcified carotid atheroma. *Oral Surgery, Oral Medicine, Oral Pathology, Oral Radiology and Endodontology*, *103*(4), 543–548. https://doi.org/10.1016/j.tripleo.2006.06.048

Magnani, J. W., Mujahid, M. S., Aronow, H. D., Cené, C. W., Dickson, V. V., Havranek, E., Morgenstern, L. B., Paasche-Orlow, M. K., Pollak, A., & Willey, J. Z. (2018). Health Literacy and Cardiovascular Disease: Fundamental Relevance to Primary and Secondary Prevention: A Scientific Statement From the American Heart Association. *Circulation*, *138*(2), e48–e74. https://doi.org/10.1161/CIR.0000000000000579

Mai, V., Taneja, A., Larjava, H., Chehroudi, B., MacDonald, D., & Luong, C. (2024). Calcified carotid artery atheroma on standard dental radiographs: A public health opportunity for cardiovascular risk reduction. *American Journal of Preventive Cardiology*, *19*. https://doi.org/10.1016/j.ajpc.2024.100714

Marwaha, K. (2022). Examining the Role of Psychosocial Stressors in Hypertension. *Journal of Preventive Medicine and Public Health*, *55*(6), 499. https://doi.org/10.3961/JPMPH.21.266

Mason, D. (2011). SU-E-T-33: Pydicom: An Open Source DICOM Library. *Medical Physics*, *38*(6Part10), 3493–3493. https://doi.org/10.1118/1.3611983

Massad Marwa Qadadha Mervett Isbeih Khalid Abu Saman, S., Shakhra Nancy Falah, K., & Abed Rabah Al-Jamal Nebal Ismael, N. (2022). *Work Team Technical Team • World Health Organization*.

Mateen, F. J., Grau-Perez, M., Pollak, J. S., Moon, K. A., Howard, B. V., Umans, J. G., Best, L. G., Francesconi, K. A., Goessler, W., Crainiceanu, C., Guallar, E., Devereux, R. B., Roman, M. J., & Navas-Acien, A. (2017). Chronic arsenic exposure and risk of carotid artery disease: The Strong Heart Study. *Environmental Research*, *157*, 127–134. https://doi.org/10.1016/J.ENVRES.2017.05.020

McGill, H. C., McMahan, C. A., & Gidding, S. S. (2008). Preventing heart disease in the 21st century: Implications of the pathobiological determinants of atherosclerosis in youth (PDAY) study. *Circulation*, *117*(9), 1216–1227. https://doi.org/10.1161/CIRCULATIONAHA.107.717033

Messner, B., & Bernhard, D. (2014). Smoking and cardiovascular disease: mechanisms of endothelial dysfunction and early atherogenesis. *Arteriosclerosis, Thrombosis, and Vascular Biology*, *34*(3), 509–515. https://doi.org/10.1161/ATVBAHA.113.300156

Moshfeghi, M., Taheri, J. B., Bahemmat, N., Evazzadeh, M. E., & Hadian, H. (2014). Relationship Between Carotid Artery Calcification Detected in Dental Panoramic Images and Hypertension and Myocardial Infarction. *Iranian Journal of Radiology*, *11*(3), e8714. https://doi.org/10.5812/IRANJRADIOL.8714

Möst, T., Winter, L., Ballheimer, Y. E., Kappler, C., Schmid, M., Adler, W., Weber, M., Kesting, M. R., & Lutz, R. (2023). Prevalence of carotid artery calcification detected by different dental imaging techniques and their relationship with cardiovascular risk factors, age and gender. *BMC Oral Health*, *23*(1), 1–11. https://doi.org/10.1186/S12903-023-03564-0/FIGURES/6

Münzel, T., Gori, T., Babisch, W., & Basner, M. (2014). Cardiovascular effects of environmental noise exposure. *European Heart Journal*, *35*(13), 829. https://doi.org/10.1093/EURHEARTJ/EHU030

Münzel, T., & Sørensen, M. (2017). Noise Pollution and Arterial Hypertension. *European Cardiology Review*, *12*(1), 26. https://doi.org/10.15420/ECR.2016:31:2

Naqvi, T. Z., & Lee, M. S. (2014). Carotid Intima-Media Thickness and Plaque in Cardiovascular Risk Assessment. *JACC: Cardiovascular Imaging*, *7*(10), 1025–1038. https://doi.org/10.1016/J.JCMG.2013.11.014

National Imaging Associates, Inc. (2025). *Clinical guideline: Neck MRA/MRV*.

Nelson, J., Vaddi, A., & Tadinada, A. (2024). Can convolutional neural networks identify external carotid artery calcifications? *Oral Surgery, Oral Medicine, Oral Pathology and Oral Radiology*, *138*(1), 142–148. https://doi.org/10.1016/j.oooo.2023.01.017

Nguyen, Q. C., Waddell, E. N., Thomas, J. C., Huston, S. L., Kerker, B. D., & Gwynn, R. C. (2011). Awareness, Treatment, and Control of Hypertension and Hypercholesterolemia

Among Insured Residents of New York City, 2004. *Preventing Chronic Disease*, *8*(5), A109. https://pmc.ncbi.nlm.nih.gov/articles/PMC3181182/

Organización Mundial de la Salud (OMS). (2021). WHO global air quality guidelines. *Particulate Matter (PM2.5 and PM10), Ozone, Nitrogen Dioxide, Sulfur Dioxide and Carbon Monoxide*, 1–360.

Osborne, M. T., Shin, L. M., Mehta, N. N., Pitman, R. K., Fayad, Z. A., & Tawakol, A. (2020). Disentangling the Links Between Psychosocial Stress and Cardiovascular Disease. *Circulation: Cardiovascular Imaging*, *13*(8), E010931. https://doi.org/10.1161/CIRCIMAGING.120.010931

Pae, B. J., Lee, S. K., Kim, S., Siddiquee, A. T., Hwang, Y. H., Lee, M. H., Kim, R. E. Y., Kim, S. H., Lee, M., & Shin, C. (2023). Effect of physical activity on the change in carotid intima-media thickness: An 8-year prospective cohort study. *PLOS ONE*, *18*(6), e0287685. https://doi.org/10.1371/JOURNAL.PONE.0287685

Palaniswamy, C., Sekhri, A., Aronow, W. S., Kalra, A., & Peterson, S. J. (2011). Association of Warfarin Use With Valvular and Vascular Calcification: A Review. *Clinical Cardiology*, *34*(2), 74. https://doi.org/10.1002/CLC.20865

Park, J., Kwon, Y., & Park, H. (2017). Effects of 24-Week Aerobic and Resistance Training on Carotid Artery Intima-Media Thickness and Flow Velocity in Elderly Women with Sarcopenic Obesity. *Journal of Atherosclerosis and Thrombosis*, *24*(11), 1117. https://doi.org/10.5551/JAT.39065

Petersen, K. S., Clifton, P. M., & Keogh, J. B. (2014). The association between carotid intima media thickness and individual dietary components and patterns. *Nutrition, Metabolism and Cardiovascular Diseases*, *24*(5), 495–502. https://doi.org/10.1016/j.numecd.2013.10.024

Piercy, K. L., Troiano, R. P., Ballard, R. M., Carlson, S. A., Fulton, J. E., Galuska, D. A., George, S. M., & Olson, R. D. (2018). The Physical Activity Guidelines for Americans. *JAMA*, *320*(19), 2020–2028. https://doi.org/10.1001/JAMA.2018.14854

Pizer, S. M., Amburn, E. P., Austin, J. D., Cromartie, R., Geselowitz, A., Greer, T., ter Haar Romeny, B., Zimmerman, J. B., & Zuiderveld, K. (1987). Adaptive histogram equalization and its variations. *Computer Vision, Graphics, and Image Processing*, *39*(3), 355–368. https://doi.org/10.1016/S0734-189X(87)80186-X

Prados-Privado, M., García Villalón, J., Blázquez Torres, A., Martínez-Martínez, C. H., Prados-Frutos, J. C., & Ivorra, C. (2022). Are Panoramic Images a Good Tool to Detect Calcified Carotid Atheroma? A Systematic Review. *Biology*, *11*(11). https://doi.org/10.3390/BIOLOGY11111684

Professor, A., Ibrahim Mousa, A., Mohamed Hesham, N., Ahmed Hamza, S., & Mamdouh Mohamed, E. (2025). Article is licensed under a Creative Commons Attribution 4.0 International License THE PREVALENCE OF CAROTID ARTERY

CALCIFICATION DETECTED FROM THE PANORAMIC RADIOGRAPHS OF A SAMPLE OF THE EGYPTIAN POPULATION: A RETROSPECTIVE STUDY. *DENTAL JOURNAL*, *71*, 2143. https://doi.org/10.21608/edj.2025.373220.3437

Provost, E. B., Madhloum, N., Panis, L. I., De Boever, P., & Nawrot, T. S. (2015). Carotid Intima-Media Thickness, a Marker of Subclinical Atherosclerosis, and Particulate Air Pollution Exposure: the Meta-Analytical Evidence. *PLOS ONE*, *10*(5), e0127014. https://doi.org/10.1371/JOURNAL.PONE.0127014

Ren, L., Cai, J., Liang, J., Li, W., & Sun, H. (2015). Impact of Cardiovascular Risk Factors on Carotid Intima-Media Thickness and Degree of Severity: A Cross-Sectional Study. *PLOS ONE*, *10*(12), e0144182. https://doi.org/10.1371/JOURNAL.PONE.0144182

Roth, G. A., Mensah, G. A., Johnson, C. O., Addolorato, G., Ammirati, E., Baddour, L. M., Barengo, N. C., Beaton, A., Benjamin, E. J., Benziger, C. P., Bonny, A., Brauer, M., Brodmann, M., Cahill, T. J., Carapetis, J. R., Catapano, A. L., Chugh, S., Cooper, L. T., Coresh, J., … Fuster, V. (2020). Global Burden of Cardiovascular Diseases and Risk Factors, 1990-2019: Update From the GBD 2019 Study. *Journal of the American College of Cardiology*, *76*(25), 2982–3021. https://doi.org/10.1016/j.jacc.2020.11.010

Saito, M., Miyake, Y., Tanaka, K., Nagata, C., Senba, H., Hasebe, Y., Miyata, T., Higaki, T., Kimura, E., Matsuura, B., Yamaguchi, O., & Kawamoto, R. (2024). Smoking and secondhand smoke exposure and carotid intima-media thickness: Baseline data from the Aidai Cohort Study in Japan. *Tobacco Induced Diseases*, *22*, 10.18332/tid/175632. https://doi.org/10.18332/TID/175632

Sala-Vila, A., Romero-Mamani, E. S., Gilabert, R., Núñez, I., De La Torre, R., Corella, D., Ruiz-Gutiérrez, V., López-Sabater, M. C., Pintó, X., Rekondo, J., Martínez-González, M. Á., Estruch, R., & Ros, E. (2014). Changes in ultrasound-assessed carotid intima-media thickness and plaque with a Mediterranean diet: a substudy of the PREDIMED trial. *Arteriosclerosis, Thrombosis, and Vascular Biology*, *34*(2), 439–445. https://doi.org/10.1161/ATVBAHA.113.302327

Saleh, C., Ilia, T. S., Schöpfer, R., Seidl, U., Deraita, J., Todua-Lennigk, S., Lieb, J., Budincevic, H., Trzcinska, M., Hovhannisyan, K., Boviatsis, K. A., & Saleh, F. M. (2024). Atherosclerosis and depression: is carotid intima-media thicker in patients with depression compared to matched control individuals? A systematic review and meta-analysis. *Journal of Psychiatric Research*, *173*, 216–224. https://doi.org/10.1016/j.jpsychires.2024.03.012

Santos, J.-M.-O., Soares, G.-C., Alves, A.-P.-N.-N., Kurita, L.-M., Silva, P.-G.-D. B., & Costa, F.-W.-G. (2018). *Prevalence of carotid artery calcifications among 2,500 digital panoramic radiographs of an adult Brazilian population*. *23*(3), 256–261. https://doi.org/10.4317/medoral.22350

Sara, J. D. S., Toya, T., Ahmad, A., Clark, M. M., Gilliam, W. P., Lerman, L. O., & Lerman, A. (2022). Mental Stress and Its Effects on Vascular Health. *Mayo Clinic Proceedings*, *97*(5), 951–990. https://doi.org/10.1016/J.MAYOCP.2022.02.004

Schmidt, F., Kolle, K., Kreuder, K., Schnorbus, B., Wild, P., Hechtner, M., Binder, H., Gori, T., & Münzel, T. (2014). Nighttime aircraft noise impairs endothelial function and increases blood pressure in patients with or at high risk for coronary artery disease. *Clinical Research in Cardiology*, *104*(1), 23. https://doi.org/10.1007/S00392-014-0751-X

Schmidt, F. P., Basner, M., Kröger, G., Weck, S., Schnorbus, B., Muttray, A., Sariyar, M., Binder, H., Gori, T., Warnholtz, A., & Münzel, T. (2013). Effect of nighttime aircraft noise exposure on endothelial function and stress hormone release in healthy adults. *European Heart Journal*, *34*(45), 3508–3514. https://doi.org/10.1093/EURHEARTJ/EHT269

Schurgers, L. J., Uitto, J., & Reutelingsperger, C. P. (2013). Vitamin K-dependent carboxylation of matrix Gla-protein: a crucial switch to control ectopic mineralization. *Trends in Molecular Medicine*, *19*(4), 217–226. https://doi.org/10.1016/J.MOLMED.2012.12.008

Schwendicke, F., Samek, W., & Krois, J. (2020). Artificial Intelligence in Dentistry: Chances and Challenges. *Journal of Dental Research*, *99*(7), 769–774. https://doi.org/10.1177/0022034520915714

Shea, M. K., O'Donnell, C. J., Hoffmann, U., Dallal, G. E., Dawson-Hughes, B., Ordovas, J. M., Price, P. A., Williamson, M. K., & Booth, S. L. (2009). Vitamin K supplementation and progression of coronary artery calcium in older men and women1. *The American Journal of Clinical Nutrition*, *89*(6), 1799. https://doi.org/10.3945/AJCN.2008.27338

Shu, D., Chen, F., Zhang, C., Guo, W., & Dai, S. (2022). Environmental tobacco smoke and carotid intima–media thickness in healthy children and adolescents: a systematic review. *Open Heart*, *9*(1), e001790. https://doi.org/10.1136/OPENHRT-2021-001790

Sinjab, A. Z., Soman, C., & Sahab, L. A. (2021). Prevalence of carotid artery calcifications in Riyadh from digital panoramic radiographs and its relationship with cardiovascular disorders. *Saudi Journal of Oral Sciences*, *8*(1), 28–32. https://doi.org/10.4103/SJOS.SJORALSCI_78_20

Song, Y. Bin, Jeong, H. G., Kim, C., Kim, D., Kim, J., Kim, H. J., & Park, W. (2022). Comparison of detection performance of soft tissue calcifications using artificial intelligence in panoramic radiography. *Scientific Reports*, *12*(1), 1–10. https://doi.org/10.1038/S41598-022-22595-1;SUBJMETA

Srour, B., Fezeu, L. K., Kesse-Guyot, E., Allès, B., Méjean, C., Andrianasolo, R. M., Chazelas, E., Deschasaux, M., Hercberg, S., Galan, P., Monteiro, C. A., Julia, C., & Touvier, M. (2019). Ultra-processed food intake and risk of cardiovascular disease:

prospective cohort study (NutriNet-Santé). *BMJ*, *365*. https://doi.org/10.1136/BMJ.L1451

Stein, J. H., Smith, S. S., Hansen, K. M., Korcarz, C. E., Piper, M. E., Fiore, M. C., & Baker, T. B. (2020). Longitudinal effects of smoking cessation on carotid artery atherosclerosis in contemporary smokers: The Wisconsin Smokers Health Study. *Atherosclerosis*, *315*, 62–67. https://doi.org/10.1016/J.ATHEROSCLEROSIS.2020.11.010

Tarighatnia, A., Amanzadeh, M., Hamedan, M., Mohammadnia, A., & Nader, N. D. (2025). Deep learning-based evaluation of panoramic radiographs for osteoporosis screening: a systematic review and meta-analysis. *BMC Medical Imaging*, *25*(1), 1–11. https://doi.org/10.1186/S12880-025-01626-Z/FIGURES/6

Tassoker, M., Öziç, M. Ü., & Yuce, F. (2024). Performance evaluation of a deep learning model for automatic detection and localization of idiopathic osteosclerosis on dental panoramic radiographs. *Scientific Reports*, *14*(1), 4437. https://doi.org/10.1038/s41598-024-55109-2

The Palestinian Ministry of Health. (2022). https://www.moh.gov.ps/portal/wp-content/uploads/2023/07/annual-english-202218-7-2023.pdf?utm

Theofilis, P., Oikonomou, E., Lazaros, G., Vogiatzi, G., Anastasiou, M., Mystakidi, V. C., Goliopoulou, A., Christoforatou, E., Bourouki, E., Vavouranaki, G., Marinos, G., & Tousoulis, D. (2022). The association of diabetes mellitus with carotid atherosclerosis and arterial stiffness in the Corinthia study. *Nutrition, Metabolism and Cardiovascular Diseases*, *32*(3), 567–576. https://doi.org/10.1016/J.NUMECD.2021.12.013

Tomasi, C., & Manduchi, R. (1998). *Bilateral Filtering for Gray and Color Images*.

Turosz, N., Chęcińska, K., Chęciński, M., Brzozowska, A., Nowak, Z., & Sikora, M. (2023). Applications of artificial intelligence in the analysis of dental panoramic radiographs: an overview of systematic reviews. *Dentomaxillofacial Radiology*, *52*(7). https://doi.org/10.1259/dmfr.20230284

Tuzoff, D. V., Tuzova, L. N., Bornstein, M. M., Krasnov, A. S., Kharchenko, M. A., Nikolenko, S. I., Sveshnikov, M. M., & Bednenko, G. B. (2019). Tooth detection and numbering in panoramic radiographs using convolutional neural networks. *Dentomaxillofacial Radiology*, *48*(4), 20180051. https://doi.org/10.1259/dmfr.20180051

Valdivielso, J. M., Rodríguez-Puyol, D., Pascual, J., Barrios, C., Bermúdez-López, M., Sánchez-Niño, M. D., Pérez-Fernández, M., & Ortiz, A. (2019). Atherosclerosis in Chronic Kidney Disease. *Arteriosclerosis, Thrombosis, and Vascular Biology*, *39*(10), 1938–1966. https://doi.org/10.1161/ATVBAHA.119.312705

Vallat, R., Shah, V. D., Redline, S., Attia, P., & Walker, M. P. (2020). Broken sleep predicts hardened blood vessels. *PLOS Biology*, *18*(6), e3000726. https://doi.org/10.1371/JOURNAL.PBIO.3000726

van Kempen, E., Casas, M., Pershagen, G., & Foraster, M. (2018). WHO Environmental Noise Guidelines for the European Region: A Systematic Review on Environmental Noise and Cardiovascular and Metabolic Effects: A Summary. *International Journal of Environmental Research and Public Health*, *15*(2), 379. https://doi.org/10.3390/IJERPH15020379

Vashisht, R., Sharma, A., Kiran, T., Jolly, S. S., Brar, P. K., & Puri, J. V. (2024). Artificial intelligence in dentistry — A scoping review. *Journal of Oral and Maxillofacial Surgery, Medicine, and Pathology*, *36*(4), 579–592. https://doi.org/10.1016/J.AJOMS.2024.04.009

Vinayahalingam, S., van Nistelrooij, N., Xi, T., Heiland, M., Bressem, K., Rendenbach, C., Flügge, T., & Gaudin, R. (2024). Detection of carotid plaques on panoramic radiographs using deep learning. *Journal of Dentistry*, *151*. https://doi.org/10.1016/j.jdent.2024.105432

Vlasschaert, C., Goss, C. J., Pilkey, N. G., McKeown, S., & Holden, R. M. (2020). Vitamin K Supplementation for the Prevention of Cardiovascular Disease: Where Is the Evidence? A Systematic Review of Controlled Trials. *Nutrients 2020, Vol. 12, Page 2909*, *12*(10), 2909. https://doi.org/10.3390/NU12102909

Vranckx, M., Van Gerven, A., Willems, H., Vandemeulebroucke, A., Ferreira Leite, A., Politis, C., & Jacobs, R. (2020). Artificial Intelligence (AI)-Driven Molar Angulation Measurements to Predict Third Molar Eruption on Panoramic Radiographs. *International Journal of Environmental Research and Public Health*, *17*(10), 3716. https://doi.org/10.3390/ijerph17103716

Waclawovsky, A. J., de Brito, E., Smith, L., Vancampfort, D., da Silva, A. M. V., & Schuch, F. B. (2021). Endothelial dysfunction in people with depressive disorders: A systematic review and meta-analysis. *Journal of Psychiatric Research*, *141*, 152–159. https://doi.org/10.1016/j.jpsychires.2021.06.045

Wadia, R. (2021). Carotid artery calcification on dental radiographs. *British Dental Journal*, *230*(2), 92. https://doi.org/10.1038/S41415-021-2626-7;KWRD

Wang, Y., Wu, H., Sun, J., Wei, M., Wang, J., Li, H., Wu, X., & Wu, J. (2022). Effect of Exercise on Carotid Artery Intima-Media Thickness in Adults: A Systematic Review and Meta-Analysis. *Journal of Physical Activity & Health*, *19*(12), 855–867. https://doi.org/10.1123/JPAH.2022-0372

Wilmot, E. G., Edwardson, C. L., Achana, F. A., Davies, M. J., Gorely, T., Gray, L. J., Khunti, K., Yates, T., & Biddle, S. J. H. (2012). Sedentary time in adults and the association with diabetes, cardiovascular disease and death: systematic review and meta-analysis. *Diabetologia*, *55*(11), 2895–2905. https://doi.org/10.1007/S00125-012-2677-Z

World Health Organization. (2017). *Guidelines for Drinking-water Quality FOURTH EDITION INCORPORATING THE FIRST ADDENDUM*.

World Health Organization. (2023). Health conditions in the occupied Palestinian territory, including east Jerusalem, and in the occupied Syrian Golan Report by the Director-General. *SEVENTY-SIXTH WORLD HEALTH ASSEMBLY Provisional Agenda Item 18*. https://www.cbs.gov.il/he/publications/doclib/2022/3.shnatonhealth/st03_05.pdf,

World Health Organization. (2025). *Cardiovascular diseases (CVDs)*. https://www.who.int/news-room/fact-sheets/detail/cardiovascular-diseases-%28cvds%29?

Wozniak, G., Khan, T., Gillespie, C., Sifuentes, L., Hasan, O., Ritchey, M., Kmetik, K., & Wynia, M. (2015). Hypertension Control Cascade: A Framework to Improve Hypertension Awareness, Treatment, and Control. *The Journal of Clinical Hypertension*, *18*(3), 232. https://doi.org/10.1111/JCH.12654

Wu, Z., Li, X., Wen, Q., Tao, B., Qiu, B., Zhang, Q., & Wang, J. (2022). Serum LDL-C/HDL-C ratio and the risk of carotid plaques: a longitudinal study. *BMC Cardiovascular Disorders*, *22*(1), 501. https://doi.org/10.1186/S12872-022-02942-W

Xie, J., Girshick, R., & Farhadi, A. (2016). *Unsupervised Deep Embedding for Clustering Analysis*. http://arxiv.org/abs/1511.06335

Yoo, S. W., Yang, S., Kim, J. E., Huh, K. H., Lee, S. S., Heo, M. S., & Yi, W. J. (2024). CACSNet for automatic robust classification and segmentation of carotid artery calcification on panoramic radiographs using a cascaded deep learning network. *Scientific Reports*, *14*(1), 1–15. https://doi.org/10.1038/S41598-024-64265-4;SUBJMETA

Yoon, S. J., Shim, S. K., Lee, J. S., Kang, B. C., Lim, H. J., Kim, M. S., & Kim, S. H. (2014). Interobserver agreement on the diagnosis of carotid artery calcifications on panoramic radiographs. *Imaging Science in Dentistry*, *44*(2), 137–141. https://doi.org/10.5624/ISD.2014.44.2.137

Yoon, S. J., Yoon, W., Kim, O. S., Lee, J. S., & Kang, B. C. (2008). Diagnostic accuracy of panoramic radiography in the detection of calcified carotid artery. *Dento Maxillo Facial Radiology*, *37*(2), 104–108. https://doi.org/10.1259/DMFR/86909790

Yu, Z., Yang, H., Shou, B., Cheng, Z., Jiang, C., & Xu, J. (2024). Association between pulse pressure and carotid plaques in old adults with uncontrolled hypertension: results from a community-based screening in Hangzhou, China. *BMC Cardiovascular Disorders*, *24*(1), 1–10. https://doi.org/10.1186/S12872-024-03914-Y/FIGURES/5

Zaghden, O., Jaziri, R., Kammoun, R., Chaabani, I., & Alaya, T. Ben. (2023). Benefit of Panoramic Radiography in the Detection of Carotid Calcifications: Clinical Case Reports and Review of the Literature. *Case Reports in Dentistry*, *2023*, 1–13. https://doi.org/10.1155/2023/3989502

Appendix A: Letter of Research Ethical Committee (REC) approval

Al-Quds University
Jerusalem
Deanship of Scientific Research

بسم الله الرحمن الرحيم

جامعة القدس
القدس
عمادة البحث العلمي

Research Ethics Committee
Committee's Decision Letter

Date: September 28, 2024
Ref No: 427/REC/2024

Dears Dr. Radwan Qasrawi, Ms. Nadeen Erekat, Mr. Suleiman Thwib,

Thank you for submitting your application seeking approval for research ethics. After a thorough review of your submission titled "Predicting Stroke and Ischemic Heart Diseases from Carotid Calcifications in Panoramic Radiographs: Deep Learning Approach", the Research Ethics Committee (REC) at Al-Quds University is pleased to confirm that your application aligns with our research ethics guidelines.
Please be aware that while this approval authorizes your research, it does not replace any departmental or other necessary approvals. These may include permissions for sample shipment, data sharing, or administrative approval to distribute questionnaires.

Additionally, we kindly request that you provide us with a copy of your final research report or publication once it is available.

Thank you once again for your commitment to conducting ethical research. We extend our best wishes for a productive research endeavor that benefits your research subjects.

Please note that this ethical approval letter is valid for two years from the date of issuance.
If your research extends beyond this timeframe, a renewal request will be necessary. This approval remains valid as long as there are no changes to the data collection procedures or any aspect of the research protocol.

Sincerely,

Suheir Ereqat, PhD
Associate Professor of Molecular Biology
Research Ethics Committee Chair

Cc. Prof. Imad Abu Kishek - President
Cc. Members of the committee
Cc. file

Abu-Dies, Jerusalem P.O.Box 20002
Tel-Fax: #970-02-2791293
research@admin.alquds.edu
أبوديس، القدس ص.ب. 20002
تلفاكس: #970-02-2791293

Appendix B: Consent form and questionnaire

نموذج الموافقة المستنيرة للمشاركة في الاستبيان

عزيزي/عزيزتي المشارك/ة،
نشكرك على تخصيص وقتك للمشاركة في هذا الاستبيان الذي يهدف إلى تقييم عوامل الخطر للسكتة الدماغية وأمراض نقص تروية القلب. المعلومات التي تقدمها ستكون سرية تمامًا، ولن يتم استخدامها إلا لأغراض البحث الطبي وتحسين الخدمات الصحية.

يرجى ملاحظة ما يلي:

- المشاركة في هذا الاستبيان اختيارية، ويمكنك التوقف في أي وقت دون أي تأثير على رعايتك الصحية.
- جميع البيانات التي يتم جمعها ستُستخدم فقط للأغراض البحثية، ولن يتم مشاركتها مع أي طرف دون موافقتك.
- من خلال الموافقة على المشاركة، فإنك تؤكد فهمك لأهداف الاستبيان وموافقتك على استخدام بياناتك المجهولة لأغراض البحث الطبي.

1. هل توافق على المشاركة في هذا الاستبيان؟:

☐نعم

☐لا

نموذج تقييم عوامل الخطر للسكتة الدماغية وأمراض نقص تروية القلب

القسم أ: المعلومات العامة

1. اسم المريض: _____

القسم ب: المعلومات الاجتماعية والديموغرافية

2. العمر: _____ سنة
3. الجنس: ☐ ذكر ☐ أنثى
4. مكان الإقامة: ☐ حضري ☐ ريفي ☐ مخيم لاجئين
5. الحالة الاجتماعية: ☐ أعزب ☐ متزوج ☐ أرمل ☐ مطلق
6. المستوى التعليمي: ☐ بدون تعليم رسمي ☐ ابتدائي ☐ ثانوي ☐ جامعي
7. المهنة: ☐ موظف ☐ يعمل لحسابه الخاص ☐ عاطل عن العمل ☐ متقاعد
8. عدد أفراد الأسرة: _____ فرد
9. وضع الدخل: ☐ قليل ☐ متوسط ☐ كبير

القسم ج: التاريخ الطبي والأمراض المصاحبة

10. هل تعاني أو سبق لك أن عانيت من أي من الحالات التالية؟ (اختر كل ما ينطبق)
- ☐ ارتفاع ضغط الدم
- ☐ السكري النوع الأول
- ☐ السكري النوع الثاني
- ☐ ارتفاع الكوليسترول/الدهون الثلاثية
- ☐ أمراض القلب التاجية
- ☐ قصور القلب
- ☐ عدم انتظام ضربات القلب
- ☐ الربو
- ☐ أمراض الكلى
- ☐ السمنة ((BMI ≥30
- ☐ أمراض الغدة الدرقية
- ☐ أمراض نفسية (اكتئاب، قلق)
- ☐ لا شيء مما سبق

11. هل تراجع طبيبًا بشكل دوري؟ ☐نعم ☐لا

12. هل أجريت فحوصات للقلب خلال آخر 12 شهرًا؟
- ☐ تخطيط قلب
- ☐ إيكو
- ☐ اختبار جهد
- ☐ لا شيء

13. أمراض القلب والأوعية الدموية في العائلة ☐نعم ☐لا

14. السكتة الدماغية في العائلة ☐نعم ☐لا

15. أمراض صحية أخرى ذات أهمية _____

القسم د: التغذية والسلوك الغذائي

16. عدد الوجبات الرئيسية يوميًا: 3 ☐ 2 ☐ 1 ☐

17. عدد الوجبات الخفيفة يوميًا: +2 ☐ 1 ☐ 0 ☐

18. هل تتناول وجبة الإفطار يوميًا؟ ☐دائمًا ☐ أحيانًا ☐ نادرًا

19. كم مرة تتناول الوجبات السريعة (بيتزا، برغر، بطاطا مقلية...إلخ) أسبوعيًا؟
☐ لا ☐ 1–2 ☐ 3–5 ☐أكثر

20. كم مرة تتناول ما يلي أسبوعيًا؟

نوع الطعام	أبدًا	1–2	3–5	يوميًا
الخضروات الطازجة	☐	☐	☐	☐
الفواكه الطازجة	☐	☐	☐	☐
اللحوم الحمراء	☐	☐	☐	☐
الدجاج/السمك	☐	☐	☐	☐
الألبان والأجبان	☐	☐	☐	☐
الحلويات والمعجنات	☐	☐	☐	☐
المشروبات المُحلّاة	☐	☐	☐	☐
المياه المعدنية (لتر)	☐أقل من 1	1–2 ☐	☐أكثر من 2	—

21. هل تتبع حمية غذائية خاصة (مثل كيتو، نباتي...إلخ)؟
☐ نعم ☐لا | إذا نعم، حدد_____ :

22. من يقوم بتحضير الطعام في المنزل؟
☐ أنت ☐أحد أفراد العائلة ☐ شراء خارجي

23. هل تأكل عادة بسرعة؟
☐ نعم ☐لا

24. هل تستمر بالأكل حتى الشبع الزائد؟
☐ دائمًا ☐أحيانًا ☐ نادرًا

القسم هـ: العوامل السلوكية ونمط الحياة

25. هل تدخن؟ ☐لا ☐ نعم، حاليًا ☐ نعم، سابقًا
26. نوع التدخين:
☐ سجائر (عدد يوميًا: ___)
☐ أرجيلة (عدد الجلسات أسبوعيًا: ___)
☐ إلكترونية
☐ أخرى: _____

27.مدة التدخين بالأعوام: ___

28.هل حاولت الإقلاع عن التدخين؟ □نعم □ لا

29. كم مرة تمارس الرياضة أسبوعيًا؟ □لا □ 5–3 □ 2–1 □ يوميًا

30.نوع التمارين: □مشي □ جري □ سباحة □ تمارين مقاومة □ أخرى

31.كم ساعة تقضيها جالسًا يوميًا (عمل، تلفاز، موبايل)؟

□ أقل من 4 □ 6–4 □أكثر من6

32. هل تستعمل الدرج أم المصعد عادة؟ □درج □ مصعد

33. عدد ساعات النوم اليومية: ___

34. هل تعاني من الأرق؟ □نعم □ لا

35. ما هو مستوى نشاطك البدني خلال يومك المعتاد؟:

□ هادئ

□ متوسط المجهود

□ مجهد بدنيًا أو نفسيًا

36. العادات الغذائية (اختر جميع ما ينطبق):

□ غني بالفواكه والخضروات

□ قليل الفواكه والخضروات

□ غني بالأطعمة المعالجة

□ نظام غذائي عالي الملح: □ نعم □ لا

□ نظام غذائي عالي السكر: □ نعم □ لا

□ نظام غذائي عالي الدهون: □ نعم □ لا

القسم و: البيانات السريرية والأعراض

37. الطول: _____ سم

38. الوزن: _____ كغم

39.الأعراض (اختر جميع ما ينطبق)

□ألم في الصدر

□دوخة

□ضيق في التنفس

□صداع شديد

□ضعف أو تنميل (خاصة في جانب واحد من الجسم)

□صعوبة في التحدث أو فهم الكلام

40. الأدوية الحالية: _____

القسم ز: العوامل البيئية والوبائية

41. المصدر الأساسي للمياه: ☐ عام ☐ بئر خاص ☐ معبأة
42. جودة الهواء: ☐ جيدة ☐ متوسطة ☐ سيئة
43. التعرض لتلوث الهواء: ☐ نادراً ☐ أحياناً ☐ كثيراً
44. التعرض للضوضاء: ☐ نعم ☐ لا

القسم ح: التوعية والوصول إلى الرعاية الصحية

45. التثقيف حول مخاطر أمراض القلب والأوعية الدموية: ☐ نعم ☐ لا
46. الوصول إلى مقدم رعاية صحية منتظم: ☐ نعم ☐ لا
47. عدد زيارات الرعاية الصحية:
☐ نادراً ☐ مرة واحدة في السنة ☐ عدة مرات في السنة
48. الاهتمام بالتطبيقات الصحية على الهواتف: ☐ نعم ☐ لا
49. هل سمعت عن السكتة القلبية المفاجئة من قبل؟ ☐نعم ☐ لا
50. هل تعرف الفرق بين النوبة القلبية والسكتة القلبية؟ ☐نعم ☐ لا
51. إذا فقد شخص الوعي أمامك، ماذا تفعل أولًا؟
☐ اتصل بالإسعاف ☐أبدأ بالإنعاش القلبي الرئوي ☐ لا أعرف
52. هل حضرت دورة في الإسعافات الأولية؟ ☐نعم ☐ لا

القسم ح: الحالة النفسية

53. مقياس الاكتئاب: اختر عدد مرات شعورك في آخر أسبوعين

العنصر	أبداً (0)	أيام قليلة(1)	نصف الأيام(2)	كل الأيام(3)
قلة الاهتمام أو الاستمتاع بالأشياء	☐	☐	☐	☐
شعور بالاكتئاب أو الإحباط	☐	☐	☐	☐
اضطرابات النوم	☐	☐	☐	☐
الإرهاق أو فقدان الطاقة	☐	☐	☐	☐

العنصر	أبداً (0)	أيام قليلة(1)	نصف الأيام(2)	كل الأيام(3)
تغيرات الشهية	☐	☐	☐	☐
الإحساس بعدم القيمة أو الذنب	☐	☐	☐	☐
صعوبة التركيز	☐	☐	☐	☐
بطء الحركة أو العصبية	☐	☐	☐	☐
أفكار عن الموت أو الأذى بالنفس	☐	☐	☐	☐

إذا كان المجموع ≤10، يُنصح بإجراء تقييم نفسي إضافي.

54. مقياس التوتر والقلق ***DASS***-21 (7 أسئلة مختارة)

العنصر	**نادرًا (1)**	**أحيانًا (2)**	**كثيرًا (3)**	**لا ينطبق (0)**
أشعر بصعوبة في الاسترخاء	☐	☐	☐	☐
أشعر بالخوف غير المبرر	☐	☐	☐	☐
أتوتر بسهولة	☐	☐	☐	☐
لا أستمتع بالأشياء التي كانت تهمني	☐	☐	☐	☐
أشعر بالانزعاج أو الغضب دون سبب واضح	☐	☐	☐	☐
أشعر أني غير قادر على التحكم في ضغوطي	☐	☐	☐	☐
أعاني من تسارع ضربات القلب أو توتر عضلي	☐	☐	☐	☐

التنبؤ بخطر الأمراض القلبية الوعائية من تكلسات الشريان السباتي الظاهرة في صور الأشعة البانورامية للأسنان باستخدام التجميع العميق غير المُراقَب

إعداد: نادين خالد إبراهيم عريقات

المشرف: د. رضوان القصراوي

المشرف المشارك: د. حسين المصري

الملخص:

تُعد أمراض القلب والأوعية الدموية من أهم أسباب الوفاة عالميًا، ويظل الاكتشاف المبكر للخطورة الوعائية وتوجيه الإحالة الوقائية تحدّيًا في كثير من الأنظمة الصحية. من المؤشرات التي اكتسبت اهتمامًا سريريًا متزايدًا تكلسات الشريان السباتي التي قد تظهر عرضيًا في صور الأشعة البانورامية للأسنان، حيث يمكن أن تعكس عبئًا تصلبيًا يرتبط بخطر أعلى لأحداث قلبية ودماغية مستقبلية. إلا أن رصد هذه التكلسات يدويًا يعتمد على خبرة الفاحص وقد يتأثر بمقلدات تشريحية شائعة، كما أن كثيرًا من حلول الذكاء الاصطناعي المنشورة تعتمد على التعلم المُراقب وتتطلب بيانات موسومة بكثافة، وهو ما قد يحد من التعميم والتطبيق العملي. تهدف هذه الرسالة إلى تطوير إطار غير مُراقب قائم على التجميع العميق لتحليل مناطق الشريان السباتي في الصور البانورامية، مع توسيع منظور "تصنيف الخطورة" عبر تحليل عوامل الخطورة المستندة إلى الاستبيانات.

تُعد هذه الدراسة (single-center retrospective cross-sectional observational) وقد اعتمدت على قاعدة بيانات مكونة من 1107 صورة بانورامية لمرضى خضعوا لفحوصات سنية روتينية في عيادات الأبراج السنية التابعة لجامعة القدس، وبالتعاون مع كلية طب الأسنان، وذلك خلال الفترة بين February 2025 و August 2025 كما أُجريت دراسة فرعية استبيانية مقطعية مستعرضة بشكل Prospectivelyعلى عينة فرعية (n=438) لاستقصاء عوامل الخطورة القلبية الوعائية ودعم التحليلات غير التصويرية. شملت العينة التصويرية 48% ذكور و52% إناث، بمدى عمري من 18 إلى 85 سنة ومتوسط يقارب 40 سنة. تضمن خط المعالجة تحسين التباين باستخدام تقنية CLAHE ، ثم استخراج منطقتين للاهتمام لكل مريض تمثلان منطقتي الشريان السباتي الأيسر والأيمن اعتمادًا على مواضع معيارية متسقة، مع توحيد الأبعاد إلى 128×128 بكسل لتقليل التباين الحسابي بين الصور.

في تمثيل السمات، استخدمت الرسالة مقاربة مزدوجة تجمع بين السمات القابلة للتفسير والسمات العميقة. تم احتساب سمات يدوية لوصف توزيع الشدة، الملمس، الحواف، وبعض المؤشرات الشكلية المرتبطة

باحتمال التكلس، ثم تمت معايرتها باستخدام Robust Scaler للتقليل من تأثير القيم الشاذة. بالتوازي، تم تدريب مُشفّر تلقائي التفافي لاستخراج تمثيل كامن منخفض الأبعاد (تمثيل كامن منخفض الأبعاد) بعد تدريب مسبق لمدة 300 حقبة باستخدام دالة خطأ متوسط مربع الخطأ، وذلك للحصول على تمثيل مضغوط يحافظ على البنية المرئية ذات الصلة داخل مناطق الاهتمام.

بعد استخراج التمثيلات، تمت مقارنة أربع طرق للتجميع: K-Means ، التجميع الهرمي، نموذج الخلط الغاوسي (GMM) ، وطريقة DEC (التجميع المضمّن العميق). تم تقييم جودة العناقيد باستخدام مؤشرات داخلية تشمل Silhouette و Davies–Bouldin و Calinski–Harabasz. ولربط النتائج بسياق سريري، تم اعتماد تحقق على مستوى المريض (يسار/يمين) بدلًا من مستوى القصاصة المفردة، مع استخدام مجموعة تحقق عالية الخطورة مكونة من 21 مريضًا مُعرّفين اعتمادًا على تاريخ قلبي وعائي مؤكد أو تكلسات موثقة في السجلات السريرية، ثم حُسبت الدقة بحسب قدرة الطريقة على تجميع غالبية هؤلاء المرضى ضمن العنقود السائد عالي الخطورة. كما استُخدمت GradCAM++ لدعم قابلية التفسير بصريًا وإبراز مناطق التركيز ضمن.ROI

أظهرت النتائج تفوق DEC على الطرق الأخرى، محققة أفضل مؤشرات داخلية (Silhouette=0.214، Davies–Bouldin=1.752، Calinski–Harabasz=524)، ما يدل على عناقيد أكثر تماسكًا وانفصالًا أفضل. وعلى مستوى التحقق السريري بالمريض، حققت DEC دقة 95.2% في تجميع حالات الخطورة العالية ضمن عنقود رئيسي مع عدد أقل من الحالات الشاذة مقارنةً بالطرق التقليدية.

ولتعزيز التنبؤ متعدد الأبعاد، حللت الدراسة بيانات استبيان لعوامل الخطورة لعدد 438 مشاركًا (220 عالية الخطورة و218 منخفضة). تم إجراء اختبارات كاي-تربيع معCramér’s V ، وأظهرت النتائج ارتباطات ملحوظة مع العمر، النشاط البدني، ساعات النوم، وقت الجلوس، أنماط غذائية محددة، بعض مؤشرات الوعي الصحي، إضافة إلى مؤشرات نفسية مثل صعوبة الاسترخاء والشعور بانعدام القيمة. كما تم تدريب نموذج غابة عشوائية للتنبؤ بفئة الخطورة اعتمادًا على الاستبيان، وحقق أداء مرتفعًا (Accuracy=0.9318، ROC-AUC=0.9821، F1=0.9291) ، مع بروز مؤشرات اجتماعية اقتصادية ومؤشرات ضيق نفسي ضمن السمات الأعلى تأثيرًا إلى جانب عوامل نمط الحياة والعمر.

تخلص الرسالة إلى أن التجميع العميق غير المُراقب لمناطق الشريان السباتي في الصور البانورامية يمكن أن ينتج أنماطًا ذات معنى سريري، وأن دمجه مع عوامل الخطورة المستخرجة من الاستبيانات قد يدعم مسارًا عمليًا للتحري المبكر والإحالة الوقائية. وتوصي الأعمال المستقبلية بتأكيد النتائج بمرجع ذهبي وعائي مثل دوبلر السباتي أو التصوير الوعائي، وبالتحقق الخارجي متعدد المراكز وربط النتائج بمتابعة طولية للأحداث القلبية والدماغية لضمان الاعتمادية السريرية والتعميم.

الكلمات المفتاحية: الأشعة البانورامية، تكلسات الشريان السباتي، التجميع العميق، DEC، المُشفّر التلقائي الالتفافي، CLAHE، عوامل الخطورة القلبية الوعائية، الغابة العشوائية، ++GradCAM.